Universidade do Minho
Escola de Medicina

Samuel Martins Gonçalves

Metabolic regulation of antifungal immunity: from basic mechanisms to clinical translation

setembro de 2022

Metabolic regulation of antifungal immunity: from basic mechanisms to clinical translation
Samuel Martins Gonçalves
UMinho | 2022

Universidade do Minho
Escola de Medicina

Samuel Martins Gonçalves

Metabolic regulation of antifungal immunity: from basic mechanisms to clinical translation

Tese de Doutoramento
Doutoramento em Ciências da Saúde

Trabalho efetuado sob a orientação do
Doutor Agostinho Albérico Rodrigues de Carvalho
e da
Doutora Cristina Amorim Cunha

setembro de 2022

DIREITOS DE AUTOR E CONDIÇÕES DE UTILIZAÇÃO DO TRABALHO POR TERCEIROS

ACKNOWLEDGMEMENTS

Agradeço aos meus orientadores, Doutor Agostinho Carvalho e Doutora Cristina Cunha, por todo o apoio prestado no desenvolvimento desta tese e pela excecional capacidade de orientação que me têm proporcionado nos últimos 7 anos. Quero agradecer também, sem individualizar, a todos os membros do meu grupo e a todos os colaboradores que, de alguma forma, contribuíram para que eu pudesse concluir mais uma etapa. Por último, mas não menos importante, agradeço também à minha família por todo o suporte prestado.

FINANCIAL SUPPORT

The work presented in this thesis was performed in the Life and Health Sciences Research Institute (ICVS), University of Minho, Braga, Portugal. Support was provided by the Fundação para a Ciência e a Tecnologia (FCT) (SFRH/BD/136814/2018, PTDC/SAU-SER/29635/2017, PTDC/MED-GEN/28778/2017, PTDC/MED-OUT/112/2021, UIDB/50026/2020, and UIDP/50026/2020); the Northern Portugal Regional Operational Program (NORTE 2020), under the Portugal 2020 Partnership Agreement, through the European Regional Development Fund (ERDF) (NORTE-01-0145-FEDER-000039); the European Union's Horizon 2020 research and innovation program under grant agreement no. 847507; the "la Caixa" Foundation (ID 100010434) and FCT under the agreement LCF/PR/HR17/52190003; the Gilead Research Scholars Program - Antifungals; and the ICVS Scientific Microscopy Platform, member of the national infrastructure PPBI - Portuguese Platform of Bioimaging (PPBI-POCI-01-0145-FEDER-022122.

STATEMENT OF INTEGRITY

I hereby declare having conducted this academic work with integrity. I confirm that I have not used plagiarism or any form of undue use of information or falsification of results along the process leading to its elaboration.

I further declare that I have fully acknowledged the Code of Ethical Conduct of the University of Minho.

RESUMO

Regulação metabólica da imunidade antifúngica: dos mecanismos básicos à aplicação clínica

Aspergillus fumigatus é um fungo oportunista responsável por um largo espectro de doenças com manifestações clínicas, que podem ir desde a colonização a síndromes alérgicos, até formas invasivas de infeção. Até à data, não existem vacinas aprovadas para a aspergilose e os métodos usados para o diagnóstico desta doença não apresentam sensibilidade e especificidade adequadas, o que resulta em altas taxas de morbilidade e mortalidade após infeção. É assim, de extrema importância, que a compreensão dos mecanismos de defesa do hospedeiro seja aprimorada, de forma a permitir o desenvolvimento de tratamentos ou de abordagens profiláticas mais eficazes.

No conjunto das células do sistema imune inato, os macrófagos são considerados essenciais para a prevenção da germinação do fungo e da invasão dos tecidos logo após a infeção. Como resposta à infeção, os macrófagos adaptam os seus programas metabólicos, entre os quais o aumento da glicólise que alimenta as funções efetoras microbicidas. Neste trabalho, demonstrámos que em resposta à infeção com *A. fumigatus*, os macrófagos reprogramam o seu metabolismo, ativando o metabolismo glicolítico, essencial para a eliminação do fungo e sobrevivência dos macrófagos. Demonstrámos ainda que a ativação da glicólise é dependente da melanina, expressa na parede celular fúngica. Através da remodelação da maquinaria intracelular de cálcio e do bloqueio da sua sinalização via calmodulina, a melanina induz sinais imunometabólicos que ativam a molécula HIF-1α e recrutam a molécula mTOR para o fagossoma, culminando na ativação da glicólise. Adicionalmente, a contribuição da glicólise para a imunidade antifúngica é também suportada neste trabalho pela identificação de variantes genéticas no gene que codifica a enzima glicolítica PFKFB3, que atuam como cQTLs e que predispõem recetores de transplantes de progenitores hematopoiéticos para o desenvolvimento de aspergilose pulmonar invasiva (API) como resultado de uma desregulação na reprogramação do seu metabolismo celular.

Em suma, os nossos dados demonstram um mecanismo fundamental na regulação imunometabólica durante a infeção fúngica e destacam a manipulação metabólica das células imunes como uma estratégia para prevenir ou tratar a aspergilose. Adicionalmente, este trabalho destaca o papel da variação genética em genes metabólicos na suscetibilidade à API e reforça a importância do perfil genético na identificação dos pacientes com maior risco de desenvolverem a doença, e que poderão beneficiar de uma profilaxia antifúngica mais especifica ou de um diagnóstico célere.

Palavras-chave: *A. fumigatus;* Aspergilose; Imunometabolismo; Macrófago; Variabilidade genética

ABSTRACT

Metabolic regulation of antifungal immunity: from basic mechanisms to clinical translation

The opportunistic fungal pathogen *Aspergillus fumigatus* can cause a wide spectrum of diseases with clinical manifestations that range from colonization to allergic syndromes, to invasive forms of infection. Because there are no licensed vaccines and the currently available tests for the diagnosis of invasive pulmonary aspergillosis (IPA) lack accuracy, mortality rates after infection remain unacceptably high. Therefore, an improved understanding of host defense mechanisms allowing the development of more effective treatment or control measures for IPA remains a pressing demand.

Among the cells from the innate immune system, macrophages are considered critical in preventing fungal germination and tissue invasion early after infection. In response to infection, macrophages rapidly adapt their metabolic programs whereby enhanced glycolysis fuels specialized antimicrobial effector functions. Here, we demonstrated that in response to *A. fumigatus* infection, macrophages reprogram their metabolism toward glycolysis, critical to fungal elimination and macrophage survival. Moreover, we establish fungal melanin as an essential molecule required for the metabolic rewiring of macrophages during infection with *A. fumigatus*. By remodeling the intracellular calcium machinery and impairing signaling via calmodulin, fungal melanin drives an immunometabolic signaling axis toward glycolysis with activation of HIF-1α and phagosomal recruitment of mTOR. The contribution of glucose homeostasis to antifungal immunity was further supported by the identification of variants in the gene coding for the glycolytic enzyme PFKFB3 that act as cytokine quantitative trait loci and predispose recipients of stem-cell transplantation to IPA as the result of a deregulated reprogramming of cellular metabolism.

In summary, our data demonstrate a pivotal mechanism in the immunometabolic regulation during fungal infection and highlight the metabolic repurposing of immune cells as a potential strategy to prevent or treat IPA. Additionally, this work highlights the role of genetic variation in metabolic genes in susceptibility to IPA and reinforces the importance of the genetic profile in the identification of high-risk patients who would benefit from targeted antifungal prophylaxis or a more intensive diagnostic work–up.

Keywords*: A. fumigatus*; Aspergillosis; Genetic variability; Immunometabolism; Macrophage

TABLE OF CONTENTS

LIST OF ABBREVIATIONS

IFIs	Invasive fungal infections
HSCT	Hematopoietic stem cell transplantation
SOT	Solid organ transplantation
COVID-19	Coronavirus disease 2019
HIV	Immunodeficiency virus
GAG	Galactosaminogalactan
PAMPs	Pathogen-associated molecular patterns
NADPH	Nicotinamide adenine dinucleotide phosphate
ROS	Reactive oxygen species
LAP	LC3-associated phagocytosis
ABPA	Allergic bronchopulmonary aspergillosis
CPA	Chronic pulmonary aspergillosis
IPA	Invasive pulmonary aspergillosis
CGD	Chronic granulomatous disease
EORTC	European Organization for the Research and Treatment of Cancer
MSG	Mycoses Study Group
BAL	Bronchoalveolar lavage
GM	Galactomannan
HDT	Host-directed therapies
DCs	Dendritic cells
PRRs	Pattern recognition receptors
TLRs	Toll-like receptors
CLRs	C-type lectin receptors
DAMPs	Damage-associated molecular patterns
APCs	Antigen presenting cells
MHC	Major histocompatibility complex
TCR	T cell receptor
Th	T helper
COPD	Chronic obstructive pulmonary disease

Treg	T regulatory
NLRs	NOD–like receptors
RIG	Retinoic acid–inducible gene
Syk	Spleen tyrosine kinase
CARD9	Caspase recruitment domain–containing protein 9
DC-SIGN	DC–specific ICAM3–grabbing non–integrin
MR	Mannose receptor
MelLec	Melanin-sensing C-type lectin receptor
DHN	Dihydroxynaphthalene
IDO1	Indoleamine-2,3-dioxygenase 1
ECs	Epithelial cells
PTX3	Pentraxin-3
SAP	Serum amyloid P
SP	Surfactant protein
CaM	Calmodulin
CXCL	C-X-C motif chemokine ligand
NETs	Neutrophil extracellular traps
Kyn	Kynurenines
mTOR	Mammalian target of rapamycin
HIF-1α	Hypoxia-inducible factor-1α
PFKFB3	6-phosphofructo-2-kinase/fructose-2,6-biphosphatase 3
IRG1	Immune-responsive gene 1
SDH	Succinate dehydrogenase
RVVC	Recurrent vulvovaginal candidiasis
BCG	Bacillus Calmette-Guérin
MPLA	Monophosphoryl lipid A
2-DG	2-deoxy-D-glucose
SNPs	Single nucleotide polymorphisms
GWAS	Genome-wide association studies
QTLs	Quantitative trait loci

LIST OF FIGURES

LIST OF TABLES

Chapter I

General Introduction

This chapter was partially published in:

Goncalves SM, Ferreira AV, Cunha C, et al. Targeting immunometabolism in host-directed therapies to fungal disease. Clin Exp Immunol. 2022 Jun 11;208(2):158-166

Goncalves SM, Cunha C, Carvalho A. Understanding the genetic basis of immune responses to fungal infection. Expert Rev Anti Infect Ther. 2022 Apr 13:1-10

1.1 Human fungal infections

Fungal infections are currently a global health problem, associated with high morbidity and mortality rates as well as with problematic socioeconomic consequences [1,2]. Fungal pathogens are estimated to lead to more than 1.7 million deaths every year worldwide, with a global burden exceeding one billion [3]. Nonetheless, fungal diseases have been substantially underestimated and neglected by healthcare authorities [2,4]. Over the past two decades, the prevalence of invasive fungal infections (IFIs) has increased considerably, and currently more than 150 million people develop severe fungal infections, with a major clinical impact [3]. This increased incidence is particularly relevant in the case of healthcare-associated IFIs [5-7], for which a call to action was recently issued by the scientific community [8]. This increase is a consequence of the expanding population of at-risk patients for IFIs, namely immunocompromised patients due to recent advances in medical care. Severely impaired immune status, e.g., neutropenia, hematopoietic stem cell transplantation (HSCT), solid organ transplantation (SOT) and the associated prescription of immune-modulatory drugs as well as the excessive antibiotic use are classical examples of predisposing conditions [9,10]. Clinical and epidemiological studies have also recently revealed an expanding frequency of severe fungal infections among critically ill patients that occur in the context of viral pneumonia, e.g., influenza and coronavirus disease 2019 (COVID-19) [11,12]. Endemic fungal infections also pose a significant health threat in selected geographical areas, mainly due to environmental changes, population growth, and increasing rates of human immunodeficiency virus (HIV) infection [13].

Among patients at-risk, the airborne opportunistic fungi *Aspergillus* spp., *Cryptococcus* spp., and *Pneumocystis* spp., as well as the human-associated commensal fungal species *Candida albicans* remain the major fungal pathogens responsible for most cases of serious fungal diseases in the world. These fungi are responsible for more than 90% of all reported fungal disease-related deaths [14-16]. The latest estimates of the annual burden of fungal diseases amount to more than 14 million cases for all diseases within the pulmonary aspergillosis spectrum, over 200,000 cases of cryptococcal meningitis, 500,000 cases of *Pneumocystis jirovecii* pneumonia, 700,000 cases of invasive candidiasis, and over 10 million cases of asthma with fungal sensitization [3,14,17]. Despite the global burden of fungal infections associated with high mortality rates and healthcare costs, and the emergence of antifungal resistance [18], no fungal vaccines have been approved to date [19]. There is, therefore, an urgent need to further elucidate the pathogenetic mechanisms that predispose individuals to infection and foster the development of more effective diagnostic and therapeutic measures for fungal infections.

1.2 *Aspergillus* and pulmonary aspergillosis

Among the wide range of fungal pathogens able to infect a susceptible host, the ascomycetes of the *Aspergillus* genus stand out as a paradigm of environmental microbes that turn into opportunistic pathogens under "permissive" host conditions [20]. In fact, *Aspergillus* spp. are the most frequently isolated filamentous fungi in humans and animals [21-23]. The *Aspergillus* genus consists of over 250 species of ubiquitous saprophytic molds particularly common in the soil, compost, and decaying vegetable matter. Aspergilli are also found in indoor environments, such as surfaces of buildings, household appliances and air, and play important roles in carbon and nitrogen recycling. While many species of this genus are used in industrial applications, around 40 species of *Aspergillus* have been found to be pathogenic to humans [24]. These fungi present remarkable phenotypic plasticity in their ecology and stress responses, which is the basis of their success as opportunistic pathogens. Among the pathogenic species, *Aspergillus fumigatus* possesses a combination of biological characteristics that make it responsible for the vast majority of related infections [22,24]. The growth rate, ease of dissemination, high adaptation, nutritional versatility, thermotolerance, and other aspects of its ecophysiology collectively contribute to the efficacy of *A. fumigatus* as a pathogen [23,25]. *A. fumigatus* produces large quantities of spores (termed conidia), with 2-3 μm in diameter, through asexual reproduction [20], that enter the human lungs by inhalation and that can penetrate and access pulmonary alveoli due to their small size. *A. fumigatus* can also reproduce sexually, allowing the inheritance of virulence factors, resulting in strains with increased virulence [26].

In a hostile environment, the fungal cell wall is the first line of defense against the host immune system. Therefore, the cell wall plays an important role in host-*Aspergillus* interactions and fungal survival, providing integrity and physical protection to the cell. The inner cell wall of *A. fumigatus* is composed of an alkali-insoluble fibrillar skeleton, which is made of branched β-1,3-glucans to which chitin, galactomannan and β-1,3-glucans/β-1,4-glucans are covalently bound. The fibrillar core of the cell wall is embedded in an amorphous alkali-soluble cement, which is mainly composed of α-1,3-glucans and the galactose-containing polysaccharides galactomannan and galactosaminogalactan (GAG) [20]. The surface rodlet layer is responsible for the unique surface of the conidium and its hydrophobic characteristics and provides resistance to harsh environmental conditions and host defenses [27,28]. The hydrophobic RodA proteins that comprise the rodlet layer on the conidial surface mediate immune evasion both *in vitro* and *in vivo* [29], and together with α-mannans and melanin form a dense layer around the conidium [20]. These conidial surface molecules mask pathogen-associated molecular patterns (PAMPs) that are present

in the cell wall and avoid fungal recognition by immune cells. Melanin also plays a potent anti-phagocytic and immune evading function, since it blocks the acidification of the phagosome [30], inhibits the nicotinamide adenine dinucleotide phosphate (NADPH) oxidase complex [31], responsible for the production of antifungal reactive oxygen species (ROS), and blocks LC3-associated phagocytosis (LAP), a critical mechanism for the intracellular elimination of conidia by monocytes and macrophages [31,32]. Of note, disruption of the melanin biosynthetic pathway in *A. fumigatus* results in an attenuation of virulence in animal models, which highlights its critical role in immune evasion by the fungus [33]. When conidia start to swell and germinate, the fungus sheds its outer melanin and rodlet layer, exposing additional PAMPs, allowing hyphal growth (and GAG expression) to occur (Fig. 1).

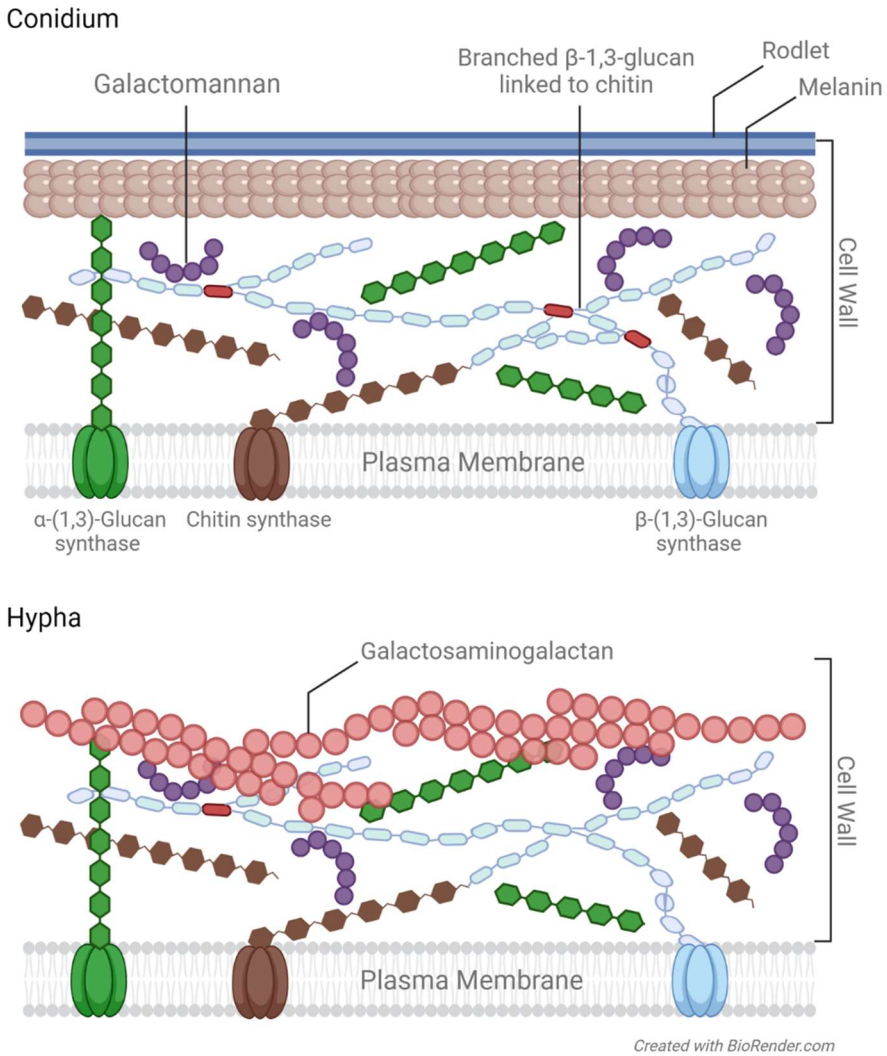

Figure 1. Schematic representation of the *A. fumigatus* conidium and hypha cell walls. Note that despite the structural components of the cell wall of the conidium and hypha are mostly shared, the composition of the outer layer of these two morphotypes is distinct, with a rodlet layer and melanin expressed on the conidium, and galactosaminogalactan (GAG) covering the mycelium .

1.2.1 Pulmonary aspergillosis: a wide spectrum of diseases

On a daily basis, any individual will inhale approximately 100–1,000 conidia of *A. fumigatus* [20]. Immunocompetent individuals will efficiently clear most of the inhaled conidia through mucociliary movements, while the remaining conidia will be phagocytosed and eliminated mostly by tissue-resident alveolar macrophages [34]. However, depending on the underlying immune status of the host , *Aspergillus* spp. can lead to a variety of pathologies. There are three broad categories of pulmonary aspergillosis with distinct pathogenetic mechanisms and clinical manifestations: allergic bronchopulmonary aspergillosis (ABPA), chronic pulmonary aspergillosis (CPA) and invasive pulmonary aspergillosis (IPA) [35] (Fig. 2).

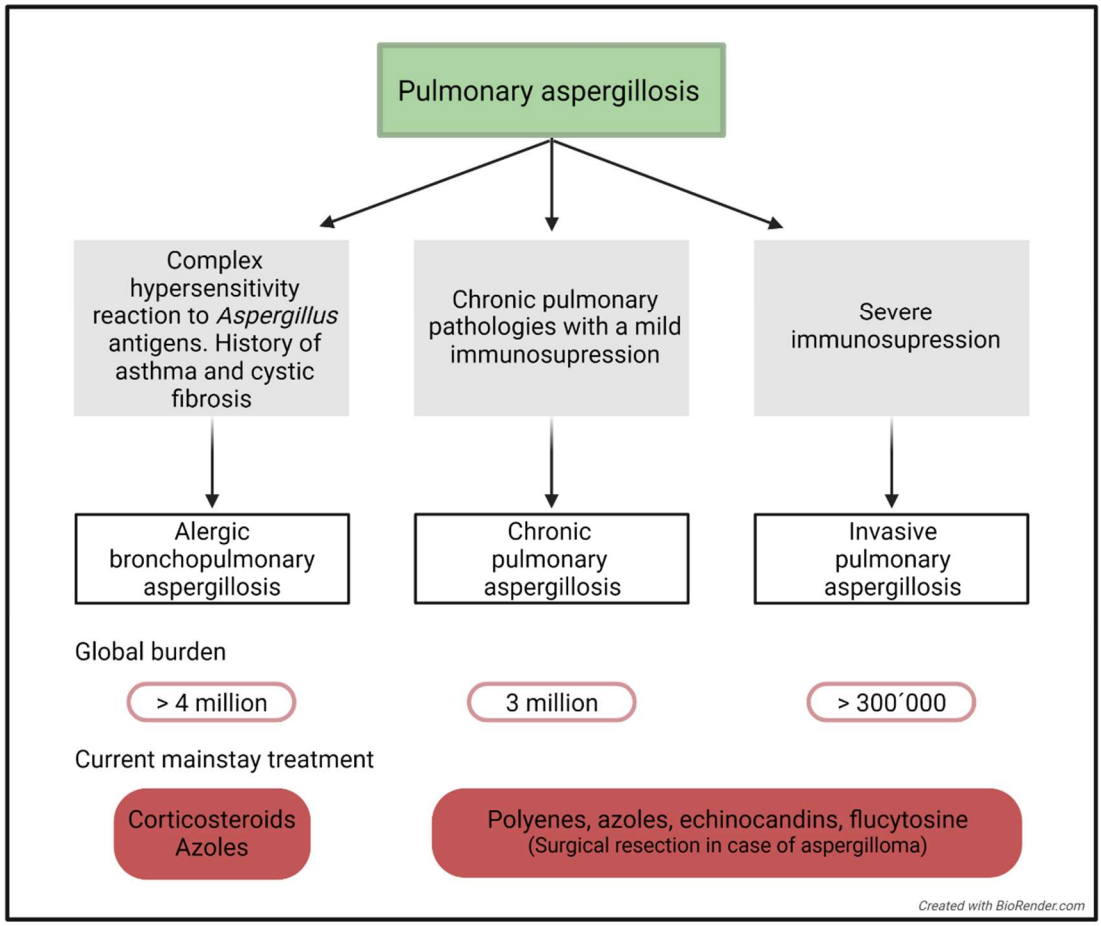

Figure 2. The general spectrum of pulmonary aspergillosis. Following inhalation of conidia, *Aspergillus* spp. can cause a variety of pathologies, if not proper eliminated by mucociliary clearance or macrophage phagocytosis. Depending on the immune status of the host, pulmonary aspergillosis can range from allergic reactions (hypersensitivity) to life-threatening invasive infections (severe immunosuppression). The current burden and treatment options are also depicted.

The interplay between the pathogen and the host immune dysfunction or hyperactivity determines which clinical syndrome is more likely to develop [36]. Due to the widespread use of chemotherapeutic and immunosuppressive agents, the overlap between these categories is becoming increasingly recognized [37]. As such, pulmonary aspergillosis should be regarded as a semi-continuous spectrum of allergic, non-invasive and invasive diseases [35].

1.2.2 Epidemiology of invasive pulmonary aspergillosis

Invasive pulmonary aspergillosis (IPA), a life-threatening infection caused mainly by *A. fumigatus*, was first described in 1953 [38], and is the most serious clinical entity on the spectrum of pulmonary aspergillosis. IPA has a global incidence of more than 300,00 cases per year with mortality rates ranging from 30 to 80% [3,17,39]. IPA implies the invasion of lung tissue by *Aspergillus* hyphae that can be followed by hematogenous dissemination to distant organs, including the central nervous system, liver, spleen and skin, whose function is often irreversibly compromised [40]. Patients at-risk are predominantly HSCT recipients and patients with hematological malignancies undergoing intensive chemotherapy [23]. Additionally, patients undergoing SOT, patients treated with corticosteroids, individuals with genetic immunodeficiencies (e.g., chronic granulomatous disease, CGD), or infected with HIV [14,21,36] are also at high risk for IPA. More recently, there has also been an increase in reports of cases of IPA developing in immunocompetent patients following severe influenza [41,42] and COVID-19 [43-45].

The number of patients undergoing HSCT has grown exponentially in the last 30 years and IPA has become a leading cause of death among these patients, accounting for 10% of all deaths in this population [46]. In this setting, most experts agree that there is a hierarchy of risk based not only on the type of transplant, but also on the underlying disease, comorbid conditions, and other variables. Currently, IPA mostly occurs late (40 to 80 days) and very late (80+ days) after stem-cell engraftment. Despite the significant progress in treating and preventing IPA, its incidence within HSCT patients has increased since the first reports in surveillance clinical studies in the late 1990s [23]. In 2010, the Transplant–Associated Infection Surveillance Network (TRANSNET), a network of 23 United States transplant centers that prospectively enrolled HSCT recipients between March 2001 and March 2006 revealed that, in addition to the increased cumulative incidence of IPA, the overall 1–year mortality among HSCT patients with IPA was approximately 75% [47]. Other large epidemiological studies performed in several European countries have confirmed the predominance of IPA over other IFIs in HSCT patients [48-51]. Moreover, because of

its prevalence and costly treatments, IPA has also become the most expensive fungal disease in the hospital setting [52]. Altogether, these data emphasize the clinical relevance of this disease, particularly in this setting, and show that there is still much to do to fight IPA.

1.2.3 Diagnosis of invasive pulmonary aspergillosis

The unacceptably high mortality rates associated with IPA stem primarily from difficulties in the diagnostic and therapeutic options. Timely and accurate diagnosis of IPA is needed to improve disease outcome, however, despite recent improvements, it remains a critical challenge nowadays for clinicians worldwide. One difficulty in the diagnosis of IPA is defining the precise criteria required to establish the diagnosis. Along this line, the development of standardized diagnostic criteria for IPA by the European Organization for the Research and Treatment of Cancer (EORTC)/Mycoses Study Group (MSG) represents a major contribution [53,54].

The clinical presentations and radiological changes in IPA are non-specific and become evident late in the course of the disease, especially in neutropenic patients [23]. The gold standard for securing diagnosis remains the identification of the organism by histopathology and/or growth in culture from tissue biopsy or aspirate from a sterile site, but this is frequently contraindicated in critical ill patients. Besides the fact that these approaches are undoubtedly the most labor intensive, colonization can be difficult to discriminate from a true invasive infection, and detection of *Aspergillus* by traditional blood culture is often not possible since fungi rarely circulate in the bloodstream [55]. Although histopathological detection of *Aspergillus* in the tissue remains essential to define the highest level of certainty in diagnostic criteria, less invasive and more rapid methods have already overtaken this approach in most settings. As IPA patients typically do not produce anti-*Aspergillus* antibodies, in contrast to immunocompetent patients, detection of *Aspergillus* molecules circulating in the biological fluids is the reference to diagnose an invasive infection. Therefore, serum and bronchoalveolar lavage (BAL) biomarkers such as galactomannan (GM) and β-D-glucan are being increasingly employed to establish the diagnosis. While BAL testing for GM is the most sensitive method for the diagnosis of IPA, serum GM testing is easier to perform and serial sampling can be used to monitor the response to antifungal therapy [55,56]. However, these tests vary in sensitivity and specificity, depending on the patient population involved and the assay used [56]. Another important circulating molecule considered for diagnosis of IPA is fungal DNA. Different polymerase chain reaction (PCR) protocols have been published so far, but they lack standardization. Although PCR is more accurate in detecting *Aspergillus* in the sputum and BAL when compared to culture,

the heterogeneity of the assays employed along with their lack of clinical validity renders its diagnostic value unclear [35]. Additionally, PCR is often associated with false-positive results because it does not discriminate between colonization and infection. The use of PCR remains controversial and has not been included in the consensus definitions of the EORTC. Additionally, fungal RNA [57] and microRNA detection [58], as well as the analysis of the volatile organic compounds of *A. fumigatus* in the exhaled breath condensates of patients with IPA have also been proposed as diagnostic tools [23,59,60].

Currently, none of the antigen-based diagnosis approaches is 100% reliable for the diagnosis of IPA, suggesting that a combination of diagnostic tests is the best option to significantly increase the detection rate. In fact, when *Aspergillus* PCR in BAL was used in combination with GM, diagnosis of IPA was made earlier, and therapy was more effective [61]. Finally, the inability of molecular diagnostic assays to distinguish between the different stages of the disease, from colonization to chronic non-invasive infection to IPA (all of which can coexist in the same patient), together with the lack of a gold standard for diagnosis, have hampered the performance of the current diagnostic methods.

1.2.4 Treatment of invasive pulmonary aspergillosis

Prompt initiation of therapy in IPA decreases mortality and is essential to prevent disease progression, even when a proven diagnosis is not readily available [35]. In this regard, medical mycology is also facing a gap, since there are no licensed antifungal vaccines and the therapeutic options are restricted to four antifungal drug classes - polyenes, azoles, echinocandins and the pyrimidine analogue flucytosine (5-FC) - targeting different parts of the fungal cell [62] (Fig. 2). These drugs are frequently associated with intrinsic and acquired resistance [63], because of the target similarity between the fungal and host cells, resulting in high toxicity and various side effects [64].

The polyene amphotericin B (AmB) deoxycholate was the first therapy for IPA and has been used in prophylaxis or to treat suspicion of *A. fumigatus* infection. However, this drug causes serious side effects including nephrotoxicity, electrolyte disturbances and hypersensitivity [65]. In the early 1990's, a new class of antifungal drugs containing azoles was generated. Fluconazole was the first azole to be used, but since the year 2000, the emergence of resistant fungal strains rendered the use of this drug in therapy almost obsolete. Currently, voriconazole is considered the gold standard for the treatment of IPA [39]. Another class of antifungals used for treatment are echinocandins. These drugs are fungistatic to molds such as *A. fumigatus*, and their mechanism of action occurs trough the inhibition of the synthesis of

fungal β-1,3 glucan [66]. Nevertheless, as echinocandins are not fungicidal, they are less effective in severely immunocompromised patients, which suggests that these drugs should be used in combination with other antifungal drugs to increase fungal elimination. Despite the availability of these antifungal drugs, mortality rates in IPA patients that receive treatment remain unacceptably high.

To address the increasing need for new therapeutic options against fungal infections, alternative approaches are being explored, which include host-directed therapies (HDT). In this context, HDTs based on cytokine therapy, vaccine development and in cellular immunotherapy have been explored to modulate host antifungal response by mitigating inflammation and promoting the antimicrobial activity of immune cells [67], with the crucial advantage of avoiding the development of drug resistance [68]. Despite these advances, however, IPA remains difficult to diagnose and to treat. The aim for future antifungal management should be a targeted personalized medicine approach whereby high-risk patients are identified and prophylactically treated. In this regard, genetic profiling to stratify patients with different risk patterns is expected to become clinically relevant soon [69].

1.3 Fungal recognition and antifungal immune response

The primary function of the immune system is to sense and remove invading pathogens through a variety of host resistance effector mechanisms. While resistance is defined as the capacity to reduce pathogen burden during infection, tolerance is meant to alleviate the substantial cost of resistance systems to host fitness [70]. Therefore, host immune responses during IPA must balance the clearance of the pathogen, while limiting tissue damage.

From an immunological perspective, the defense against inhaled conidia begins in the anatomical barriers of the respiratory tract. Most inhaled conidia are deposited against the airway surface fluid due to turbulent airflow caused by the branching pattern of the bronchial tree [34]. The trapped conidia are then removed by the ciliary action of the respiratory epithelium [71]. This mechanism represents the first line of defense in the lung. Due to their small size, some of the inhaled conidia can overcome the anatomical barriers and reach the respiratory alveoli. When this occurs, conidia will be challenged by cells of the innate immune system, including resident alveolar macrophages and dendritic cells (DCs), as well as recruited inflammatory cells, mainly polymorphonuclear neutrophils. A rapid and efficient immune response relies largely on the selective recognition of PAMPs by pattern recognition receptors (PRRs) expressed on phagocytes. The maturation of conidia within the alveoli will trigger a morphological change leading to the loss of the thin hydrophobic RodA protein layer, thus exposing fungal PAMPs, such as β-

1,3-glucans, mannans, chitin and melanin [72]. The main PRRs involved in fungal recognition are Toll-like receptors (TLRs) and C-type lectin receptors (CLRs), but other receptors such as integrins and scavenger receptors also function as PRRs [73]. Engagement of PRRs initiates signaling cascades that result in pathogen engulfment by professional phagocytes, initiation of inflammation, and secretion of cytokines and chemokines (Fig. 3). The cytokine environment contributes to the recruitment of other innate immune effectors, such as inflammatory monocytes and neutrophils, which mediate killing of conidia that have escaped initial recognition or that have germinated into hyphae. In addition, soluble proteins such as collectins, pentraxins, ficolins, and proteins from the complement system can act as opsonins to facilitate phagocytosis and promote direct fungicidal activity through the recruitment of complement components [74]. PRRs also respond to products released from damaged host cells during infection, including nucleic acids, alarmins, and metabolites, collectively termed damage-associated molecular patterns (DAMPs) [75]. While some PRRs and soluble molecules exert a redundant function during fungal infection, an efficient antifungal immunity requires the coordinated regulation of individual or multiple receptors.

The induction of innate immunity via PRRs shapes the development of the adaptive immune response. DCs are key cells that bridge the innate and adaptive immune responses to *A. fumigatus*. As antigen presenting cells (APCs), DCs transport fungal antigens from the airways to the draining lymph nodes, where they interact with naïve T cells through the major histocompatibility complex (MHC) and T cell receptor (TCR), resulting in the secretion of various cytokines driving protective T helper 1 (Th1) and Th17 responses against *A. fumigatus* [46,76] (Fig. 3).

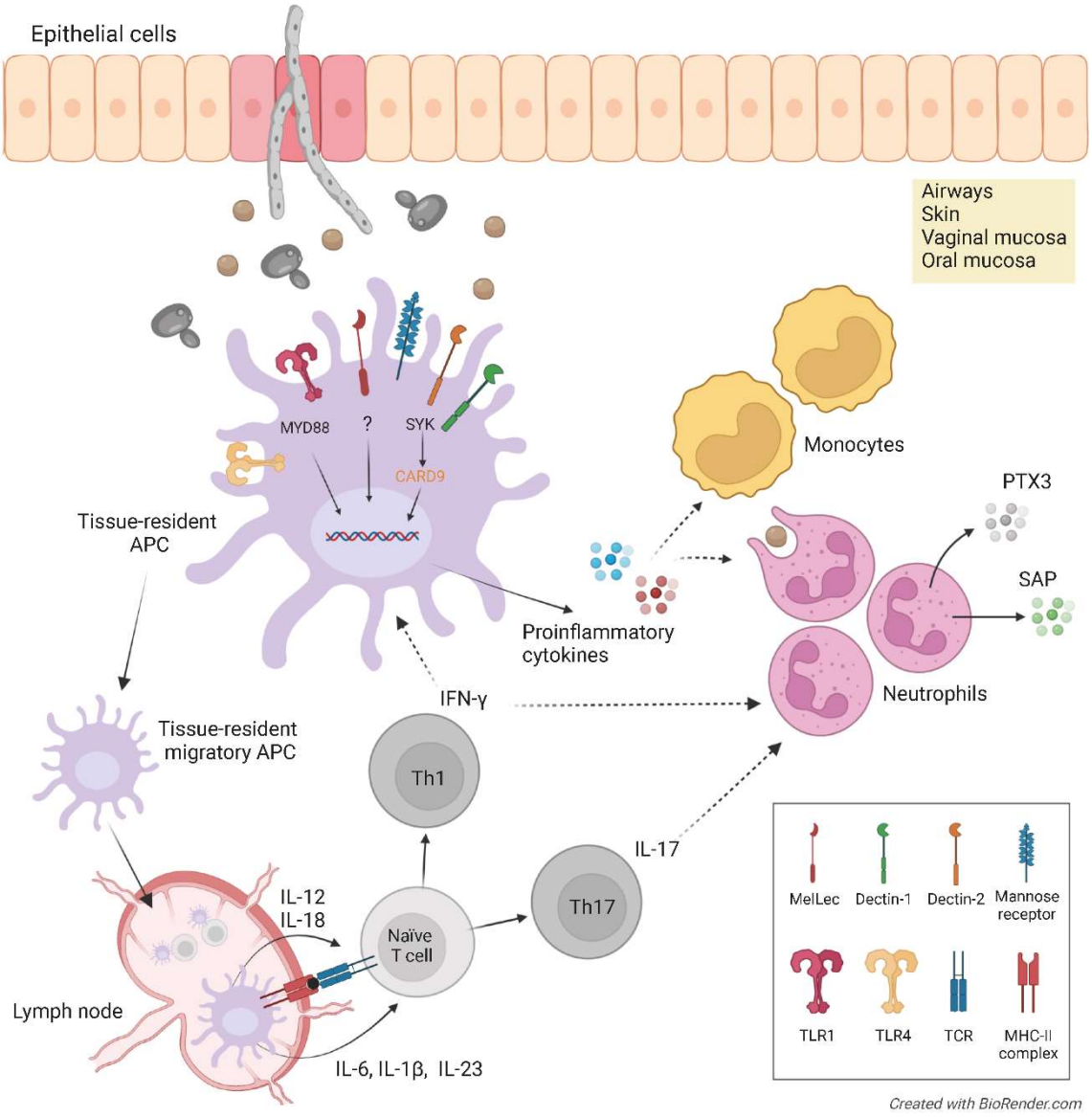

Figure 3. General overview of the molecular and cellular processes involved in the innate and adaptive immune responses to fungal pathogens. APC, antigen-presenting cell; PTX3, long pentraxin PTX3; SAP, serum amyloid P.

The activation of specific T cell subsets is dependent on the fungal antigen, PRR signaling pathways and the mode of antigen routing and presentation in DCs [77]. Th1 responses driven by IL-12 are critically required for the development of protective immunity to the fungus in mice and humans [78,79], as well as to experimental fungal vaccines [77]. This protective immunity develops through the secretion of the pro-inflammatory cytokines tumor necrosis factor (TNF) and interferon gamma (IFN-γ), which promote antifungal activity of macrophages and neutrophils at the site of infection [80-82]. Interestingly, Th1 cells

have been shown to induce a fungus-specific Th1 immunity to the immunogenic epitope of the *A. fumigatus* cell wall glucanase (Crf1) that can be presented by three common MHC class II alleles, and that induces memory CD4+ Th1 cells with a diverse T-cell receptor repertoire that is cross-reactive to *C. albicans* [83]. The role of Th17 responses in antifungal immunity to *A. fumigatus* is less clear, both in humans and in murine models [14,84]. In humans, *A. fumigatus* fails to induce the production of IL-17, and as such, is it acknowledged that human host defense against *Aspergillus* relies more prominently on Th1 rather than Th17 responses [85]. However, recently, Jolink and collaborators showed that Th17 cells may play a more important role in the immune response than was appreciated until now [86]. In this work, the authors stimulated lung-derived mononuclear cells (LMC), from chronic obstructive pulmonary disease (COPD) patients, with a mixture of overlapping peptides of six *A. fumigatus* proteins and found that the lung-derived *Aspergillus*-specific T-cells exhibited a Th17 phenotype, producing mainly IL-17 and low amounts of IFN-γ [86]. These data indicate that, like in other fungal infections, Th17 cells play a role at the site of infection in response to *A. fumigatus* infection [86]. Lastly, regulatory T (Treg) cells have been shown to regulate the inflammatory response elicited by a strong Th1 response in the early phase of *A. fumigatus* infection [87], but may conversely promote fungal persistence and immunosuppression. In fact, Treg cells are relevant producers of IL-10, which is instead linked to disease progression in IPA [46].

1.4 Recognition of *A. fumigatus* by membrane-associated PRRs

Pathogen recognition is crucial to initiate adequate immune defenses and is facilitated by recognition receptors expressed on phagocytes. Currently, PRRs are categorized into four classes: CLRs ; TLRs; nuclear oligomerization domain (NOD)–like receptors (NLRs) and retinoic acid–inducible gene (RIG)-I–like receptors [88-90].

The best characterized PRR for *A. fumigatus* is the CLR type II transmembrane protein dectin-1. This receptor is highly expressed in macrophages, neutrophils and DCs, and is crucial for mediating a proinflammatory response against *A. fumigatus* in the respiratory tract [91], as shown by the increased susceptibility of immunocompetent mice deficient in dectin-1 to *A. fumigatus* infection [92]. Dectin-1 recognizes the cell wall constituent β-1,3-glucan [93] on swollen and germinating conidia but does not respond to resting conidia, thus allowing macrophages to distinguish between the different morphological forms of *A. fumigatus* [94]. Dectin-1 can stimulate a variety of cellular responses via the spleen tyrosine

kinase (Syk)/caspase recruitment domain–containing protein 9 (CARD9) signaling pathway [95]. Interaction of dectin-1 with *A. fumigatus* conidia promotes their phagocytosis, enhances macrophage activation, and induces proinflammatory responses including the secretion of IL-1β and TNF. In addition, dectin-1 mediates the recruitment of the autophagy protein LC3-II to the phagosomes in monocytes [96] and has an important role in neutrophil recruitment [93]. Dectin-2 has also recently been shown to be implicated in the innate immune response against *A. fumigatus*. In contrast to dectin-1, dectin-2 recognizes α-mannans, which are found in the outer layer of the fungal cell wall [97,98], thereby masking β-glucans. This observation suggests that, upon inhalation, conidia are more likely to be recognized by dectin-2 before detection by dectin-1. Dectin-2 is expressed at high levels by alveolar macrophages in the human lung in response to *A. fumigatus* [98] and is also expressed in DCs. Furthermore, dectin-2 was shown to mediate an NF-κB-dependent proinflammatory response against swollen conidia. Blocking of dectin-2 resulted in significantly reduced conidial killing by THP-1 macrophages, thus further emphasizing the role of this receptor in host defense against *A. fumigatus* [98,99]. Of note, recognition of *A. fumigatus* hyphae by human plasmacytoid DCs was shown to be mediated by dectin-2 [100]. Recently, dectin-2 was also found to recognize *A. fumigatus* galactomannan [101]. In addition, DC–specific ICAM3–grabbing non–integrin (DC-SIGN) has also been suggested to recognize galactomannan [102]. DC-SIGN is expressed at the surface of DCs and some macrophages with specificity for high mannose moieties [34,103] and, together with mannose receptor (MR), recognize branched *N*–linked mannans. Both receptors can direct mannosylated fungal antigens to the endocytic pathway of DCs, thereby promoting antigen processing and presentation to T cells [104,105]. Likewise, MR has been shown to be involved in the promotion of antifungal Th17 cell responses [106]. More recently, the melanin-sensing C-type lectin receptor (MelLec) was identified as an essential receptor in both mice and humans, with a role in the recognition of the naphthalene-diol unit of 1,8-dihydroxynaphthalene (DHN)-melanin, an immunologically active component commonly found on melanized fungi [107].

Among PRRs, TLRs were the first to be identified and are the best characterized. This family is critical to the recognition of *A. fumigatus* and comprises 10 members in humans (TLR1–10) and 12 in mouse (TLR1–9, TLR11–13) [108]. As TLRs are membrane-bound, they can be found either at the cell surface (TLR1, TLR2, TLR4-6 and TLR10) or in endocytic compartments (TLR3, TLR7-9), and recognize distinct PAMPs and DAMPs. Upon recognition, TLRs recruit toll/interleukin-1 receptor (TIR) domain-containing adaptor proteins such as myeloid differentiation primary response 88 (MyD88) and TIR-domain-containing adapter-inducing interferon-β TRIF [108] which initiate a signaling cascade leading to the activation of

transcriptional factors such as NF-κB, capable of controlling the expression of pro- and anti-inflammatory cytokines and chemokines [109]. TLR2 has been implicated in the recognition of yet unidentified ligands of conidia and hyphae, whereas TLR4 is only associated with the recognition of conidial ligands [110]. Interestingly, in response to hyphae, TLR4 signaling is lost, and hyphae, but not conidia, stimulate instead the production of IL-10 via TLR2, suggesting that a phenotypic switch from conidia to hyphae may represent an immune evasion mechanism of *A. fumigatus* [110,111]. Moreover, both TLR2 and TLR4 enhance pro-inflammatory cytokine production in response to *A. fumigatus* [111]. In fact, cytokine production by *A. fumigatus*-stimulated bone marrow-derived macrophages (BMDMs) from both TLR2 and TLR4-deficient mice is severely dampened [112]. The activation of TLR2 by *A. fumigatus* was observed with the formation of a heterodimer with TLR1 or TLR6 in mouse cells, and with TLR1, but not TLR6, in human cells [112]. Several reports have indicated that some TLRs can also recognize fungal nucleic acids, namely TLR9 [113-116] and TLR3 [77,117,118]. TLR9 recognizes the fungal unmethylated CpG DNA, and its absence abolished cytokine production by BMDCs stimulated with fungal DNA [119]. Regarding TLR3, the activation of a TLR3/TRIF–dependent pathway converging on indoleamine-2,3-dioxygenase 1 (IDO1) on epithelial cells (ECs) was found to confer protective tolerance to *A. fumigatus* [118] and TLR3 sensing of fungal RNA by DCs was essentially required for the activation of protective MHC class I–restricted memory CD8+ T cell responses to aspergillosis in mice and in human patients [117].

The intracellular NLRs can also activate immune signaling pathways following the recognition of *A. fumigatus*. Along this line, NOD2 has been implicated in the recognition of *A. fumigatus* [120]. *In vitro* stimulation of murine macrophages with *A. fumigatus* conidia resulted in a significantly increased expression of NOD2 protein and RIP2 kinase, a signaling component of NODs. Upregulation of NF-κB and downstream cytokine production were increased simultaneously after conidia exposure, and these features were not observed in NOD2-knockout cells [120], suggesting that this receptor can potentially contribute to the innate immune response against *A. fumigatus*. A role for the NLRP3 (NOD-, LRR- and pyrin domain-containing protein 3) inflammasome during *A. fumigatus* infection was also demonstrated *in vitro* [121] and *in vivo* [122]. Hyphae, but not conidia, were shown to induce IL-1β production in THP-1 cells, which was significantly reduced in cells with silenced *NLRP3* and *ASC* genes. NLRP3 inflammasome activation by *A. fumigatus* was found to occur through a pathway requiring ROS production and the Syk tyrosine kinase [121]. More recently, *A. fumigatus* GAG was reported as a novel PAMP that

activates the NLRP3 inflammasome to provide host protection [123]. Of note, double knockout mice for both *Nlrp3* and absent in melanoma 2 (*Aim2*) are susceptible to IPA [124].

1.5 Recognition of *A. fumigatus* by soluble PRRs

Fungal recognition is facilitated by molecules of the humoral arm of the innate immune system including pentraxins, complement proteins, ficolins and collectins [125-127]. Pentraxin-3 belongs to the family of long pentraxins and is secreted as a multimeric protein by numerous cells, including neutrophils, DCs, mononuclear phagocytes, and pulmonary epithelial cells in response to inflammatory mediators [128]. PTX3 binds to *A. fumigatus* conidia and facilitates recognition by phagocytes such as alveolar macrophages [129,130]. The critical role of PTX3 in host antifungal defense was demonstrated *in vivo* by the remarkable susceptibility of immunocompetent PTX3-deficient mice to IPA, and by the observation that administration of exogenous PTX3 restored antifungal effector functions in these animals [129]. Another pentraxin, serum amyloid P component (SAP), also known as PTX2, is also an essential element of resistance against *A. fumigatus*. Murine and human SAP were found to bind conidia, activate the complement cascade and enhance phagocytosis by neutrophils [131]. In immunosuppressed mice, SAP administration protects hosts against *A. fumigatus* infection and associated mortality [131]. In addition, pulmonary collectins, which include lung surfactant proteins A and D (SP-A and SP-D, respectively), also serve as opsonins. Binding of SP-A and SP-D to *A. fumigatus* conidia has been shown to result in conidial agglutination, enhanced phagocytic capacity and increased fungicidal effects of alveolar macrophages and neutrophils [132]. Moreover, SP-A and SP-D were shown to be potent chemoattractants for neutrophils [132].

1.6 Innate effector mechanisms

Alveolar macrophages, neutrophils and epithelial cells constitute the first line of defense against inhaled *A. fumigatus* conidia [34]. Inside the alveolar lumen, alveolar macrophages are the first immune cells to interact with inhaled conidia of *A. fumigatus* and control most of the fungal germination [133]. These cells are professional phagocytes, characterized by a remarkable ability to engulf particulate material, ranging from resting conidia to apoptotic cells or even latex beads [134].

Alveolar macrophages efficiently eliminate phagocytosed conidia within a few hours in acidified phagolysosomes [135-138]. Studies on *Aspergillus* phagosome biogenesis have reported a rapid

acquisition of markers of the early and late endosomal/lysosomal pathways within the first hour after phagocytosis, a process regarded as a normal phagosome maturation [135,137]. In contrast to the rapid acquisition of certain lysosomal markers, conidial killing by alveolar macrophages was delayed 3 to 6 hours after phagocytosis and was associated with delayed phagosome acidification, intracellular swelling of *Aspergillus* conidia and NADPH oxidase-dependent ROS production [135,137]. This generation of ROS occurs in response to swollen but not resting conidia, which results in the recruitment of cytosolic proteins to the plasma membrane that, together with membrane-bound flavocytochrome units, form the complex called NADPH oxidase [139]. The NADPH oxidase complex regulates several crucial pathways in host defense against *A. fumigatus* [20]. Its key function is highlighted by the extreme susceptibility of patients who are deficient in the NADPH oxidase complex, such as CGD patients, to IPA [20]. Likewise, even immunosuppressed mice displayed a lower susceptibility to IPA than $p47^{phox}$ deficient mice, which are defective in NADPH ROS generation [140]. Specifically, $p47^{phox}$ deficient alveolar macrophages were unable to control the growth of phagocytosed conidia in contrast to wild-type cells [140]. Moreover, the ability of neutrophils to damage hyphae, but not kill conidia, was dependent on the function of the NADPH oxidase complex [141]. Besides the well-established role of NADPH oxidase and ROS production in macrophages and neutrophils and in other innate effector cells, mitochondrial ROS (mtROS) have recently been disclosed to be relevant to antifungal immunity [142]. Exposure of murine macrophages to swollen conidia of *A. fumigatus* increased mtROS production compared to untreated macrophages, or those treated with resting conidia [142]. Exposure of macrophages to swollen conidia increased the activity of the complex II of the respiratory chain and raised mitochondrial membrane potential, suggesting that mtROS are produced via reverse electron transport (RET). In fact, preventing mtROS generation via RET by treatment with rotenone lowered the production of pro-inflammatory cytokines TNF and IL-1β, and impaired the fungicidal activity of macrophages [142]. The importance of mtROS for alveolar macrophages was also demonstrated in a recent study by Shlezinger and collaborators [143]. In this study, murine innate immune cells, including alveolar macrophages, monocyte-derived DCs, and neutrophils, were also found to generate mtROS in response to fungal infection [143]. Of note, neutralizing the mtROS constituent hydrogen peroxide (H_2O_2) via a catalase expressed in the mitochondria of innate immune cells substantially diminished the fungicidal properties of alveolar macrophages, but not of other innate immune cells, pointing mtH_2O_2 as a novel alveolar macrophage killing mechanism against *Aspergillus* conidia [143].

The importance of ROS production goes beyond their direct antifungal activity. In fact, NADPH oxidase-mediated ROS production is necessary for the recruitment of LC3 to the *Aspergillus*-containing phagosomes and subsequent initiation of LAP [31,144], a critical process in antifungal immunity against *A. fumigatus*. Indeed, macrophage or monocyte killing of *A. fumigatus* is dependent on the noncanonical autophagy pathway LAP [31,144]. LAP links the activation of selected PRRs with phagosome biogenesis and inflammatory cytokine responses [145], and has an important role in immunity against *A. fumigatus*, since mice that lack components of LAP are more susceptible to IPA [146]. Intracellular swelling of *A. fumigatus* conidia and β-glucan-mediated activation of Dectin1/Syk kinase/NADPH oxidase signaling is a prerequisite for activation of LAP, phagosome maturation, and fungal killing [23,144], providing a link between pattern recognition by CLRs and NADPH oxidase-mediated host defense. Melanin, a major component of the conidial cell wall, is intracellularly removed from the *A. fumigatus* cell wall when the conidia germinate. Melanin inhibits LAP without interfering with Dectin-1/Syk signaling regulating cytokine responses. Fungal pathogenicity is therefore regulated by melanin-induced LAP blockade, since the attenuated virulence of melanin-deficient *A. fumigatus* is restored in *Atg5*-deficient macrophages and in mice upon conditional inactivation of Atg5 in hematopoietic cells [31]. Of note, this melanin-induced LAP blockade depends on Ca^{2+} sequestration by *Aspergillus* melanin inside the phagosome, which abrogates activation of Ca^{2+}-calmodulin (CaM) signaling to inhibit LAP [147].

Alveolar macrophages orchestrate a robust inflammatory response through the activation of PRRs and cytokine and chemokine production, which include key mediators of neutrophil recruitment such as macrophage inflammatory protein-2 (MIP-2/CXCL2) and CXCL1 [148]. Neutrophil recruitment is crucial to help alveolar macrophages in antifungal defense, namely when larger doses of conidia are present in the lung [135]. Moreover, conidia that escape macrophage killing start to germinate, forming germ tubes and hyphae which then penetrate through the alveolar surface [40]. Neutrophils can kill both germinating conidia and hyphae. Neutrophils bind and phagocytose swollen conidia to trigger the respiratory burst and degranulation. The size of the hyphae prevents phagocytosis, so direct contact with neutrophils can induce damaging oxidative and non-oxidative mechanisms, including NADPH oxidase-mediated generation of ROS, production of lactoferrin and the discharge of antimicrobial proteases by degranulation [14]. Another extracellular killing mechanism used by neutrophils against hyphae is the ROS-mediated release of neutrophil extracellular traps (NETs) consisting of nuclear DNA decorated with fungicidal proteins [149]. NETosis was found to be maximal against hyphae but reduced against resting and swollen conidia [149]. NET formation occurs both *in vitro* and *in vivo*, although it does not play a major role in

killing of *A. fumigatus* [149], suggesting that NETs may have a fungistatic effect and may prevent further spreading.

Furthermore, respiratory epithelial cells, i.e., bronchial and alveolar epithelial cells [23,34,150,151] and human peripheral blood monocytes [152], both classical and non-classical [153], have also been shown to participate in the innate immune response against *A. fumigatus*, besides the already well documented role of DCs [76,154].

1.7 Immunometabolism of fungal infection

In recent years, the identification of several factors and mechanisms related to the immune response has provided exciting developments to our understanding of the pathogenesis of fungal infections [20,155]. The reprogramming of cellular metabolism has recently emerged as a central mechanism through which the effector functions of immune cells are supported during host antifungal defense [156]. An improved understanding of the immunometabolic signatures that orchestrate antifungal immunity may therefore reveal new targets amenable to adjunctive host-directed therapies, which are currently limited to cytokines, monoclonal antibodies, or cellular immunotherapy [157]. In this section, we discuss recent findings on the immunometabolic signatures activated in response to fungal infection and highlight targetable pathways and mechanisms that show promising potential as adjuncts for host-directed therapies.

1.7.1 Metabolic regulation of the host-fungus interaction

Metabolism is a determining factor of immune cell function [158]. Upon infection, immune cells sense molecular patterns from pathogens and remodel their metabolic outputs beyond their normal energy requirements (Fig. 4). Different metabolites are used as signaling molecules, enzymatic cofactors, and substrates that support the activation of immune effector functions, including phagocytosis, cytokine production, cell surface receptor expression, antigen presentation, and the control of long-term responses. In turn, pathogens can sense the metabolites produced by activated immune cells and reshape their ligand repertoire to hide from or subvert the immune response [159]. These observations highlight the profound impact of coordinated metabolic networks on the outcome of the host-pathogen interaction.

Glucose metabolism of immune cells is at the center of antifungal immune responses, potentiating the production of proinflammatory cytokines and other inflammatory mediators, and ROS [156]. In the

context of fungal infections, this metabolic route in immune cells has been predominantly studied in response to *C. albicans* [160-164] but has also recently been shown to occur during infection with *A. fumigatus* [165] and *Cryptococcus gattii* [166]. Although glycolysis is often induced in a context of reduced oxidative phosphorylation, leading to the so-called Warburg effect [164], human monocytes challenged with *C. albicans* are nonetheless endowed with functional oxidative phosphorylation [161]. This implies that immunometabolic signatures vary in intensity and nature according to the microbial insult or the receptor involved [167]. Likewise, the metabolic remodeling in response to infection with *C. albicans* also depends on the fungal morphotype [161]. While monocytes stimulated with the yeast form rely on glycolysis and glutaminolysis to mount cytokine responses, hyphal stimulation primarily drives the activation of glycolysis. These divergent profiles are likely due to the variable expression of the β-glucan polysaccharide in the yeast and hyphal cell wall. In this regard, β-glucan masking was shown to be induced by lactate-mediated signals that control the expression of cell wall-related genes [168]. Moreover, by taking advantage of its efficient metabolic fitness, *C. albicans* exploits the terminal commitment of macrophages to glycolysis by competing for and depleting available glucose, ultimately leading to rapid cell death [164]. These findings depict crucial virulence traits from fungi that, by exploiting or subverting host metabolism, contribute to evasion from the immune system (Fig. 4).

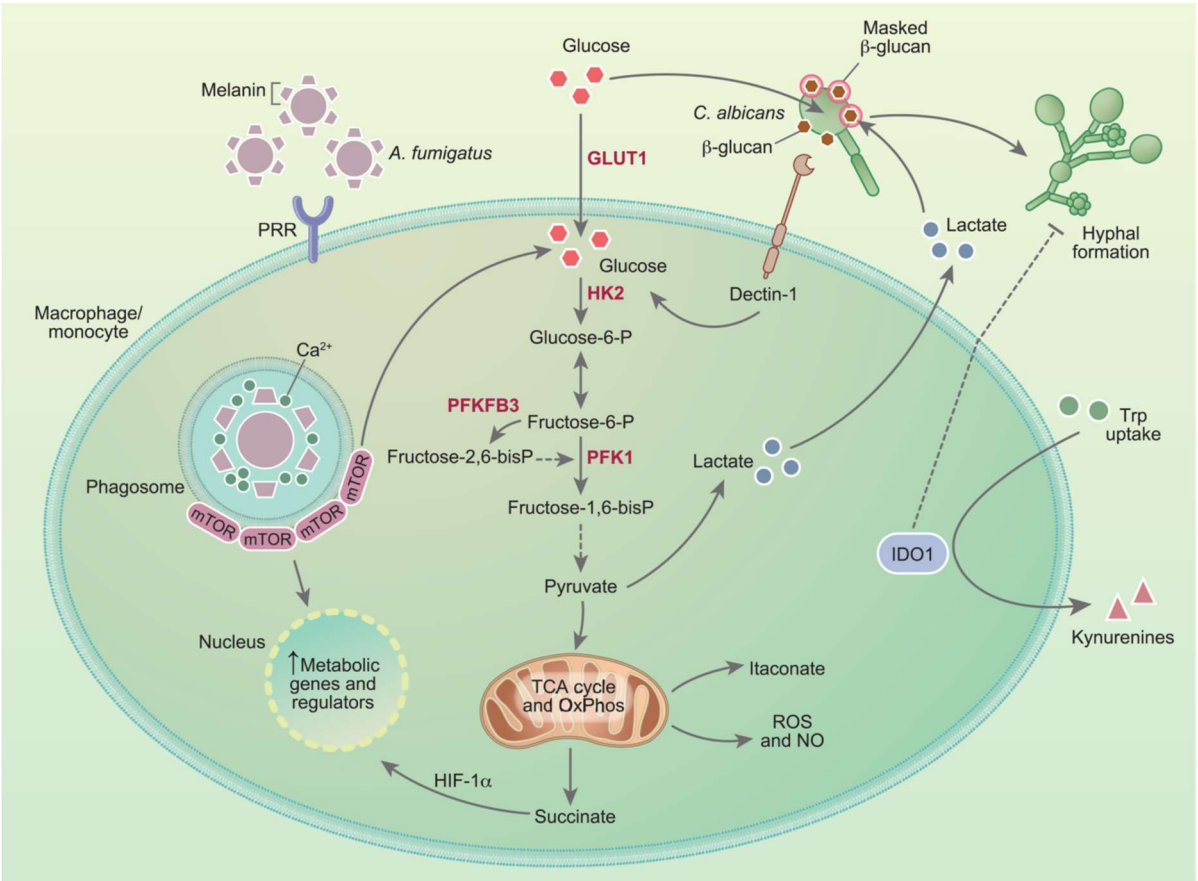

Figure 4. Metabolic reprogramming of myeloid cells in response to fungal infection. Recognition of fungal pathogens by pathogen recognition receptors (PRRs) is accompanied by the upregulation of glycolysis and production of lactate. In these conditions, the TCA cycle and oxidative phosphorylation (OxPhos) are often repressed, resulting in the accumulation of intermediates such as succinate and itaconate, and enhancing the generation of reactive oxygen and nitrogen species. In response to *C. albicans*, the activation of glycolysis is triggered by the recognition of β-glucan by dectin-1, a process that can be in turn exploited by the fungus through its ability to compete for glucose and ultimately promote macrophage death. Sensing of lactate secreted by immune cells also drives the masking of β-glucans in the fungal cell wall and immune evasion. The activation of glycolysis during infection with *A. fumigatus* is instead triggered by the release of melanin during germination. By sequestering calcium within the phagosome, melanin promotes the recruitment of mTOR which, in turn, mediates the activation of downstream metabolic genes and regulators. The catabolism of tryptophan (Trp) by the indoleamine-2,3-dioxygenase 1 (IDO1) enzyme also regulates antifungal immune responses and controls fungal morphology through its downstream catabolites, collectively referred to as kynurenines (Kyn).

In contrast to *C. albicans*, the expression of β-glucan in the cell wall of *A. fumigatus* appears instead to be largely dispensable to the activation of glycolysis in macrophages [165]. Instead, the phagosomal release of melanin from the surface of conidia was shown to regulate calcium-dependent signals leading to enhanced glycolysis through the activation of mammalian target of rapamycin (mTOR) and hypoxia-inducible factor-1α (HIF-1α) (Fig. 4). These findings are in line with the requirement for HIF-1α to the modulation of cytokine release by human dendritic cells upon infection with *A. fumigatus* [169] and the non-redundant role of HIF-1α in mouse models of aspergillosis [170]. Of note, the metabolic reprogramming induced by fungal melanin appears to occur regardless of its recently identified receptor MelLec [107]. Instead, the germination process associated with the active removal of melanin within the phagosome is required for host cells to rewire their metabolism. In support of this, germination has been shown to promote fungal clearance, as faster-growing CEA10-derived strains are cleared more efficiently *in vivo* than slower-growing Af293-derived strains [171]. This enhanced fungal elimination could thus be explained by cell wall rearrangements culminating with melanin release during germination and the activation of host glycolysis. Whatever the mechanism(s), the efficient regulation of glycolysis is required for resistance to aspergillosis in humans. This is illustrated by the recent finding that genetic variation in 6-phosphofructo-2-kinase/fructose-2,6-biphosphatase 3 (PFKFB3), a critical regulator of glucose metabolism, was found to impair antifungal effector functions of macrophages and predispose recipients of allogeneic hematopoietic stem-cell transplantation to the development of IPA [172]. PFKFB3 is

upregulated in bacterial infections and PFKFB3-driven glycolysis in macrophages is critical for antiviral defense [173], pinpointing this gene as a possible therapeutic target across infectious diseases. Moreover, the similar regulation of glycolysis in immune cells in response to different infectious agents [174] highlights the attractive possibility of exploiting genetic variants in metabolic genes and their effects on immunometabolic signatures as a tool to identify and stratify the patients most at risk of infectious diseases.

1.7.2 Immunoregulatory functions of host metabolites in fungal infection

The metabolic switch to glycolysis results in the accumulation of several intermediates of the tricarboxylic acid (TCA) cycle that act as signals to link metabolism and immunity. In recent years, the metabolite itaconate has been explored for its broad immunomodulatory properties. Activated myeloid cells display enhanced expression of the immune-responsive gene 1 (IRG1) mitochondrial enzyme, which catalyzes the decarboxylation of the TCA cycle intermediate *cis*-aconitate to itaconate [175]. The molecular mechanisms under control by itaconate vary, but the net function is thought to be anti-inflammatory. Itaconate inhibits the succinate dehydrogenase (SDH), which is both an enzyme of the TCA cycle and the complex II of the electron transport chain, leading to succinate accumulation and impaired mitochondrial respiration, and suppressing the production of inflammatory cytokines [176]. Moreover, itaconate enables the activation of the transcription factors NRF2 and ATF3, and the increased expression of downstream genes with antioxidant and anti-inflammatory properties, and the modulation of type I interferon responses [177].

Itaconate plays an important role across several infections, decreasing tissue injury in a mouse model of tuberculosis [178] and enhancing the bactericidal activity of macrophage-lineage cells in zebrafish [179]. During infection with the Zika virus, itaconate was found to alter the neuronal metabolism to suppress viral replication [180], indicating that its modulatory effects are not restricted to myeloid cells. The direct antimicrobial functions of itaconate are thought to rely largely on the inhibition of isocitrate lyase, an enzyme of the glyoxylate shunt that is essential for growth under glucose-poor conditions, and that is required for the virulence of several pathogens, including *C. albicans* [178,181,182]. In contrast, bacteria often harbor genes involved in itaconate degradation, allowing them to counter the inhibitory mechanisms deployed by itaconate and survive inside the host [183]. Moreover, pathogens such as *Staphylococcus aureus* and *Pseudomonas aeruginosa* were recently shown to adapt to itaconate-rich

environments and use this metabolite as a carbon source for the production of biofilms, contributing to the establishment and progression of infection [184,185]. The therapeutic administration of inhaled itaconate has been shown to improve pulmonary fibrosis in mice [186], a disease that often develops due to exposure to airborne fungi [187] and that, in turn, further potentiates the development of respiratory fungal infections [188]. Whether itaconate plays a role in the immune response to fungal pathogens other than *C. albicans* remains to be explored, although the metabolism of acetate, a carbon source metabolized also through the glyoxylate shunt, impacts virulence traits and the pathogenicity of *A. fumigatus* [189].

In response to inflammatory stimuli, macrophages accumulate succinate that, in turn, acts as a proinflammatory redox signal to the transcription factor HIF-1α and the production of IL-1β [190]. Succinate oxidation also potentiates the generation of mitochondrial ROS [191], which represent critical effectors required for antifungal immunity [142]. Indeed, the balance between the production of ROS and reactive nitrogen species by the host and the fungal stress response is a key feature of the host-fungus interaction [192]. The production of nitric oxide (NO) is modulated by the metabolism of amino acids, which also plays an important role in macrophage polarization [193]. In this regard, C*. albicans* was shown to upregulate arginase activity and limit NO production in macrophages via chitin-mediated signals, skewing macrophage polarization towards an anti-inflammatory profile which ultimately restrains antimicrobial functions and mediates fungal survival [194]. In contrast, granulocyte-mediated clearance of *A. fumigatus* occurred independently of arginine availability [195], a finding that supports distinct pathogen-driven metabolic strategies to subvert antifungal immune responses.

The catabolism of tryptophan via the activity of IDO1 also represents an essential mechanism in the modulation of antifungal immunity [196]. IDO1 acts as a physiological checkpoint that controls immune homeostasis through its downstream catabolites – referred to as kynurenines – and provides the host with adequate protective immune mechanisms [197]. In particular, IDO1 activity induces differentiation of T regulatory cells, while inhibiting the development of Th17 cells, thus playing a central role in cell lineage commitment across experimental fungal infections in the context of detrimental inflammation, including CGD and cystic fibrosis [198,199]. The airway expression of IDO1 was also found to inhibit pathogenic T cells in response to fungal antigens [200], a finding consistent with the requirement for IDO1 activity in the non-hematopoietic cell compartment for protective tolerance against *A. fumigatus* [118]. Tryptophan-derived metabolites may also be produced through the activity of bacterial communities in the intestinal microbiota, which establishes a highly tolerant immunological

microenvironment allowing the commensalism of *C. albicans* in the gut [201]. Of note, IDO1 activity was found to be required to inhibit the yeast-to-hyphae transition of *C. albicans* [202].

The expression and function of IDO1 are influenced by common human genetic variation [203]. Accordingly, single nucleotide polymorphisms in *IDO1* that impair its expression were found to influence the risk of developing recurrent vulvovaginal candidiasis (RVVC) [204], as well as aspergillosis in patients with cystic fibrosis and recipients of allogeneic hematopoietic stem-cell transplantation [205]. Remarkably, *A. fumigatus* was recently found to harbor genes encoding fungal IDO1-like enzymes and their deletion resulted in increased virulence in a mouse model of aspergillosis [206], thus highlighting the crucial role of the interplay between fungal and host tryptophan metabolic routes in shaping host-fungus interactions. Collectively, the bulk of available data suggests that drugs capable of potentiating IDO1 expression and activity may represent valuable therapeutic tools and that IDO1-based immunotherapeutics could be more effective if tailored to the genetic profile of individual patients [207].

1.7.3 Trained immunity as a therapeutic strategy to rescue immune impairments

A growing body of evidence has revealed alterations of the innate immune system that potentiate responses and ultimately generate characteristics of memory [208]. Trained immunity, a *de facto* innate immune memory, allows for a long-lasting and broad-spectrum resistance to pathogens. In this context, macrophage exposure to the vaccine Bacillus Calmette-Guérin (BCG), fungal β-glucan, or oxidized low-density lipoprotein enhanced effector functions toward subsequent heterologous stimuli, while it conferred protection against secondary lethal infections in mouse models, namely by *C. albicans* [209-211].

Trained cells harbor altered metabolic programs that sustain the rewiring of the epigenetic landscape and allow for enhanced immune effector functions. Trained macrophages rely on a highly energetic metabolism characterized by enhanced glycolysis, TCA cycle, and oxidative phosphorylation [209]. In accordance, the mTOR/HIF-1α axis was demonstrated to mediate the metabolic and functional reprogramming of β-glucan-trained macrophages [160]. Cholesterol biosynthesis is also a central pathway for trained immunity as shown by its induction by the intermediate mevalonate [212]. Trained immunity is also conferred by the epigenetic and metabolic reprogramming of hematopoietic stem cells and their skewing towards myelopoiesis [213,214]. The broad clinical relevance of this molecular process was emphasized in a recent randomized clinical trial that showed that BCG vaccination of elderly individuals decreased the incidence of new respiratory infections [215]. The induction of trained immunity

thus represents an interesting tool to harness the potential of innate immunity in patients with immune impairments (Fig. 5). However, increasing immune responses may be particularly challenging in selected pathologies. Not only can immune cells be epigenetically encoded to dampen responses to inflammatory stimuli, but also the decreased number of circulating immune cells might not be sufficient even if their activity is potentiated.

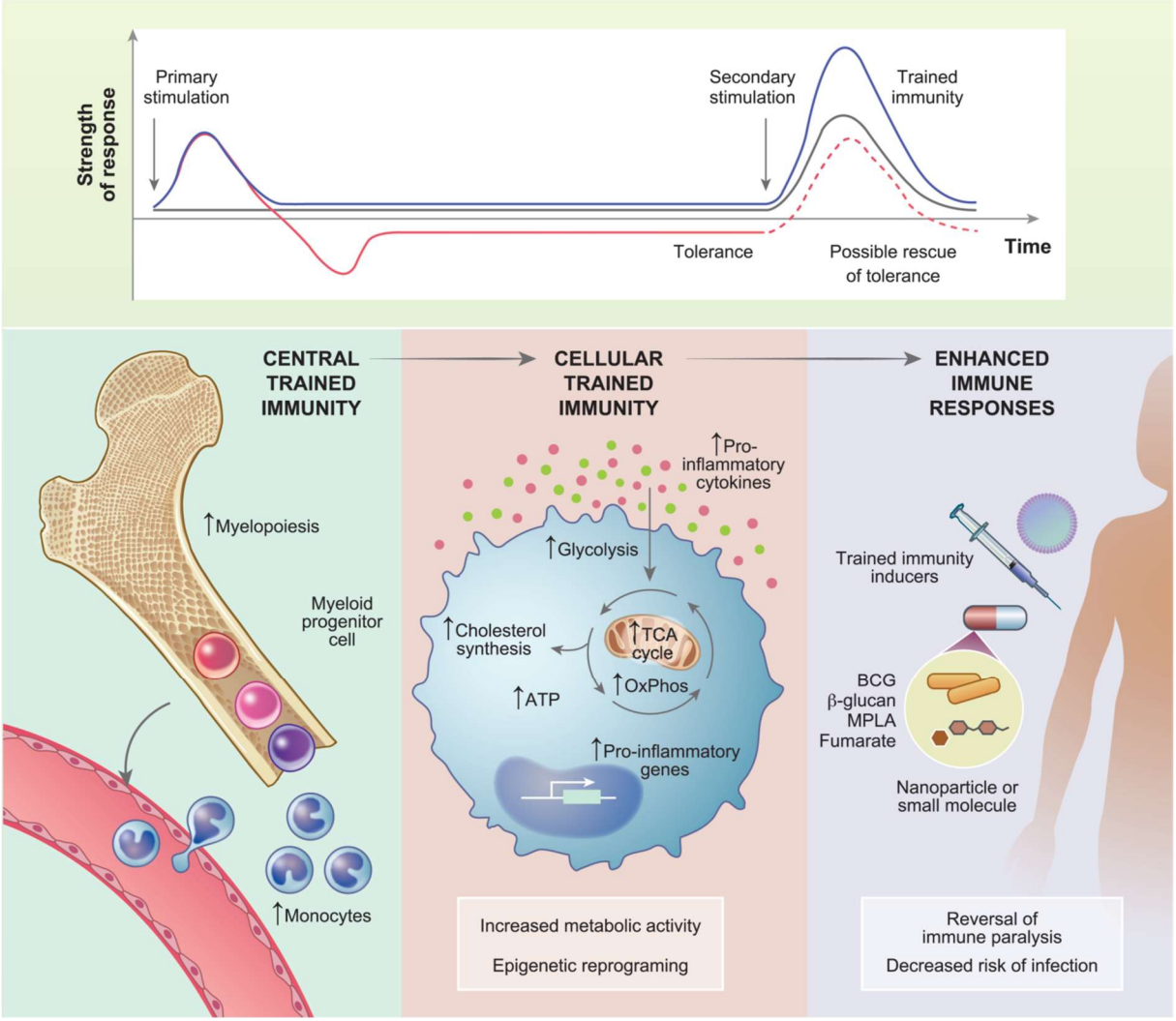

Figure 5. Trained immunity as a tool to potentiate host defense. Microbial or endogenous stimuli activate innate immune cells. Depending on the dose or stimuli, innate immune function may be increased when encountering a secondary stimulation (trained immunity) or cells may become unresponsive or anti-inflammatory (tolerance). Trained immunity confers long-term protection thought the myelopoietic skewing of hematopoietic stem cells, giving rise to monocytes with enhanced effector functions. They rely on metabolic changes, such as increased glycolysis and OxPhos, which supports epigenetic rewiring that promotes the expression of proinflammatory genes culminating in the increased secretion of cytokines. Thus, trained immunity inducers may be an attractive

therapeutic tool to revert tolerance, possibly rescuing states of immune paralysis in sepsis and decreasing the risk of secondary infections.

In patients under intensive care, fungal infections often give rise to sepsis, which involves the hyperactivation of the immune system followed by tolerance or immune paralysis. Immune paralysis also comprehends epigenetic and metabolic changes [216] but, in contrast to trained immunity programs, these changes ultimately increase the susceptibility to secondary infections [70,217]. Exposure to β-glucan restored the responsive phenotype of human monocytes tolerized with LPS, a finding that was confirmed in a human endotoxemia model [218]. The integrity of the TCA cycle in LPS-stimulated macrophages was maintained by β-glucan through the inhibition of *IRG1* expression [219]. Of note, while the anti-inflammatory properties of itaconate make it an interesting target for the reversal of immune paralysis, at the same time, itaconate may also represent a valuable therapeutic tool to decrease detrimental and exacerbated antifungal immune responses.

Another functional feature of patients with sepsis regards the defective activation of LAP, a non-canonical autophagy pathway that plays a non-redundant role in the resistance to infection with *A. fumigatus* [144,146,147]. Recently, monocytes from patients with sepsis were found to display a defective activation of LAP, which was reversed by the administration of recombinant IL-6 [220]. It is thus tempting to consider the modulation of LAP as a promising immunotherapeutic intervention in sepsis, particularly given the ability of β-glucan to increase the expression of Rubicon [221], a critical effector molecule of LAP. The induction of trained immunity could thus also represent a promising avenue for the treatment of fungal sepsis.

Several trained immunity inducers are already under clinical use. For example, muramyl tripeptide is employed in the treatment of osteosarcoma and BCG is in clinical use for bladder cancer [222]. Notably, trained immunity was found to be elicited by dimethyl fumarate [223], a drug currently under use for the management of multiple sclerosis [224]. Also approved for human use is the vaccine adjuvant and TLR4 agonist monophosphoryl lipid A (MPLA). MPLA has been shown to not only improve resistance to several pathogens, including *C. albicans* [225] but also to induce the metabolic rewiring of macrophages characterized by a sustained increase in glycolysis and oxidative phosphorylation [225] in a similar manner to other inducers of trained immunity. Collectively, these molecules represent attractive candidates for repurposing toward the induction of trained immunity in immunocompromised patients.

1.7.4 Targeting metabolic homeostasis at the host-fungus interface

During infection, the host and the pathogen compete for limiting levels of nutrients, such as glucose. It is thus not surprising that a glucose-rich diet has been found to improve the survival of mice in a model of disseminated candidiasis [164]. Importantly, induction of trained immunity may also prevent macrophage death due to glucose starvation. Trained macrophages not only present increased glycolysis but also display increased oxidative phosphorylation, and thus trained cells might not be committed to glycolysis for energy production. A benefit of the enhanced glucose uptake is also envisaged in uremic individuals, who exhibit a hyperinflammatory state and are at increased risk of developing fungal infections. Uremia downregulates the phosphatidylinositol-4,5-bisphosphate 3-kinase (PI3K)/AKT pathway, causing hyperactivation of the glycogen synthase kinase 3β (GSK3β) and thus inhibiting glucose uptake [226]. Accordingly, the pharmacological blockade of GSK3β using the specific inhibitor SB415286 or lithium chloride restored glucose uptake, but also ROS production and the candidacidal activity of neutrophils, in a mouse model of kidney disease with systemic fungal infection. The preclinical efficacy of GSK3β inhibition was confirmed by the rescue of the fungal killing capacity in neutrophils isolated from hemodialysis patients. Nutritional supplementation was also protective against influenza infection and viral sepsis, but it was instead detrimental in bacterial sepsis by *Listeria monocytogenes* [227]. Therefore, although favoring glucose metabolism may represent a promising therapeutic possibility, the opposing effects of fasting metabolism on different infections suggest its utility on a pathogen-dependent basis.

Exacerbated immune responses to infection may also drive fungal sepsis. In this scenario, it might be advantageous to combine antifungal agents with inhibitors of glucose uptake and glycolysis to ultimately decrease inflammation. In this regard, the glucose analog 2-deoxy-D-glucose (2-DG) that blocks glucose metabolism was found to decrease cytokine production in mouse models of infection with *C. albicans* [161] and *A. fumigatus* [165]. Moreover, metformin, a widely used drug in the treatment of type 2 diabetes as a glucose-lowering agent, which activates the AMP kinase and inhibits mTOR, or the mTOR blockade itself, decreased cytokine production and survival in experimental disseminated candidiasis [161,164]. Other inhibitors of glucose uptake or glycolysis, such as the HIV-protease inhibitor ritonavir [228], the pyruvate dehydrogenase kinase inhibitor dichloroacetate [229], and the small-molecule competitive lactate dehydrogenase inhibitor FX11 [230] might also be of future interest in the context of fungal infections.

The rewiring of metabolic pathways may consume or compartmentalize metabolites, restricting pathogen access to nutrients, as depicted for glucose accessibility during infection. Interestingly, the pulmonary niche was found to impose a decreased responsiveness of alveolar macrophages, by impairing glycolysis and promoting pathways of lipid metabolism [231]. These findings highlight the crucial role of the tissue milieu for both immune responses and the virulence of pathogens, including fungi. Moreover, the metabolic profiles differ at different tissues, providing substrates that regulate not only fungal fitness, but also immune cell function and their interaction. Another example of compartmentalization derives from anemia of inflammation, which arises due to infections or autoimmune disorders that promote a proinflammatory state [232]. Host and invading pathogens compete for iron availability, as it is an essential co-factor for several proteins relevant for a myriad of processes, such as DNA replication and mitochondrial function. Iron is especially relevant for highly proliferative cells, and lack of iron blunts T and B cell responses [233]. Systemic immune activation of the host induces changes in iron intestinal absorption, trafficking, and cellular retention, thus decreasing iron availability to pathogens. To counter this, fungi produce siderophores that capture iron from host iron-binding proteins in human serum, while restricting iron access to host immune cells and modulating their activity [234]. Accordingly, elevated circulating iron levels have been associated with an increased risk of systemic fungal infection in hematological patients [235]. Moreover, the iron chelator deferiprone was shown to decrease fungal burden in a mouse model of cornea infection by *A. fumigatus* [236] and improve survival of mice infected with the mucormycete *Rhizopus oryzae* [138]. Ciclopirox, a potent topical antifungal agent, exerts its effects partly by chelating polyvalent metal cations such as iron [237]. Inhibition of fungal iron uptake, namely via targeted iron chelation therapies, represents thus an interesting therapeutic strategy.

Iron is not only a limiting nutrient for pathogen virulence [238,239], but it also plays a regulatory role in host immune responses [240]. For example, iron-loaded macrophages exhibited a proinflammatory phenotype in diverse disease contexts, such as spinal cord injury [241], multiple sclerosis [242], and cancer [243]. On the other hand, acute iron chelation promotes an anti-inflammatory shift, as seen by the decrease in LPS-induced cytokine production by human macrophages [244]. This acute iron deprivation also enhanced glycolysis and lipid droplet formation while it downregulated oxidative phosphorylation, possibly due to the disruption of the iron-containing complex II of the respiratory chain. Interestingly, labile heme induces a trained immunity program that confers protection against LPS-induced sepsis in mice [245]. Thus, the targeted modulation of iron accessibility, be it by iron chelation

when a proinflammatory phenotype is maladaptive, or by the delivery of iron in nanoparticles or heme to promote inflammation [246] is an attractive avenue to tailor immune metabolism and function.

1.8 The genetic basis of immune responses to fungal infection

Fungal infections are characterized by significant interindividual variability in their onset, progression, and outcome. While virulence factors and mechanisms of adaptation of the pathogen contribute to infection, a dominant role for heritable host factors has also been emphasized [247-249]. Our current knowledge of the genetic basis of fungal infection has stemmed primarily from the investigation of patients with rare monogenic defects and from cohort-based studies that identified common single nucleotide polymorphisms (SNPs) associated with infection [250]. In addition, fundamental studies comparing profiles of susceptibility between inbred mouse strains have provided support to the concept of genetic susceptibility to fungal infection [251].

An in-depth understanding of the molecular mechanisms involved in the genetic control of antifungal immunity is therefore expected to generate unprecedented opportunities for patient-tailored and more efficient management of fungal infection [69]. In this section, we address recent advances in our understanding of the genetic factors that influence antifungal immune responses. In particular, we discuss insights from candidate gene studies and genome-wide approaches performed in different experimental and clinical models, and how these contribute to generating a common framework for human susceptibility to fungal infection and unveiling novel targets and pathways amenable to clinical intervention.

1.8.1 Candidate gene approaches to study complex susceptibility to fungal infections

Family-based approaches have been historically used to identify rare mutations that confer monogenic forms of predisposition to fungal infection. Monogenic patterns of susceptibility to fungal infection are covered in several excellent recent reviews [250,252] and will not be addressed in detail here. We will instead focus the discussion on the most recent and robust advances in our understanding of the common genetic factors that influence antifungal immune responses.

1.8.2 PRRs

Pathogens have long been recognized as important sources of evolutionary pressure [253]. Immune-related genes are consequently the most variable genes in the human genome, suggesting an evolutionary advantage of a diversified immune response. It is therefore not surprising that genetic variation in PRRs has been described to influence susceptibility to infection by a wide range of fungal pathogens [247]. This concept has emerged primarily from association studies of genes selected for their biological plausibility based on evidence from preclinical models. One of the early breakthroughs in the field was provided by the association of a haplotype consisting of the coding variants rs4986790 (D299G) and rs2986791 (T399I) in TLR4 with an increased risk of IPA after allogeneic hematopoietic stem-cell transplantation [254]. The association with IPA was validated in independent transplant cohorts [255,256], but also in immunocompetent individuals suffering from chronic pulmonary aspergillosis [257]. However, the precise mechanisms whereby TLR4 variants compromise antifungal immune responses remain unknown, particularly since no fungal ligands or DAMPs released during infection able to activate TLR4 have been identified to date.

Additional relevant studies have also highlighted genetic variation in TLRs other than TLR4 as a critical risk factor for fungal infection. The unexpected discovery that TLR3, a canonical receptor for viral double-stranded RNA, also participated in the recognition of *A. fumigatus* was corroborated by the association of the regulatory variant rs3775296 in TLR3 with the risk of IPA [117]. Mechanistically, cross-presenting DCs from variant carriers displayed an impaired expression of TLR3 and recognition of fungal RNA, which ultimately resulted in defective priming of memory $CD8^+$ T cell responses. Therefore, besides influencing fungal sensing and innate immune responses, genetic defects in TLRs (and other PRRs) may also compromise the efficient activation of protective adaptive immunity. In the context of candidemia, several genetic variants in TLR1 were described as important risk factors [258]. Although the exact mechanisms whereby these variants influence the risk of infection remains elusive, the non-synonymous variant rs5743618 (I602S) in TLR1 was shown to impair the trafficking of the receptor to the cell surface and restrain NF-κB activation and cytokine production in response to TLR1 agonists [259].

Considering their central role in the regulation of antifungal immunity, the impact of genetic variation in CLRs in susceptibility to fungal infection has been widely studied. The critical role for genetic variability of dectin-1 (CLEC7A) in antifungal immunity was initially demonstrated in patients with recurrent fungal infections carrying the early stop codon polymorphism rs16910526 (Y238X) [260]. This SNP truncates dectin-1 at the carbohydrate recognition domain and leads to impaired surface expression of the receptor

and defective production of cytokines by myeloid cells, particularly IL-17, in response to stimulation with *C. albicans*. As a result, Y238X has been implicated in mucosal and gastrointestinal fungal colonization [204,261], but not in candidemia [262]. The non-synonymous variant rs16910527 (I223S) in dectin-1 was instead associated with lower levels of IFN-γ and an increased risk of oropharyngeal candidiasis in HIV patients [263]. This suggests that different pathogenetic variations in dectin-1 with specific structural consequences may elicit distinct susceptibility mechanisms and fungal disease entities.

The Y238X SNP in dectin-1 was also reported to enhance the risk of IPA after stem-cell transplantation, when present in either the donor or patient genomes [92], a model of association that was independently validated [264]. These findings highlight the requisite role for dectin-1 function in both immune and non-immune cell types to promote protective antifungal immunity. Additional regulatory variants in dectin-1, but also dectin-2 and DC-SIGN (CD209), were likewise associated with the development of IPA in hematological patients [265,266]. Because the cellular localization of different dectin-1 isoforms dictates the signaling quality of antifungal immunity [267,268], this variability may represent another potential mechanism whereby the Y238X SNP predisposes to infection. Moreover, recognition of β-glucan mediated by dectin-1 has been demonstrated to confer innate immune memory to infection by regulating selected pathways of cellular metabolism [160,223]. It is thus plausible that Y238X and other dectin-1 variants predispose patients to infection by impairing the induction of "natural" trained immunity emerging from our constant exposure to fungi.

The relevance of CLRs to antifungal immunity is further illustrated by the presence of mutations in the adaptor molecule CARD9 in patients suffering from mucocutaneous fungal infections [269]. Nonetheless, the fungicidal defect of neutrophils from CARD9-deficient patients is independent of dectin-1 and NADPH oxidase activity, a finding that might explain, at least partly, the variable clinical presentation of fungal infection in patients with dectin-1 and CARD9 deficiency, and CGD [270]. Rare mutations in CARD9 have also been found to predispose patients to extrapulmonary aspergillosis as the result of a defective accumulation of neutrophils in infected tissues [271]. More recently, studies performed in knock-in mice expressing the common rs4077515 (S12N) SNP in CARD9 revealed a pathogenic role in the activation of NF-κB subunit RelB and the production of IL-5 by alveolar macrophages, which in turn promoted the recruitment of eosinophils that fostered Th2 responses and the development of ABPA [272].

The MelLec (CLEC1A) receptor was recently identified as the receptor for DHN-melanin in melanized fungi, such as *A. fumigatus* [107]. The functional relevance of human MelLec was confirmed by the association of the non-synonymous rs2306894 (G26A) SNP in CLEC1A with the risk of IPA [107].

Because G26A affects the cytoplasmic tail of MelLec and myeloid cells from carriers displayed a broad defect in fungal-induced cytokine production, G26A was suggested to influence intracellular signal transduction rather than recognition of DHN-melanin. Despite its protective role in IPA, MelLec was unexpectedly found to exacerbate pulmonary inflammation in experimental fungal-mediated allergy, by promoting cellular influx and the production of cytokines and chemokines, together with the development of Th17 cells [273]. Thus, while MelLec is required to control pulmonary fungal burden, the proinflammatory responses mediated by this receptor have a detrimental impact on allergy.

Until recently, the function of NOD-like receptors such as NOD1 and NOD2 in antifungal immunity was poorly understood. Genetic analyses revealed that the donor rs2066842 (P268S) SNP in NOD2 was associated with protection from IPA in the corresponding stem-cell transplant recipient [274]. This protective phenotype was correlated with an enhanced ability of mononuclear cells from P268S carriers to phagocytose and clear fungi and, likewise, NOD2-deficient mice were more resistant to experimental aspergillosis. Collectively, the detrimental impact of NOD2 activation in IPA highlights the blockade of NOD2-mediated signals as potential antifungal adjuvant therapy.

1.8.3 Soluble recognition molecules

Besides PRRs, several soluble mediators interact with and bind to microbial polysaccharides without transducing intracellular signals and function as opsonins to facilitate phagocytosis [74]. Among these, mannose-binding lectin (MBL) binds carbohydrate patterns from pathogens and activates the lectin pathway of the complement system. Several studies have disclosed common genetic variation in MBL to regulate its expression levels, functional activity, or both [275]. Except for cryptococcosis in HIV-uninfected patients [276], the contribution of genetic variation in MBL to invasive disease has not been addressed, although the levels of circulating protein were found to vary significantly during IPA [277], invasive candidiasis [278], and pneumonia by *Pneumocystis jirovecii* [279]. Likewise, SNPs in the triggering receptor expressed on myeloid cells 1 (TREM1) were found to influence the levels of soluble TREM1 as well as TREM1-mediated cytokine production in response to stimulation with *A. fumigatus* [280], despite no evidence for a direct association with human infection reported thus far.

The long pentraxin PTX3 represents another humoral immune mediator that binds to microbial moieties from a wide range of microorganisms, including bacteria, viruses, and fungi [281]. In line with an essential role in antifungal immunity in mouse models of infection [129], a haplotype in human PTX3 including the coding rs3816527 (D48A) SNP was identified as a major risk factor for IPA in recipients of

stem-cell transplant [264,282], but also in other clinical settings, including SOT [283,284] and COPD [285]. PTX3 SNPs were found to impair the phagocytic activity and fungal killing by neutrophils [282], a phenotype that was corroborated by the lack of association with IPA in patients with severe neutropenia [282,286]. Importantly, the efficacy of neutrophil effector functions was restored *in vitro* upon rescuing the genetic defect with recombinant PTX3 [282].

PTX3 has been shown to bind to myeloid differentiation protein 2 (MD-2), an adapter of the TLR4 signaling complex, to regulate cytokine production and promote protective immunity to experimental aspergillosis [287]. PTX3 SNPs were also shown to influence the levels of alveolar cytokines in hematological patients with IPA [288], a finding in line with an immune regulatory role of PTX3 in response to fungal infection. Accordingly, PTX3 SNPs were suggested to impact the ability of neutrophils to regulate B-cell function, including class switching, plasmablast expansion, and antibody production [289]. Although clinical data is so far lacking, the observations highlighted above support the potential applicability of PTX3 in novel therapeutic approaches for the treatment or prevention of IPA in patients at-risk [290].

Serum amyloid P component (also known as PTX2 and encoded by the *APCS* gene) is a fluid phase pattern recognition molecule of the pentraxin family that was recently demonstrated to bind to conidia of *A. fumigatus* and promote the activation of the complement cascade and phagocytosis by neutrophils [131]. In line with its role in experimental aspergillosis, SNPs in APCS were found to confer an increased risk of IPA. Given the overlapping functions of these pentraxins in antifungal immunity, the combined carriage of PTX3 and APCS SNPs might underlie an added risk for IPA than the single defects alone, a hypothesis that requires confirmation in larger patient cohorts.

1.8.4 Other genes involved in antifungal immune responses

Several associations between genetic variants in cytokines and chemokines and susceptibility to fungal infection have been reported [249]. One relevant example regards the involvement of the promoter rs1800896 SNP in the immunoregulatory cytokine IL-10 in the development of IPA in hematological patients undergoing chemotherapy [291] and stem-cell transplant recipients [292]. The latter association was validated in a large, two-stage genetic study which demonstrated also that this SNP contributed to risk, at least in part, by promoting a shift towards an anti-inflammatory cytokine profile in patients carrying high-producing genotypes for IL-10 [293]. This finding is in line with the observation that PBMCs from patients with IPA display a marked expansion of *A. fumigatus*-specific T cells that produce IL-10 [294].

Genetic variation in IL-1β and beta-defensin 1 (DEFB1) was also associated with susceptibility to mold infection after SOT through altered production of monocyte-derived proinflammatory cytokines [295]. In addition, the promoter rs2069705 SNP in IFN-γ was found to confer resistance to IPA through a mechanism that involved the enhanced fungicidal activity of macrophages [296]. Recent work based on homozygosity mapping of blastomycosis patients from endemic areas in the US implicated a block of variants near IL-6 [297]. Endemic carriers were found to display impaired IL-6 and Th17 responses compared to European donors, a finding consistent with population differences in IL-6-mediated responses and T cell development. Cellular immunity to fungal infection, particularly in the context of RVVC, was also shown to be affected by genetic variation in IL-22 [204]. In this case, the risk variant was associated with decreased production of IL-22 and downstream defects in calprotectin levels in patients.

As for chemokines, a haplotype in C-X-C motif chemokine ligand 10 (CXCL10) was associated with the risk for IPA [298]. Dendritic cells from carriers of the risk variant exhibited a defect in CXCL10 expression and, importantly, IPA survivors displayed higher CXCL10 levels compared to non-infected patients. Of note, and in line with the marked susceptibility of C-X-C motif chemokine receptor 1 (CXCR1)-deficient mice to systemic candidiasis, the rs2234671 (S276T) SNP in CXCR1 was found to increase the risk of candidemia by impairing neutrophil degranulation and fungal killing [299]. More recently, in a two-stage association study, SNPs in the C-X3-C motif chemokine receptor 1 (CX3CR1) receptor were also associated with the risk of developing IPA [300]. Functional studies revealed that macrophages from carriers of the risk variant displayed a deregulated immune response to fungal infection.

Besides the early recognition of fungal pathogens, innate immune cells can activate molecular functions that allow them to eliminate the invading fungus. Among these, the specialized autophagy pathway LAP was found to be essential for fungal killing [32]. In turn, fungal melanin was identified as a major virulence factor capable of blocking this effector mechanism [31]. Given its central role in antifungal immunity, genetic variation in molecular players that regulate the activation of LAP was reported to influence the susceptibility of IPA. The rs12885713 SNP in the core promoter of calmodulin 1 (CALM1) was found to increase the risk of IPA, an association that was supported by the requirement for calcium signals and calmodulin recruitment to the phagosome – and that was blocked by fungal melanin – in the regulation of several molecular components of LAP, including Rubicon and the NADPH oxidase NOX2 [147]. Inhibition of calmodulin activity by fungal melanin was also found to impair flotillin function and lipid raft formation, required for the maturation of functional phagolysosomes against fungal infection [301]. Likewise, the intronic rs3094127 SNP in flotillin 1 (FLOT1) increased the risk of IPA by affecting

the production of monocyte-derived cytokines, although no effects on phagolysosome function and fungal clearance were reported.

The reprogramming of cellular metabolism represents another mechanism whereby innate immune cells promote protective antifungal immunity [164,165]. Therefore, several candidates involved in cellular metabolism have emerged with regards to susceptibility to fungal infection. For example, a SNP in cystathionine γ-lyase (CTH) was found to cause a reduction in cellular persulfidation, a process required for antifungal effector functions of lung resident cells, and promote an increased risk of IPA. Importantly, the levels of host persulfidation determined the levels of fungal persulfidation, reflecting a host-pathogen functional correlation and highlighting the crucial role of the interplay between fungal and host sulfur metabolic routes in shaping host-fungus interactions.

The catabolism of tryptophan via the activity of IDO1 also denotes an essential metabolic pathway in the modulation of antifungal immunity [201]. The expression and function of IDO1 are influenced by common genetic variation [203]. Accordingly, SNPs in IDO1 were found to influence the risk of developing RVVC [204], as well as aspergillosis in patients with cystic fibrosis and stem-cell transplant recipients [205]. Collectively, the available data suggest the need for evaluating interindividual variability in immunometabolic cell function in the assessment of the performance of immune-based diagnostic and therapeutic approaches for fungal infection [302].

1.8.5 Genome-wide association studies of fungal infection

As discussed above, many studies over the past decade have implicated human genetic variation in the development of fungal infection, particularly in individuals with predisposing clinical conditions. With a few exceptions, however, these studies involved small patient cohorts from single centers and addressed candidate genes emerging from previous preclinical knowledge without considering the full complexity of the human genome. Recent advances in sequencing platforms and imputation tools have allowed the generation of high-resolution maps of human genetic variation, and have opened unique possibilities for a detailed understanding of the causative alleles and the molecular mechanisms whereby genetic variants influence the immune response and the risk of fungal infection. For example, whole-genome and whole-exome sequencing are the most widely used unbiased approaches to study rare monogenic defects associated with susceptibility to fungal infections. In the context of complex disease, exome sequencing has also been applied to a leukemic patient with mucormycosis and revealed the presence of several

putative risk-associated variants in genes such as *PTX3*, *TLR6*, and *NOD2* [303]. These studies demonstrate unbiased genome-wide approaches as promising and affordable tools to discover novel causative mutations and polymorphisms in small numbers of individuals or even single patients.

By resorting to arrays that contain millions of genetic variants, the comparison of patient and matched control genomes through genome-wide association studies (GWAS) has driven the initial unbiased efforts to identify variants associated with fungal infection. The first example was provided by a study in which the genome of children with either frequent or occasional infection with *Trichophyton tonsurans* was sequenced, with several genes involved in leukocyte function, remodeling of extracellular matrix and wound repair, and cutaneous permeability being found to account for over 60% of the variability in infection rates [304]. Another GWAS based on the use of the Immunochip SNP array identified three new susceptibility loci for candidemia, namely CD58, late cornified envelope 4A (LCE4A)-C1orf68, and T cell activation RhoGTPase activating protein (TAGAP) [305]. Functional analysis of the implicated genes and variants using in vitro and mouse models of infection confirmed their role in antifungal effector functions, including cytokine production and inhibition of fungal germination. Of note, these markers overlapped with other immune-mediated diseases besides candidemia, suggesting that the genetic architecture of autoimmune diseases in modern human populations may have been evolutionarily driven by exposure to pathogens. More recently, a GWAS of volunteers from the 23andMe database identified significant associations between yeast infection and variants downstream of protein kinase C eta type (PRKCH), and within desmoglein 1 (DSG1) and C14orf177 [306]. Although African populations are underrepresented in studies of genetic susceptibility, a GWAS of cryptococcosis in HIV patients of African descent identified several loci upstream of the macrophage colony-stimulating factor (CSF1) that were significantly associated with susceptibility to cryptococcosis [307].

1.8.6 Understanding the genetic basis of antifungal immunity through functional genomics

Given the complexity of the host-fungus interaction, conventional experimental approaches to study individual molecular components of the host or the pathogen do not allow a holistic interpretation of the mechanisms involved in the interaction and that underlie disease pathogenesis. Genome-wide approaches can thus be combined with datasets from other omics platforms, such as transcriptomics, proteomics, epigenomics, and metabolomics, to prioritize novel infection-associated genes, pathways,

and cell types [308]. In this regard, functional genomics has been demonstrated as a powerful tool for a multilayered study of the genetics of complex diseases, including fungal infections (Fig. 6).

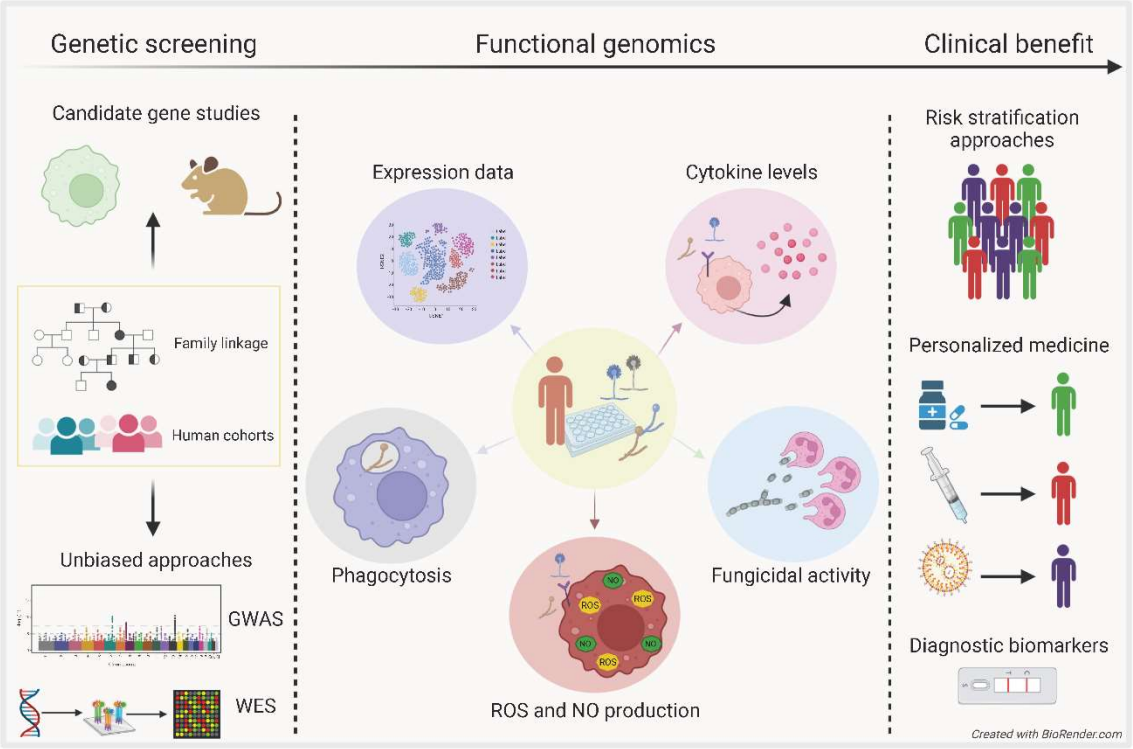

Figure 6. Candidate gene and unbiased research methodologies, and their integration into functional genomics approaches to foster the development of novel strategies of personalized medicine to treat or prevent fungal infections. GWAS, genome-wide association studies; WES, whole-exome sequencing; ROS, reactive oxygen species; NO, nitric oxide.

Genome-wide data is typically considered to provide a "static" overview of genetic variation. However, physiological responses to fungal infection require the coordinated regulation of gene expression and function [309]. These molecular events vary markedly between individuals and influence phenotypes such as protein levels, cell morphology and function, and immunity to infection. Significant efforts have been made in mapping functional traits to the underlying genetic sequence as a quantitative trait and identifying quantitative trait loci (QTLs) [310]. QTL mapping represents therefore a powerful strategy to enable critical insights into the genomic landscape and generate functional maps useful for the interpretation of genetic variants typically emerging from GWAS datasets. This is particularly useful for non-Mendelian immune and infectious disease phenotypes where the interaction between polygenic variants and environmental or clinical factors is required for the manifestation of the disease (as is the case of fungal infection).

The integration of genomic and transcriptomic data from human immune cells stimulated with *C. albicans* revealed a critical role for the type I IFN signaling pathway in antifungal host defense [311]. Accordingly, genetic variants in type I IFN genes were found to predispose critically ill patients to invasive candidiasis, and immunological studies *in vitro* in healthy volunteers and patients with chronic mucocutaneous candidiasis suggested defects in cytokine production and Th17-mediated immunity as the putative pathogenetic mechanism. A similar approach has also unveiled an unexpected role for the missense rs1990760 (A946T) and rs3747517 (H843R) SNPs in IFN-induced helicase C domain protein 1 (IFIH1) in the development of invasive candidiasis as the result of an altered cytokine response [90]. The added value of integrating multi-omics datasets was also confirmed by a recent study in which genes and pathways contributing to candidemia were prioritized, including the complement and hemostasis pathways [312].

Functional genomics approaches combining genome information and immunological screenings have also provided invaluable evidence about the genetic regulation of cytokine production in response to different stimuli, including fungi [313]. By correlating genome-wide genotypes with cytokine abundance in response to fungal stimulation, several variants that control cytokine production – cytokine QTLs – were identified. Among them, a genetic variant at the N-alpha-acetyltransferase 35, NatC auxiliary subunit (NAA35)/ Golgi membrane protein 1 (GOLM1) locus markedly influenced the levels of IL-6 and was associated with susceptibility to candidemia. Likewise, the integration of GWAS data with information on cytokine QTLs from different cell types stimulated with *C. albicans* prioritized lipid and arachidonic acid metabolism as potential pathways influencing cytokine production and susceptibility to candidemia [314]. Although no differences were detected at a genome-wide level, analysis of candidate genes involved in immune cell metabolism revealed also an association between SNPs in PFKFB3 and cytokine production by PBMCs stimulated with *A. fumigatus* [172]. Functional analyses using cells from risk variant carriers pinpointed the defective activation of glycolysis as the likely mechanism explaining the increased susceptibility of stem-cell transplant recipients to IPA. Finally, a similar strategy was performed to uncover the genome-wide factors that determined variation in inflammatory protein responses and identified several protein QTLs that modulated the secretion of IL-8, MCP-2, MMP-1, and CCL3 in response to *C. albicans* [315]. More importantly, one protein QTL was found to influence the levels of urokinase plasminogen activator and was strongly associated with patient survival. Altogether, these studies highlight a relevant genetic contribution to immune phenotypic variation and susceptibility to fungal infection.

Genetic variants often exert their consequences in a context- and cell-specific way. By combining bulk and single-cell transcriptome data from fungal-stimulated immune cells with GWAS data in a candidemia cohort, SNPs in lymphocyte antigen 86 (LY86) were found to play a protective role against candidemia [316]. In the context of RVVC, the integration of genomic approaches and immunological studies in two independent patient cohorts and healthy individuals has identified genetic variants in sialic acid binding Ig like lectin 15 (SIGLEC15) in fungal recognition and susceptibility to RVVC [317]. SIGLEC15 was also implicated in the immune response to *A. fumigatus*, although the extent to which genetic variation affecting its function contributes to infection remains to be investigated [318]. In addition, the GWAS analysis of infection-related phenotypes in lymphoblastoid cell lines within the Hi-HOST Phenome Project identified SNPs associated with basic fibroblast growth factor (FGF2) production in response to *Mucor circinelloides* and *C. albicans*, although whether and how the presence of these SNPs was associated with the risk of fungal infection was not addressed [319]. The studies highlighted above represent critical examples of powerful functional genomics approaches that allowed uncovering novel mechanistic insights into the pathogenesis of fungal infections.

1.9 Purpose of the Thesis

Recent medical advances have, paradoxically, resulted in an expanding population of immunocompromised patients susceptible to life-threatening fungal diseases, including IPA. Defects in innate immunity have been highlighted as key pathogenetic mechanisms underlying IPA. In this regard, the metabolic reprogramming of immune cells is crucial to the regulation of cell differentiation and proliferation, and activation of effector responses. Although the fine-tuned regulation of cellular metabolism is required for the functional activity of macrophages, how these processes are orchestrated in response to *A. fumigatus* remains undefined.

Therefore, the central purpose of this Doctoral Thesis was to investigate the mechanisms through which infection with *A. fumigatus* rewires macrophage metabolism toward efficient innate immune responses, providing critical insights into the crosstalk between immunometabolism and antifungal immunity. Given the variable risk of infection and its clinical outcome among patients with comparable predisposing clinical and microbiological factors, susceptibility to IPA is thought to rely largely on genetic predisposition, although little is known about the contribution of host genetics to disease through effects on defined biological processes. Along this line, in this Doctoral Thesis, we also aimed to understand the contribution of genetic variation within metabolic genes and regulators to the immunometabolic response to *A. fumigatus* and development of IPA.

These studies have contributed to the identification of new molecular mechanisms linking the deregulation of metabolic pathways with impaired antifungal immune responses. Ultimately, this information may pave the way to the identification of novel processes targetable by personalized immunotherapeutic approaches and may contribute to open new horizons and lay the foundations for risk stratification and preemptive approaches aimed at a more effective management of IPA.

1.10 References

1. Kainz K, Bauer MA, Madeo F, et al. Fungal infections in humans: the silent crisis. Microb Cell. 2020 Jun 1;7(6):143-145.
2. Rodrigues ML, Nosanchuk JD. Fungal diseases as neglected pathogens: a wake-up call to public health officials. PLoS Negl Trop Dis. 2020 Feb;14(2):e0007964.
3. Bongomin F, Gago S, Oladele RO, et al. Global and multi-national prevalence of fungal diseases-estimate precision. J Fungi (Basel). 2017 Oct 18;3(4).
4. Fisher MC, Hawkins NJ, Sanglard D, et al. Worldwide emergence of resistance to antifungal drugs challenges human health and food security. Science. 2018 May 18;360(6390):739-742.
5. Perlroth J, Choi B, Spellberg B. Nosocomial fungal infections: epidemiology, diagnosis, and treatment. Med Mycol. 2007 Jun;45(4):321-46.
6. Alangaden GJ. Nosocomial fungal infections: epidemiology, infection control, and prevention. Infect Dis Clin North Am. 2011 Mar;25(1):201-25.
7. Suleyman G, Alangaden GJ. Nosocomial fungal infections: epidemiology, infection control, and prevention. Infect Dis Clin North Am. 2021 Dec;35(4):1027-1053.
8. Lionakis MS, Hohl TM. Call to action: How to tackle emerging nosocomial fungal infections. Cell Host Microbe. 2020 Jun 10;27(6):859-862.
9. Friedman DZP, Schwartz IS. Emerging fungal infections: new patients, new patterns, and new pathogens. J Fungi (Basel). 2019 Jul 20;5(3).
10. Lockhart SR, Guarner J. Emerging and reemerging fungal infections. Semin Diagn Pathol. 2019 May;36(3):177-181.
11. Verweij PE, Rijnders BJA, Bruggemann RJM, et al. Review of influenza-associated pulmonary aspergillosis in ICU patients and proposal for a case definition: an expert opinion. Intensive Care Med. 2020 Aug;46(8):1524-1535.
12. Arastehfar A, Carvalho A, van de Veerdonk FL, et al. COVID-19 associated pulmonary aspergillosis (CAPA)-from immunology to treatment. J Fungi (Basel). 2020 Jun 24;6(2).
13. Thompson GR, 3rd, Le T, Chindamporn A, et al. Global guideline for the diagnosis and management of the endemic mycoses: an initiative of the european confederation of medical mycology in cooperation with the international society for human and animal mycology. Lancet Infect Dis. 2021 Dec;21(12):e364-e374.
14. Palmieri F, Koutsokera A, Bernasconi E, et al. Recent advances in fungal infections: from lung ecology to therapeutic strategies with a focus on *Aspergillus* spp. Front Med (Lausanne). 2022;9:832510.
15. Brown GD, Denning DW, Gow NA, et al. Hidden killers: human fungal infections. Sci Transl Med. 2012 Dec 19;4(165):165rv13.
16. Firacative C. Invasive fungal disease in humans: are we aware of the real impact? Mem Inst Oswaldo Cruz. 2020;115:e200430.
17. Gago S, Denning DW, Bowyer P. Pathophysiological aspects of *Aspergillus* colonization in disease. Med Mycol. 2019 Apr 1;57(Supplement_2):S219-S227.
18. Arastehfar A, Carvalho A, Houbraken J, et al. *Aspergillus fumigatus* and aspergillosis: from basics to clinics. Stud Mycol. 2021 Sep;100:100115.
19. Oliveira LVN, Wang R, Specht CA, et al. Vaccines for human fungal diseases: close but still a long way to go. NPJ Vaccines. 2021 Mar 3;6(1):33.
20. van de Veerdonk FL, Gresnigt MS, Romani L, et al. *Aspergillus fumigatus* morphology and dynamic host interactions. Nat Rev Microbiol. 2017 Nov;15(11):661-674.

21. Kousha M, Tadi R, Soubani AO. Pulmonary aspergillosis: a clinical review. Eur Respir Rev. 2011 Sep 1;20(121):156-74.
22. Paulussen C, Hallsworth JE, Alvarez-Perez S, et al. Ecology of aspergillosis: insights into the pathogenic potency of *Aspergillus fumigatus* and some other *Aspergillus* species. Microb Biotechnol. 2017 Mar;10(2):296-322.
23. Latge JP, Chamilos G. *Aspergillus fumigatus* and Aspergillosis in 2019. Clin Microbiol Rev. 2019 Dec 18;33(1).
24. Abad A, Fernandez-Molina JV, Bikandi J, et al. What makes *Aspergillus fumigatus* a successful pathogen? Genes and molecules involved in invasive aspergillosis. Rev Iberoam Micol. 2010 Oct-Dec;27(4):155-82.
25. Kwon-Chung KJ, Sugui JA. *Aspergillus fumigatus*–what makes the species a ubiquitous human fungal pathogen? PLoS Pathog. 2013;9(12):e1003743.
26. O'Gorman CM, Fuller H, Dyer PS. Discovery of a sexual cycle in the opportunistic fungal pathogen *Aspergillus fumigatus*. Nature. 2009 Jan 22;457(7228):471-4.
27. Penalver MC, Casanova M, Martinez JP, et al. Cell wall protein and glycoprotein constituents of *Aspergillus fumigatus* that bind to polystyrene may be responsible for the cell surface hydrophobicity of the mycelium. Microbiology (Reading). 1996 Jul;142 (Pt 7):1597-604.
28. Parta M, Chang Y, Rulong S, et al. HYP1, a hydrophobin gene from *Aspergillus fumigatus*, complements the rodletless phenotype in *Aspergillus nidulans*. Infect Immun. 1994 Oct;62(10):4389-95.
29. Aimanianda V, Bayry J, Bozza S, et al. Surface hydrophobin prevents immune recognition of airborne fungal spores. Nature. 2009 Aug 27;460(7259):1117-21.
30. Jahn B, Langfelder K, Schneider U, et al. PKSP-dependent reduction of phagolysosome fusion and intracellular kill of *Aspergillus fumigatus* conidia by human monocyte-derived macrophages. Cell Microbiol. 2002 Dec;4(12):793-803.
31. Akoumianaki T, Kyrmizi I, Valsecchi I, et al. *Aspergillus* cell wall melanin blocks LC3-associated phagocytosis to promote pathogenicity. Cell Host Microbe. 2016 Jan 13;19(1):79-90.
32. Chamilos G, Akoumianaki T, Kyrmizi I, et al. Melanin targets LC3-associated phagocytosis (LAP): a novel pathogenetic mechanism in fungal disease. Autophagy. 2016 May 3;12(5):888-9.
33. Jahn B, Koch A, Schmidt A, et al. Isolation and characterization of a pigmentless-conidium mutant of *Aspergillus fumigatus* with altered conidial surface and reduced virulence. Infect Immun. 1997 Dec;65(12):5110-7.
34. Park SJ, Mehrad B. Innate immunity to *Aspergillus* species. Clin Microbiol Rev. 2009 Oct;22(4):535-51.
35. Kanj A, Abdallah N, Soubani AO. The spectrum of pulmonary aspergillosis. Respir Med. 2018 Aug;141:121-131.
36. Kosmidis C, Denning DW. The clinical spectrum of pulmonary aspergillosis. Thorax. 2015 Mar;70(3):270-7.
37. Li L, Jiang Z, Shao C. Pulmonary *Aspergillus* overlap syndromes. Mycopathologia. 2018 Apr;183(2):431-438.
38. Rankin NE. Disseminated aspergillosis and moniliasis associated with agranulocytosis and antibiotic therapy. Br Med J. 1953 Apr 25;1(4816):918-9.
39. Ledoux MP, Guffroy B, Nivoix Y, et al. Invasive pulmonary aspergillosis. Semin Respir Crit Care Med. 2020 Feb;41(1):80-98.
40. Dagenais TR, Keller NP. Pathogenesis of *Aspergillus fumigatus* in invasive aspergillosis. Clin Microbiol Rev. 2009 Jul;22(3):447-65.

41. Alshabani K, Haq A, Miyakawa R, et al. Invasive pulmonary aspergillosis in patients with influenza infection: report of two cases and systematic review of the literature. Expert Rev Respir Med. 2015 Feb;9(1):89-96.
42. Crum-Cianflone NF. Invasive aspergillosis associated with severe influenza infections. Open Forum Infect Dis. 2016 Sep;3(3):ofw171.
43. Gangneux JP, Dannaoui E, Fekkar A, et al. Fungal infections in mechanically ventilated patients with COVID-19 during the first wave: the french multicentre MYCOVID study. Lancet Respir Med. 2022 Feb;10(2):180-190.
44. White PL, Springer J, Wise MP, et al. A clinical case of COVID-19-associated pulmonary aspergillosis (CAPA), illustrating the challenges in diagnosis (despite overwhelming mycological evidence). J Fungi (Basel). 2022 Jan 14;8(1).
45. David F, Morais JR, Beires F, et al. Invasive pulmonary aspergillosis after COVID-19 pneumonia. Eur J Case Rep Intern Med. 2022;9(3):003209.
46. Al-Bader N, Sheppard DC. Aspergillosis and stem cell transplantation: an overview of experimental pathogenesis studies. Virulence. 2016 Nov 16;7(8):950-966.
47. Kontoyiannis DP, Marr KA, Park BJ, et al. Prospective surveillance for invasive fungal infections in hematopoietic stem cell transplant recipients, 2001-2006: overview of the transplant-associated infection surveillance network (TRANSNET) Database. Clin Infect Dis. 2010 Apr 15;50(8):1091-100.
48. Robin C, Cordonnier C, Sitbon K, et al. Mainly post-transplant factors are associated with invasive aspergillosis after allogeneic stem cell transplantation: a study from the surveillance des aspergilloses invasives en France and societe francophone de greffe de moelle et de therapie cellulaire. Biol Blood Marrow Transplant. 2019 Feb;25(2):354-361.
49. Lortholary O, Gangneux JP, Sitbon K, et al. Epidemiological trends in invasive aspergillosis in France: the SAIF network (2005-2007). Clin Microbiol Infect. 2011 Dec;17(12):1882-9.
50. Montagna MT, Lovero G, Coretti C, et al. SIMIFF study: Italian fungal registry of mold infections in hematological and non-hematological patients. Infection. 2014 Feb;42(1):141-51.
51. Kuster S, Stampf S, Gerber B, et al. Incidence and outcome of invasive fungal diseases after allogeneic hematopoietic stem cell transplantation: a Swiss transplant cohort study. Transpl Infect Dis. 2018 Dec;20(6):e12981.
52. Benedict K, Jackson BR, Chiller T, et al. Estimation of direct healthcare costs of fungal diseases in the United States. Clin Infect Dis. 2019 May 17;68(11):1791-1797.
53. Ascioglu S, Rex JH, de Pauw B, et al. Defining opportunistic invasive fungal infections in immunocompromised patients with cancer and hematopoietic stem cell transplants: an international consensus. Clin Infect Dis. 2002 Jan 1;34(1):7-14.
54. De Pauw B, Walsh TJ, Donnelly JP, et al. Revised definitions of invasive fungal disease from the european organization for research and treatment of cancer/invasive fungal infections cooperative group and the national institute of allergy and infectious diseases mycoses study group (EORTC/MSG) consensus group. Clin Infect Dis. 2008 Jun 15;46(12):1813-21.
55. Schelenz S, Barnes RA, Barton RC, et al. British society for medical mycology best practice recommendations for the diagnosis of serious fungal diseases. Lancet Infect Dis. 2015 Apr;15(4):461-74.
56. Lass-Florl C. How to make a fast diagnosis in invasive aspergillosis. Med Mycol. 2019 Apr 1;57(Supplement_2):S155-S160.
57. Zhao Y, Paderu P, Railkar R, et al. Blood *Aspergillus* RNA is a promising alternative biomarker for invasive aspergillosis. Med Mycol. 2016 Nov 1;54(8):801-7.

58. Wu C, Xu K, Wang Z, et al. A novel microRNA miR-1165-3p as a potential diagnostic biomarker for allergic asthma. Biomarkers. 2019 Feb;24(1):56-63.
59. Heddergott C, Calvo AM, Latge JP. The volatome of *Aspergillus fumigatus*. Eukaryot Cell. 2014 Aug;13(8):1014-25.
60. Koo S, Thomas HR, Daniels SD, et al. A breath fungal secondary metabolite signature to diagnose invasive aspergillosis. Clin Infect Dis. 2014 Dec 15;59(12):1733-40.
61. Hoenigl M, Prattes J, Spiess B, et al. Performance of galactomannan, beta-d-glucan, *Aspergillus* lateral-flow device, conventional culture, and PCR tests with bronchoalveolar lavage fluid for diagnosis of invasive pulmonary aspergillosis. J Clin Microbiol. 2014 Jun;52(6):2039-45.
62. Houst J, Spizek J, Havlicek V. Antifungal Drugs. Metabolites. 2020 Mar 12;10(3).
63. Robbins N, Caplan T, Cowen LE. Molecular evolution of antifungal drug resistance. Annu Rev Microbiol. 2017 Sep 8;71:753-775.
64. Silva LN, de Mello TP, de Souza Ramos L, et al. Current challenges and updates on the therapy of fungal infections. Curr Top Med Chem. 2019;19(7):495-499.
65. Cornely OA, Maertens J, Bresnik M, et al. Liposomal amphotericin B as initial therapy for invasive mold infection: a randomized trial comparing a high-loading dose regimen with standard dosing (AmBiLoad trial). Clin Infect Dis. 2007 May 15;44(10):1289-97.
66. Patil A, Majumdar S. Echinocandins in antifungal pharmacotherapy. J Pharm Pharmacol. 2017 Dec;69(12):1635-1660.
67. Armstrong-James D, Brown GD, Netea MG, et al. Immunotherapeutic approaches to treatment of fungal diseases. Lancet Infect Dis. 2017 Dec;17(12):e393-e402.
68. Zumla A, Rao M, Wallis RS, et al. Host-directed therapies for infectious diseases: current status, recent progress, and future prospects. Lancet Infect Dis. 2016 Apr;16(4):e47-63.
69. Oliveira-Coelho A, Rodrigues F, Campos A, Jr., et al. Paving the way for predictive diagnostics and personalized treatment of invasive aspergillosis. Front Microbiol. 2015;6:411.
70. Medzhitov R, Schneider DS, Soares MP. Disease tolerance as a defense strategy. Science. 2012 Feb 24;335(6071):936-41.
71. Whitsett JA, Alenghat T. Respiratory epithelial cells orchestrate pulmonary innate immunity. Nat Immunol. 2015 Jan;16(1):27-35.
72. Hopke A, Brown AJP, Hall RA, et al. Dynamic fungal cell wall architecture in stress adaptation and immune evasion. Trends Microbiol. 2018 Apr;26(4):284-295.
73. Hatinguais R, Willment JA, Brown GD. PAMPs of the fungal cell wall and mammalian PRRs. Curr Top Microbiol Immunol. 2020;425:187-223.
74. Delliere S, Sze Wah Wong S, Aimanianda V. Soluble mediators in anti-fungal immunity. Curr Opin Microbiol. 2020 Dec;58:24-31.
75. Cunha C, Carvalho A, Esposito A, et al. DAMP signaling in fungal infections and diseases. Front Immunol. 2012;3:286.
76. Bozza S, Gaziano R, Spreca A, et al. Dendritic cells transport conidia and hyphae of *Aspergillus fumigatus* from the airways to the draining lymph nodes and initiate disparate Th responses to the fungus. J Immunol. 2002 Feb 1;168(3):1362-71.
77. De Luca A, Iannitti RG, Bozza S, et al. CD4(+) T cell vaccination overcomes defective cross-presentation of fungal antigens in a mouse model of chronic granulomatous disease. J Clin Invest. 2012 May;122(5):1816-31.
78. Decken K, Kohler G, Palmer-Lehmann K, et al. Interleukin-12 is essential for a protective Th1 response in mice infected with *Cryptococcus neoformans*. Infect Immun. 1998 Oct;66(10):4994-5000.

79. Hamza T, Barnett JB, Li B. Interleukin 12 a key immunoregulatory cytokine in infection applications. Int J Mol Sci. 2010 Feb 26;11(3):789-806.
80. Sales-Campos H, Tonani L, Cardoso CR, et al. The immune interplay between the host and the pathogen in *Aspergillus fumigatus* lung infection. Biomed Res Int. 2013;2013:693023.
81. Bellocchio S, Bozza S, Montagnoli C, et al. Immunity to *Aspergillus fumigatus*: the basis for immunotherapy and vaccination. Med Mycol. 2005 May;43 Suppl 1:S181-8.
82. Arias M, Santiago L, Vidal-Garcia M, et al. Preparations for invasion: modulation of host lung immunity during pulmonary aspergillosis by gliotoxin and other fungal secondary metabolites. Front Immunol. 2018;9:2549.
83. Stuehler C, Khanna N, Bozza S, et al. Cross-protective TH1 immunity against *Aspergillus fumigatus* and *Candida albicans*. Blood. 2011 Jun 2;117(22):5881-91.
84. Zelante T, De Luca A, Bonifazi P, et al. IL-23 and the Th17 pathway promote inflammation and impair antifungal immune resistance. Eur J Immunol. 2007 Oct;37(10):2695-706.
85. Chai LY, van de Veerdonk F, Marijnissen RJ, et al. Anti-*Aspergillus* human host defence relies on type 1 T helper (Th1), rather than type 17 T helper (Th17), cellular immunity. Immunology. 2010 May;130(1):46-54.
86. Jolink H, de Boer R, Hombrink P, et al. Pulmonary immune responses against *Aspergillus fumigatus* are characterized by high frequencies of IL-17 producing T-cells. J Infect. 2017 Jan;74(1):81-88.
87. Montagnoli C, Fallarino F, Gaziano R, et al. Immunity and tolerance to *Aspergillus* involve functionally distinct regulatory T cells and tryptophan catabolism. J Immunol. 2006 Feb 1;176(3):1712-23.
88. Latge JP. Tasting the fungal cell wall. Cell Microbiol. 2010 Jul;12(7):863-72.
89. Plato A, Hardison SE, Brown GD. Pattern recognition receptors in antifungal immunity. Semin Immunopathol. 2015 Mar;37(2):97-106.
90. Jaeger M, van der Lee R, Cheng SC, et al. The RIG-I-like helicase receptor MDA5 (IFIH1) is involved in the host defense against *Candida infections*. Eur J Clin Microbiol Infect Dis. 2015 May;34(5):963-974.
91. Gessner MA, Werner JL, Lilly LM, et al. Dectin-1-dependent interleukin-22 contributes to early innate lung defense against *Aspergillus fumigatus*. Infect Immun. 2012 Jan;80(1):410-7.
92. Cunha C, Di Ianni M, Bozza S, et al. Dectin-1 Y238X polymorphism associates with susceptibility to invasive aspergillosis in hematopoietic transplantation through impairment of both recipient- and donor-dependent mechanisms of antifungal immunity. Blood. 2010 Dec 9;116(24):5394-402.
93. Werner JL, Metz AE, Horn D, et al. Requisite role for the dectin-1 beta-glucan receptor in pulmonary defense against *Aspergillus fumigatus*. J Immunol. 2009 Apr 15;182(8):4938-46.
94. Margalit A, Kavanagh K. The innate immune response to *Aspergillus fumigatus* at the alveolar surface. FEMS Microbiol Rev. 2015 Sep;39(5):670-87.
95. Drummond RA, Brown GD. The role of Dectin-1 in the host defence against fungal infections. Curr Opin Microbiol. 2011 Aug;14(4):392-9.
96. Tam JM, Mansour MK, Khan NS, et al. Dectin-1-dependent LC3 recruitment to phagosomes enhances fungicidal activity in macrophages. J Infect Dis. 2014 Dec 1;210(11):1844-54.
97. Levitz SM. Innate recognition of fungal cell walls. PLoS Pathog. 2010 Apr 22;6(4):e1000758.
98. Sun H, Xu XY, Tian XL, et al. Activation of NF-kappaB and respiratory burst following *Aspergillus fumigatus* stimulation of macrophages. Immunobiology. 2014 Jan;219(1):25-36.

99. Sun H, Xu XY, Shao HT, et al. Dectin-2 is predominately macrophage restricted and exhibits conspicuous expression during *Aspergillus fumigatus* invasion in human lung. Cell Immunol. 2013 Jul-Aug;284(1-2):60-7.
100. Loures FV, Rohm M, Lee CK, et al. Recognition of *Aspergillus fumigatus* hyphae by human plasmacytoid dendritic cells is mediated by dectin-2 and results in formation of extracellular traps. PLoS Pathog. 2015 Feb;11(2):e1004643.
101. Reedy JL, Crossen AJ, Negoro PE, et al. The C-type lectin receptor dectin-2 is a receptor for *Aspergillus fumigatus* galactomannan. bioRxiv. 2022:2022.04.12.488040.
102. Serrano-Gomez D, Dominguez-Soto A, Ancochea J, et al. Dendritic cell-specific intercellular adhesion molecule 3-grabbing nonintegrin mediates binding and internalization of *Aspergillus fumigatus* conidia by dendritic cells and macrophages. J Immunol. 2004 Nov 1;173(9):5635-43.
103. Puig-Kroger A, Serrano-Gomez D, Caparros E, et al. Regulated expression of the pathogen receptor dendritic cell-specific intercellular adhesion molecule 3 (ICAM-3)-grabbing nonintegrin in THP-1 human leukemic cells, monocytes, and macrophages. J Biol Chem. 2004 Jun 11;279(24):25680-8.
104. Lam JS, Huang H, Levitz SM. Effect of differential N-linked and O-linked mannosylation on recognition of fungal antigens by dendritic cells. PLoS One. 2007 Oct 10;2(10):e1009.
105. Cambi A, Netea MG, Mora-Montes HM, et al. Dendritic cell interaction with *Candida albicans* critically depends on N-linked mannan. J Biol Chem. 2008 Jul 18;283(29):20590-9.
106. van de Veerdonk FL, Marijnissen RJ, Kullberg BJ, et al. The macrophage mannose receptor induces IL-17 in response to *Candida albicans*. Cell Host Microbe. 2009 Apr 23;5(4):329-40.
107. Stappers MHT, Clark AE, Aimanianda V, et al. Recognition of DHN-melanin by a C-type lectin receptor is required for immunity to *Aspergillus*. Nature. 2018 Mar 15;555(7696):382-386.
108. Kawasaki T, Kawai T. Toll-like receptor signaling pathways. Front Immunol. 2014;5:461.
109. Jannuzzi GP, de Almeida JRF, Paulo LNM, et al. Intracellular PRRs activation in targeting the immune response against fungal infections. Front Cell Infect Microbiol. 2020;10:591970.
110. Netea MG, Warris A, Van der Meer JW, et al. *Aspergillus fumigatus* evades immune recognition during germination through loss of toll-like receptor-4-mediated signal transduction. J Infect Dis. 2003 Jul 15;188(2):320-6.
111. Chai LY, Vonk AG, Kullberg BJ, et al. *Aspergillus fumigatus* cell wall components differentially modulate host TLR2 and TLR4 responses. Microbes Infect. 2011 Feb;13(2):151-9.
112. Rubino I, Coste A, Le Roy D, et al. Species-specific recognition of *Aspergillus fumigatus* by Toll-like receptor 1 and Toll-like receptor 6. J Infect Dis. 2012 Mar 15;205(6):944-54.
113. Miyazato A, Nakamura K, Yamamoto N, et al. Toll-like receptor 9-dependent activation of myeloid dendritic cells by deoxynucleic acids from *Candida albicans*. Infect Immun. 2009 Jul;77(7):3056-64.
114. Kasperkovitz PV, Khan NS, Tam JM, et al. Toll-like receptor 9 modulates macrophage antifungal effector function during innate recognition of *Candida albicans* and *Saccharomyces cerevisiae*. Infect Immun. 2011 Dec;79(12):4858-67.
115. Ramirez-Ortiz ZG, Lee CK, Wang JP, et al. A nonredundant role for plasmacytoid dendritic cells in host defense against the human fungal pathogen *Aspergillus fumigatus*. Cell Host Microbe. 2011 May 19;9(5):415-24.
116. Wang JP, Lee CK, Akalin A, et al. Contributions of the MyD88-dependent receptors IL-18R, IL-1R, and TLR9 to host defenses following pulmonary challenge with *Cryptococcus neoformans*. PLoS One. 2011;6(10):e26232.

117. Carvalho A, De Luca A, Bozza S, et al. TLR3 essentially promotes protective class I-restricted memory CD8(+) T-cell responses to *Aspergillus fumigatus* in hematopoietic transplanted patients. Blood. 2012 Jan 26;119(4):967-77.
118. de Luca A, Bozza S, Zelante T, et al. Non-hematopoietic cells contribute to protective tolerance to *Aspergillus fumigatus* via a TRIF pathway converging on IDO. Cell Mol Immunol. 2010 Nov;7(6):459-70.
119. Ramirez-Ortiz ZG, Specht CA, Wang JP, et al. Toll-like receptor 9-dependent immune activation by unmethylated CpG motifs in *Aspergillus fumigatus* DNA. Infect Immun. 2008 May;76(5):2123-9.
120. Li ZZ, Tao LL, Zhang J, et al. Role of NOD2 in regulating the immune response to *Aspergillus fumigatus*. Inflamm Res. 2012 Jun;61(6):643-8.
121. Said-Sadier N, Padilla E, Langsley G, et al. *Aspergillus fumigatus* stimulates the NLRP3 inflammasome through a pathway requiring ROS production and the Syk tyrosine kinase. PLoS One. 2010 Apr 2;5(4):e10008.
122. Briard B, Karki R, Malireddi RKS, et al. Fungal ligands released by innate immune effectors promote inflammasome activation during *Aspergillus fumigatus* infection. Nat Microbiol. 2019 Feb;4(2):316-327.
123. Briard B, Fontaine T, Samir P, et al. Galactosaminogalactan activates the inflammasome to provide host protection. Nature. 2020 Dec;588(7839):688-692.
124. Karki R, Man SM, Malireddi RKS, et al. Concerted activation of the AIM2 and NLRP3 inflammasomes orchestrates host protection against *Aspergillus* infection. Cell Host Microbe. 2015 Mar 11;17(3):357-368.
125. Bottazzi B, Doni A, Garlanda C, et al. An integrated view of humoral innate immunity: pentraxins as a paradigm. Annu Rev Immunol. 2010;28:157-83.
126. Patin EC, Thompson A, Orr SJ. Pattern recognition receptors in fungal immunity. Semin Cell Dev Biol. 2019 May;89:24-33.
127. Parente R, Doni A, Bottazzi B, et al. The complement system in *Aspergillus fumigatus* infections and its crosstalk with pentraxins. FEBS Lett. 2020 Aug;594(16):2480-2501.
128. Kang Y, Yu Y, Lu L. The role of pentraxin 3 in aspergillosis: reality and prospects. Mycobiology. 2020;48(1):1-8.
129. Garlanda C, Hirsch E, Bozza S, et al. Non-redundant role of the long pentraxin PTX3 in anti-fungal innate immune response. Nature. 2002 Nov 14;420(6912):182-6.
130. Balhara J, Koussih L, Zhang J, et al. Pentraxin 3: an immuno-regulator in the lungs. Front Immunol. 2013;4:127.
131. Doni A, Parente R, Laface I, et al. Serum amyloid P component is an essential element of resistance against *Aspergillus fumigatus*. Nat Commun. 2021 Jun 18;12(1):3739.
132. Madan T, Eggleton P, Kishore U, et al. Binding of pulmonary surfactant proteins A and D to *Aspergillus fumigatus* conidia enhances phagocytosis and killing by human neutrophils and alveolar macrophages. Infect Immun. 1997 Aug;65(8):3171-9.
133. Shah A, Kannambath S, Herbst S, et al. Calcineurin orchestrates lateral transfer of *Aspergillus fumigatus* during macrophage cell death. Am J Respir Crit Care Med. 2016 Nov 1;194(9):1127-1139.
134. Yates RM, Russell DG. Phagosome maturation proceeds independently of stimulation of toll-like receptors 2 and 4. Immunity. 2005 Oct;23(4):409-17.

135. Philippe B, Ibrahim-Granet O, Prevost MC, et al. Killing of *Aspergillus fumigatus* by alveolar macrophages is mediated by reactive oxidant intermediates. Infect Immun. 2003 Jun;71(6):3034-42.
136. Wasylnka JA, Moore MM. *Aspergillus fumigatus* conidia survive and germinate in acidic organelles of A549 epithelial cells. J Cell Sci. 2003 Apr 15;116(Pt 8):1579-87.
137. Ibrahim-Granet O, Philippe B, Boleti H, et al. Phagocytosis and intracellular fate of *Aspergillus fumigatus* conidia in alveolar macrophages. Infect Immun. 2003 Feb;71(2):891-903.
138. Andrianaki AM, Kyrmizi I, Thanopoulou K, et al. Iron restriction inside macrophages regulates pulmonary host defense against *Rhizopus* species. Nat Commun. 2018 Aug 20;9(1):3333.
139. Espinosa V, Rivera A. First Line of Defense: Innate cell-mediated control of pulmonary aspergillosis. Front Microbiol. 2016;7:272.
140. Grimm MJ, Vethanayagam RR, Almyroudis NG, et al. Monocyte- and macrophage-targeted NADPH oxidase mediates antifungal host defense and regulation of acute inflammation in mice. J Immunol. 2013 Apr 15;190(8):4175-84.
141. Gazendam RP, van Hamme JL, Tool AT, et al. Human neutrophils use different mechanisms to kill *Aspergillus fumigatus* conidia and hyphae: evidence from phagocyte defects. J Immunol. 2016 Feb 1;196(3):1272-83.
142. Hatinguais R, Pradhan A, Brown GD, et al. Mitochondrial reactive oxygen species regulate immune responses of macrophages to *Aspergillus fumigatus*. Front Immunol. 2021;12:641495.
143. Shlezinger N, Hohl TM. Mitochondrial reactive oxygen species enhance alveolar macrophage activity against *Aspergillus fumigatus* but are dispensable for host protection. mSphere. 2021 Jun 30;6(3):e0026021.
144. Kyrmizi I, Gresnigt MS, Akoumianaki T, et al. Corticosteroids block autophagy protein recruitment in *Aspergillus fumigatus* phagosomes via targeting dectin-1/Syk kinase signaling. J Immunol. 2013 Aug 1;191(3):1287-99.
145. Sanjuan MA, Dillon CP, Tait SW, et al. Toll-like receptor signalling in macrophages links the autophagy pathway to phagocytosis. Nature. 2007 Dec 20;450(7173):1253-7.
146. Martinez J, Malireddi RK, Lu Q, et al. Molecular characterization of LC3-associated phagocytosis reveals distinct roles for Rubicon, NOX2 and autophagy proteins. Nat Cell Biol. 2015 Jul;17(7):893-906.
147. Kyrmizi I, Ferreira H, Carvalho A, et al. Calcium sequestration by fungal melanin inhibits calcium-calmodulin signalling to prevent LC3-associated phagocytosis. Nat Microbiol. 2018 Jul;3(7):791-803.
148. Bhatia S, Fei M, Yarlagadda M, et al. Rapid host defense against *Aspergillus fumigatus* involves alveolar macrophages with a predominance of alternatively activated phenotype. PLoS One. 2011 Jan 5;6(1):e15943.
149. Bruns S, Kniemeyer O, Hasenberg M, et al. Production of extracellular traps against *Aspergillus fumigatus* in vitro and in infected lung tissue is dependent on invading neutrophils and influenced by hydrophobin RodA. PLoS Pathog. 2010 Apr 29;6(4):e1000873.
150. Paris S, Boisvieux-Ulrich E, Crestani B, et al. Internalization of *Aspergillus fumigatus* conidia by epithelial and endothelial cells. Infect Immun. 1997 Apr;65(4):1510-4.
151. Keizer EM, Wosten HAB, de Cock H. EphA2-Dependent Internalization of *A. fumigatus* conidia in A549 lung cells is modulated by DHN-Melanin. Front Microbiol. 2020;11:534118.
152. Schiefermeier-Mach N, Haller T, Geley S, et al. Migrating lung monocytes internalize and inhibit growth of *Aspergillus fumigatus* conidia. Pathogens. 2020 Nov 24;9(12).

153. Serbina NV, Cherny M, Shi C, et al. Distinct responses of human monocyte subsets to *Aspergillus fumigatus* conidia. J Immunol. 2009 Aug 15;183(4):2678-87.
154. Mezger M, Kneitz S, Wozniok I, et al. Proinflammatory response of immature human dendritic cells is mediated by dectin-1 after exposure to *Aspergillus fumigatus* germ tubes. J Infect Dis. 2008 Mar 15;197(6):924-31.
155. Netea MG, Joosten LA, van der Meer JW, et al. Immune defence against *Candida* fungal infections. Nat Rev Immunol. 2015 Oct;15(10):630-42.
156. Weerasinghe H, Traven A. Immunometabolism in fungal infections: the need to eat to compete. Curr Opin Microbiol. 2020 Dec;58:32-40.
157. Williams TJ, Harvey S, Armstrong-James D. Immunotherapeutic approaches for fungal infections. Curr Opin Microbiol. 2020 Dec;58:130-137.
158. O'Neill LA, Pearce EJ. Immunometabolism governs dendritic cell and macrophage function. J Exp Med. 2016 Jan 11;213(1):15-23.
159. Traven A, Naderer T. Central metabolic interactions of immune cells and microbes: prospects for defeating infections. EMBO reports. 2019 Jul;20(7):e47995.
160. Cheng SC, Quintin J, Cramer RA, et al. mTOR- and HIF-1alpha-mediated aerobic glycolysis as metabolic basis for trained immunity. Science. 2014 Sep 26;345(6204):1250684.
161. Dominguez-Andres J, Arts RJW, Ter Horst R, et al. Rewiring monocyte glucose metabolism via C-type lectin signaling protects against disseminated candidiasis. PLoS Pathog. 2017 Sep;13(9):e1006632.
162. Hellwig D, Voigt J, Bouzani M, et al. *Candida albicans* Induces metabolic reprogramming in human NK cells and responds to perforin with a zinc depletion response. Front Microbiol. 2016;7:750.
163. Quintin J, Saeed S, Martens JH, et al. *Candida albicans* infection affords protection against reinfection via functional reprogramming of monocytes. Cell Host Microbe. 2012 Aug 16;12(2):223-32.
164. Tucey TM, Verma J, Harrison PF, et al. Glucose homeostasis is important for immune cell viability during *Candida* challenge and host survival of systemic fungal infection. Cell Metabol. 2018 May 1;27(5):988-1006 e7.
165. Goncalves SM, Duarte-Oliveira C, Campos CF, et al. Phagosomal removal of fungal melanin reprograms macrophage metabolism to promote antifungal immunity. Nat Commun. 2020 May 8;11(1):2282.
166. Rosa RL, Berger M, Santi L, et al. Proteomics of rat lungs infected by *Cryptococcus gattii* reveals a potential warburg-like effect. J Proteome Res. 2019 Nov 1;18(11):3885-3895.
167. Lachmandas E, Boutens L, Ratter JM, et al. Microbial stimulation of different Toll-like receptor signalling pathways induces diverse metabolic programmes in human monocytes. Nat Microbiol. 2016 Dec 19;2:16246.
168. Ballou ER, Avelar GM, Childers DS, et al. Lactate signalling regulates fungal beta-glucan masking and immune evasion. Nat Microbiol. 2016 Dec 12;2:16238.
169. Fliesser M, Morton CO, Bonin M, et al. Hypoxia-inducible factor 1alpha modulates metabolic activity and cytokine release in anti-*Aspergillus fumigatus* immune responses initiated by human dendritic cells. Internat J Med Microbiol : IJMM. 2015 Dec;305(8):865-73.
170. Shepardson KM, Jhingran A, Caffrey A, et al. Myeloid derived hypoxia inducible factor 1-alpha is required for protection against pulmonary *Aspergillus fumigatus* infection. PLoS Pathog. 2014 Sep;10(9):e1004378.

171. Rosowski EE, Raffa N, Knox BP, et al. Macrophages inhibit *Aspergillus fumigatus* germination and neutrophil-mediated fungal killing. PLoS Pathog. 2018 Aug;14(8):e1007229.
172. Goncalves SM, Antunes D, Leite L, et al. Genetic variation in PFKFB3 impairs antifungal immunometabolic responses and predisposes to invasive pulmonary aspergillosis. mBio. 2021 Jun 29;12(3):e0036921.
173. Jiang H, Shi H, Sun M, et al. PFKFB3-driven macrophage glycolytic metabolism is a crucial component of innate antiviral defense. J Immunol. 2016 Oct 1;197(7):2880-90.
174. Ayres JS. Immunometabolism of infections. Nat Rev Immunol. 2020 Feb;20(2):79-80.
175. O'Neill LAJ, Artyomov MN. Itaconate: the poster child of metabolic reprogramming in macrophage function. Nat Rev Immunol. 2019 May;19(5):273-281.
176. Lampropoulou V, Sergushichev A, Bambouskova M, et al. Itaconate links inhibition of succinate dehydrogenase with macrophage metabolic remodeling and regulation of inflammation. Cell Metabol. 2016 Jul 12;24(1):158-66.
177. Mills EL, Ryan DG, Prag HA, et al. Itaconate is an anti-inflammatory metabolite that activates Nrf2 via alkylation of KEAP1. Nature. 2018 Apr 5;556(7699):113-117.
178. Nair S, Huynh JP, Lampropoulou V, et al. Irg1 expression in myeloid cells prevents immunopathology during *M. tuberculosis* infection. J Exp Med. 2018 Apr 2;215(4):1035-1045.
179. Hall CJ, Boyle RH, Astin JW, et al. Immunoresponsive gene 1 augments bactericidal activity of macrophage-lineage cells by regulating beta-oxidation-dependent mitochondrial ROS production. Cell Metabol. 2013 Aug 6;18(2):265-78.
180. Daniels BP, Kofman SB, Smith JR, et al. The nucleotide sensor ZBP1 and kinase RIPK3 induce the enzyme IRG1 to promote an antiviral metabolic state in neurons. Immunity. 2019 Jan 15;50(1):64-76 e4.
181. Chen M, Sun H, Boot M, et al. Itaconate is an effector of a Rab GTPase cell-autonomous host defense pathway against Salmonella. Science. 2020 Jul 24;369(6502):450-455.
182. Lorenz MC, Fink GR. The glyoxylate cycle is required for fungal virulence. Nature. 2001 Jul 5;412(6842):83-6.
183. Sasikaran J, Ziemski M, Zadora PK, et al. Bacterial itaconate degradation promotes pathogenicity. Nat Chem Biol. 2014 May;10(5):371-7.
184. Tomlinson KL, Lung TWF, Dach F, et al. *Staphylococcus aureus* induces an itaconate-dominated immunometabolic response that drives biofilm formation. Nat Commun. 2021 Mar 3;12(1):1399.
185. Riquelme SA, Liimatta K, Wong Fok Lung T, et al. *Pseudomonas aeruginosa* utilizes host-derived itaconate to redirect its metabolism to promote biofilm formation. Cell Metabol. 2020 Jun 2;31(6):1091-1106 e6.
186. Ogger PP, Albers GJ, Hewitt RJ, et al. Itaconate controls the severity of pulmonary fibrosis. Sci Immunol. 2020 Oct 23;5(52).
187. Fukuda Y, Homma T, Suzuki S, et al. High burden of *Aspergillus fumigatus* infection among chronic respiratory diseases. Chron Respir Dis. 2018 Aug;15(3):279-285.
188. Kumar N, Mishra M, Singhal A, et al. Aspergilloma coexisting with idiopathic pulmonary fibrosis: a rare occurrence. J Postgrad Med. 2013 Apr-Jun;59(2):145-8.
189. Ries LNA, Alves de Castro P, Pereira Silva L, et al. *Aspergillus fumigatus* acetate utilization impacts virulence traits and pathogenicity. mBio. 2021 Jul 27:e0168221.
190. Tannahill GM, Curtis AM, Adamik J, et al. Succinate is an inflammatory signal that induces IL-1beta through HIF-1alpha. Nature. 2013 Apr 11;496(7444):238-42.

191. Mills EL, Kelly B, Logan A, et al. Succinate dehydrogenase supports metabolic repurposing of mitochondria to drive inflammatory macrophages. Cell. 2016 Oct 6;167(2):457-470 e13.
192. Warris A, Ballou ER. Oxidative responses and fungal infection biology. Semin Cell Dev Biol. 2019 May;89:34-46.
193. Kieler M, Hofmann M, Schabbauer G. More than just protein building blocks: how amino acids and related metabolic pathways fuel macrophage polarization. FEBS J. 2021 Jan 18.
194. Wagener J, MacCallum DM, Brown GD, et al. *Candida albicans* chitin increases arginase-1 activity in human macrophages, with an impact on macrophage antimicrobial Functions. mBio. 2017 Jan 24;8(1).
195. Kapp K, Prufer S, Michel CS, et al. Granulocyte functions are independent of arginine availability. J Leukocyte Biol. 2014 Dec;96(6):1047-53.
196. Carvalho A, Cunha C, Bozza S, et al. Immunity and tolerance to fungi in hematopoietic transplantation: principles and perspectives. Front Immunol. 2012;3:156.
197. Proietti E, Rossini S, Grohmann U, et al. Polyamines and kynurenines at the intersection of immune modulation. Trends Immunol. 2020 Nov;41(11):1037-1050.
198. Iannitti RG, Carvalho A, Cunha C, et al. Th17/Treg imbalance in murine cystic fibrosis is linked to indoleamine 2,3-dioxygenase deficiency but corrected by kynurenines. Am J Resp Crit Care Med. 2013 Mar 15;187(6):609-20.
199. Romani L, Fallarino F, De Luca A, et al. Defective tryptophan catabolism underlies inflammation in mouse chronic granulomatous disease. Nature. 2008 Jan 10;451(7175):211-5.
200. Paveglio SA, Allard J, Foster Hodgkins SR, et al. Airway epithelial indoleamine 2,3-dioxygenase inhibits CD4+ T cells during *Aspergillus fumigatus* antigen exposure. Am J Resp Cell Mol Biol. 2011 Jan;44(1):11-23.
201. Zelante T, Iannitti RG, Cunha C, et al. Tryptophan catabolites from microbiota engage aryl hydrocarbon receptor and balance mucosal reactivity via interleukin-22. Immunity. 2013 Aug 22;39(2):372-85.
202. Bozza S, Fallarino F, Pitzurra L, et al. A crucial role for tryptophan catabolism at the host/*Candida albicans* interface. J Immunol. 2005 Mar 1;174(5):2910-8.
203. Orabona C, Mondanelli G, Pallotta MT, et al. Deficiency of immunoregulatory indoleamine 2,3-dioxygenase 1 in juvenile diabetes. JCI Insight. 2018 Mar 22;3(6).
204. De Luca A, Carvalho A, Cunha C, et al. IL-22 and IDO1 affect immunity and tolerance to murine and human vaginal candidiasis. PLoS Pathog. 2013;9(7):e1003486.
205. Napolioni V, Pariano M, Borghi M, et al. Genetic polymorphisms affecting IDO1 or IDO2 activity differently associate with aspergillosis in humans. Front Immunol. 2019;10:890.
206. Zelante T, Choera T, Beauvais A, et al. *Aspergillus fumigatus* tryptophan metabolic route differently affects host immunity. Cell Rep. 2021 Jan 26;34(4):108673.
207. Mondanelli G, Iacono A, Carvalho A, et al. Amino acid metabolism as drug target in autoimmune diseases. Autoimmun Rev. 2019 Apr;18(4):334-348.
208. Ferreira AV, Domiguez-Andres J, Netea MG. The role of cell metabolism in innate immune memory. J Innate Immun. 2020 Dec 30:1-9.
209. Arts RJW, Carvalho A, La Rocca C, et al. Immunometabolic pathways in BCG-induced trained immunity. Cell Rep. 2016 Dec 6;17(10):2562-2571.
210. Quintin J, Saeed S, Martens JHA, et al. *Candida albicans* infection affords protection against reinfection via functional reprogramming of monocytes. Cell Host Microbe. 2012 Aug 16;12(2):223-32.

211. Bekkering S, Quintin J, Joosten LA, et al. Oxidized low-density lipoprotein induces long-term proinflammatory cytokine production and foam cell formation via epigenetic reprogramming of monocytes. Arterioscler Thromb Vasc Biol. 2014 Aug;34(8):1731-8.
212. Bekkering S, Arts RJW, Novakovic B, et al. Metabolic induction of trained immunity through the mevalonate pathway. Cell. 2018 Jan 11;172(1-2):135-146 e9.
213. Kaufmann E, Sanz J, Dunn JL, et al. BCG educates hematopoietic stem cells to generate protective innate immunity against tuberculosis. Cell. 2018 Jan 11;172(1-2):176-190 e19.
214. Mitroulis I, Ruppova K, Wang B, et al. Modulation of myelopoiesis progenitors is an integral component of trained immunity. Cell. 2018 Jan 11;172(1-2):147-161 e12.
215. Giamarellos-Bourboulis EJ, Tsilika M, Moorlag S, et al. Activate: randomized clinical trial of BCG vaccination against infection in the elderly. Cell. 2020 Oct 15;183(2):315-323 e9.
216. Cheng SC, Scicluna BP, Arts RJ, et al. Broad defects in the energy metabolism of leukocytes underlie immunoparalysis in sepsis. Nat Immunol. 2016 Apr;17(4):406-13.
217. Shalova IN, Lim JY, Chittezhath M, et al. Human monocytes undergo functional re-programming during sepsis mediated by hypoxia-inducible factor-1alpha. Immunity. 2015 Mar 17;42(3):484-98.
218. Novakovic B, Habibi E, Wang SY, et al. beta-glucan reverses the epigenetic state of LPS-induced immunological tolerance. Cell. 2016 Nov 17;167(5):1354-1368 e14.
219. Dominguez-Andres J, Novakovic B, Li Y, et al. The itaconate pathway is a central regulatory node linking innate immune tolerance and trained immunity. Cell Metabol. 2019 Jan 8;29(1):211-220 e5.
220. Akoumianaki T, Vaporidi K, Diamantaki E, et al. Uncoupling of IL-6 signaling and LC3-associated phagocytosis drives immunoparalysis during sepsis. Cell Host Microbe. 2021 Jun 25.
221. Sun Z, Qu J, Xia X, et al. 17beta-Estradiol promotes LC3B-associated phagocytosis in trained immunity of female mice against sepsis. Int J Biol Sci. 2021;17(2):460-474.
222. Mourits VP, Wijkmans JC, Joosten LA, et al. Trained immunity as a novel therapeutic strategy. Curr Opin Pharmacol. 2018 Aug;41:52-58.
223. Arts RJ, Novakovic B, Ter Horst R, et al. Glutaminolysis and fumarate accumulation integrate immunometabolic and epigenetic programs in trained immunity. Cell Metabol. 2016 Dec 13;24(6):807-819.
224. Carlstrom KE, Ewing E, Granqvist M, et al. Therapeutic efficacy of dimethyl fumarate in relapsing-remitting multiple sclerosis associates with ROS pathway in monocytes. Nat Commun. 2019 Jul 12;10(1):3081.
225. Fensterheim BA, Young JD, Luan L, et al. The TLR4 agonist monophosphoryl lipid A drives broad resistance to infection via dynamic reprogramming of macrophage metabolism. J Immunol. 2018 Jun 1;200(11):3777-3789.
226. Jawale CV, Ramani K, Li DD, et al. Restoring glucose uptake rescues neutrophil dysfunction and protects against systemic fungal infection in mouse models of kidney disease. Sci Trans Med. 2020 Jun 17;12(548).
227. Wang A, Huen SC, Luan HH, et al. Opposing effects of fasting metabolism on tissue tolerance in bacterial and viral inflammation. Cell. 2016 Sep 8;166(6):1512-1525 e12.
228. Noor MA, Flint OP, Maa JF, et al. Effects of atazanavir/ritonavir and lopinavir/ritonavir on glucose uptake and insulin sensitivity: demonstrable differences in vitro and clinically. Aids. 2006 Sep 11;20(14):1813-21.
229. James MO, Jahn SC, Zhong G, et al. Therapeutic applications of dichloroacetate and the role of glutathione transferase zeta-1. Pharmacol Ther. 2017 Feb;170:166-180.

230. Krishnamoorthy G, Kaiser P, Abu Abed U, et al. FX11 limits *Mycobacterium tuberculosis* growth and potentiates bactericidal activity of isoniazid through host-directed activity. Dis Model Mech. 2020 Mar 30;13(3).
231. Svedberg FR, Brown SL, Krauss MZ, et al. The lung environment controls alveolar macrophage metabolism and responsiveness in type 2 inflammation. Nat Immunol. 2019 May;20(5):571-580.
232. Weiss G, Ganz T, Goodnough LT. Anemia of inflammation. Blood. 2019 Jan 3;133(1):40-50.
233. Frost JN, Tan TK, Abbas M, et al. Hepcidin-mediated hypoferremia disrupts immune responses to vaccination and infection. Med (N Y). 2021 Feb 12;2(2):164-179 e12.
234. Hissen AH, Chow JM, Pinto LJ, et al. Survival of *Aspergillus fumigatus* in serum involves removal of iron from transferrin: the role of siderophores. Infect Immun. 2004 Mar;72(3):1402-8.
235. Iglesias-Osma C, Gonzalez-Villaron L, San Miguel JF, et al. Iron metabolism and fungal infections in patients with haematological malignancies. J Clin Pathol. 1995 Mar;48(3):223-5.
236. Leal SM, Jr., Roy S, Vareechon C, et al. Targeting iron acquisition blocks infection with the fungal pathogens *Aspergillus fumigatus* and *Fusarium oxysporum*. PLoS Pathog. 2013;9(7):e1003436.
237. Subissi A, Monti D, Togni G, et al. Ciclopirox: recent nonclinical and clinical data relevant to its use as a topical antimycotic agent. Drugs. 2010 Nov 12;70(16):2133-52.
238. Almeida RS, Brunke S, Albrecht A, et al. The hyphal-associated adhesin and invasin Als3 of *Candida albicans* mediates iron acquisition from host ferritin. PLoS Pathog. 2008 Nov;4(11):e1000217.
239. Potrykus J, Stead D, Maccallum DM, et al. Fungal iron availability during deep seated candidiasis is defined by a complex interplay involving systemic and local events. PLoS Pathog. 2013;9(10):e1003676.
240. Ludwiczek S, Aigner E, Theurl I, et al. Cytokine-mediated regulation of iron transport in human monocytic cells. Blood. 2003 May 15;101(10):4148-54.
241. Kroner A, Greenhalgh AD, Zarruk JG, et al. TNF and increased intracellular iron alter macrophage polarization to a detrimental M1 phenotype in the injured spinal cord. Neuron. 2014 Sep 3;83(5):1098-116.
242. Gillen KM, Mubarak M, Nguyen TD, et al. Significance and *in vivo* detection of iron-laden microglia in white matter multiple sclerosis lesions. Front Immunol. 2018;9:255.
243. Costa da Silva M, Breckwoldt MO, Vinchi F, et al. Iron induces anti-tumor activity in tumor-associated macrophages. Front Iimmunol. 2017;8:1479.
244. Pereira M, Chen TD, Buang N, et al. Acute iron deprivation reprograms human macrophage metabolism and reduces inflammation *in vivo*. Cell Rep. 2019 Jul 9;28(2):498-511 e5.
245. Jentho E, Novakovic B, Ruiz-Moreno C, et al. Heme induces innate immune memory. bioRxiv. 2019:2019.12.12.874578.
246. Zanganeh S, Hutter G, Spitler R, et al. Iron oxide nanoparticles inhibit tumour growth by inducing pro-inflammatory macrophage polarization in tumour tissues. Nat Nanotechnol. 2016 Nov;11(11):986-994.
247. Campos CF, van de Veerdonk FL, Goncalves SM, et al. Host genetic signatures of susceptibility to fungal disease. Curr Top Microbiol Immunol. 2018 Jul 25.
248. Cunha C, Aversa F, Romani L, et al. Human genetic susceptibility to invasive aspergillosis. PLoS Pathog. 2013;9(8):e1003434.
249. Merkhofer RM, Klein BS. Advances in understanding human genetic variations that Influence innate immunity to fungi. Front Cell Infect Microbiol. 2020;10:69.

250. Lionakis MS, Levitz SM. Host control of fungal infections: lessons from basic studies and human cohorts. Annu Rev Immunol. 2018 Apr 26;36:157-191.
251. Durrant C, Tayem H, Yalcin B, et al. Collaborative cross mice and their power to map host susceptibility to *Aspergillus fumigatus* infection. Genome Res. 2011 Aug;21(8):1239-48.
252. Zhang Y, Li R, Wang X. Monogenetic causes of fungal disease: recent developments. Curr Opin Microbiol. 2020 Dec;58:75-86.
253. Barreiro LB, Quintana-Murci L. Evolutionary and population (epi)genetics of immunity to infection. Hum Genet. 2020 Jun;139(6-7):723-732.
254. Bochud PY, Chien JW, Marr KA, et al. Toll-like receptor 4 polymorphisms and aspergillosis in stem-cell transplantation. N Engl J Med. 2008 Oct 23;359(17):1766-77.
255. de Boer MG, Jolink H, Halkes CJ, et al. Influence of polymorphisms in innate immunity genes on susceptibility to invasive aspergillosis after stem cell transplantation. PloS One. 2011;6(4):e18403.
256. Koldehoff M, Beelen DW, Elmaagacli AH. Increased susceptibility for aspergillosis and post-transplant immune deficiency in patients with gene variants of TLR4 after stem cell transplantation. Transpl Infect Dis. 2013 Oct;15(5):533-9.
257. Carvalho A, Pasqualotto AC, Pitzurra L, et al. Polymorphisms in toll-like receptor genes and susceptibility to pulmonary aspergillosis. J Infect Dis. 2008 Feb 15;197(4):618-21.
258. Plantinga TS, Johnson MD, Scott WK, et al. Toll-like receptor 1 polymorphisms increase susceptibility to candidemia. J Infect Dis. 2012 Mar 15;205(6):934-43.
259. Johnson CM, Lyle EA, Omueti KO, et al. Cutting edge: a common polymorphism impairs cell surface trafficking and functional responses of TLR1 but protects against leprosy. J Immunol. 2007 Jun 15;178(12):7520-4.
260. Ferwerda B, Ferwerda G, Plantinga TS, et al. Human dectin-1 deficiency and mucocutaneous fungal infections. N Engl J Med. 2009 Oct 29;361(18):1760-7.
261. Plantinga TS, van der Velden WJ, Ferwerda B, et al. Early stop polymorphism in human *DECTIN-1* is associated with increased *candida* colonization in hematopoietic stem cell transplant recipients. Clin Infect Dis. 2009 Sep 1;49(5):724-32.
262. Rosentul DC, Plantinga TS, Oosting M, et al. Genetic variation in the dectin-1/CARD9 recognition pathway and susceptibility to candidemia. J Infect Dis. 2011 Oct 1;204(7):1138-45.
263. Plantinga TS, Hamza OJ, Willment JA, et al. Genetic variation of innate immune genes in HIV-infected african patients with or without oropharyngeal candidiasis. J Acquir Immune Defic Syndr. 2010 Sep;55(1):87-94.
264. Fisher CE, Hohl TM, Fan W, et al. Validation of single nucleotide polymorphisms in invasive aspergillosis following hematopoietic cell transplantation. Blood. 2017 May 11;129(19):2693-2701.
265. Fischer M, Spies-Weisshart B, Schrenk K, et al. Polymorphisms of Dectin-1 and TLR2 predispose to invasive fungal disease in patients with acute myeloid leukemia. PloS One. 2016;11(3):e0150632.
266. Sainz J, Lupianez CB, Segura-Catena J, et al. Dectin-1 and DC-SIGN polymorphisms associated with invasive pulmonary aspergillosis infection. PLoS One. 2012;7(2):e32273.
267. Carvalho A, Giovannini G, De Luca A, et al. Dectin-1 isoforms contribute to distinct Th1/Th17 cell activation in mucosal candidiasis. Cell Mol Immunol. 2012 May;9(3):276-86.
268. Fischer M, Muller JP, Spies-Weisshart B, et al. Isoform localization of Dectin-1 regulates the signaling quality of anti-fungal immunity. Eur J Immunol. 2017 May;47(5):848-859.

269. Glocker EO, Hennigs A, Nabavi M, et al. A homozygous CARD9 mutation in a family with susceptibility to fungal infections. N Engl J Med. 2009 Oct 29;361(18):1727-35.
270. Gazendam RP, van Hamme JL, Tool AT, et al. Two independent killing mechanisms of *Candida albicans* by human neutrophils: evidence from innate immunity defects. Blood. 2014 Jul 24;124(4):590-7.
271. Rieber N, Gazendam RP, Freeman AF, et al. Extrapulmonary *Aspergillus* infection in patients with CARD9 deficiency. JCI Insight. 2016 Oct 20;1(17):e89890.
272. Xu X, Xu JF, Zheng G, et al. CARD9(S12N) facilitates the production of IL-5 by alveolar macrophages for the induction of type 2 immune responses. Nat Immunol. 2018 May 18.
273. Tone K, Stappers MHT, Hatinguais R, et al. MelLec exacerbates the pathogenesis of *Aspergillus fumigatus*-induced allergic inflammation in mice. Front Immunol. 2021;12:675702.
274. Gresnigt MS, Cunha C, Jaeger M, et al. Genetic deficiency of NOD2 confers resistance to invasive aspergillosis. Nat Commun. 2018 6;9(1):2636.
275. Carvalho A, Cunha C, Pasqualotto AC, et al. Genetic variability of innate immunity impacts human susceptibility to fungal diseases. Int J Infect Dis. 2010 Jun;14(6):e460-8.
276. Ou XT, Wu JQ, Zhu LP, et al. Genotypes coding for mannose-binding lectin deficiency correlated with cryptococcal meningitis in HIV-uninfected chinese patients. J Infect Dis. 2011 Jun 1;203(11):1686-91.
277. Lambourne J, Agranoff D, Herbrecht R, et al. Association of mannose-binding lectin deficiency with acute invasive aspergillosis in immunocompromised patients. Clin Infect Dis. 2009 Nov 15;49(10):1486-91.
278. Damiens S, Poissy J, Francois N, et al. Mannose-binding lectin levels and variation during invasive candidiasis. J Clin Immunol. 2012 Dec;32(6):1317-23.
279. Yanagisawa K, Wichukchinda N, Tsuchiya N, et al. Deficiency of mannose-binding lectin is a risk of *Pneumocystis jirovecii* pneumonia in a natural history cohort of people living with HIV/AIDS in Northern Thailand. PLoS One. 2020;15(12):e0242438.
280. Bernal-Martinez L, Goncalves SM, de Andres B, et al. TREM1 regulates antifungal immune responses in invasive pulmonary aspergillosis. Virulence. 2021 Dec;12(1):570-583.
281. Parente R, Possetti V, Erreni M, et al. Complementary roles of short and long pentraxins in the complement-mediated immune response to *Aspergillus fumigatus* Infections. Front Immunol. 2021;12:785883.
282. Cunha C, Aversa F, Lacerda JF, et al. Genetic PTX3 deficiency and aspergillosis in stem-cell transplantation. N Engl J Med. 2014 Jan 30;370(5):421-32.
283. Cunha C, Monteiro AA, Oliveira-Coelho A, et al. PTX3-Based genetic testing for risk of aspergillosis after lung transplant. Clin Infect Dis. 2015 Dec 15;61(12):1893-4.
284. Wojtowicz A, Lecompte TD, Bibert S, et al. PTX3 polymorphisms and invasive mold infections after solid organ transplant. Clin Infect Dis. 2015 Aug 15;61(4):619-22.
285. He Q, Li H, Rui Y, et al. Pentraxin 3 gene polymorphisms and pulmonary aspergillosis in chronic obstructive pulmonary disease patients. Clin Infect Dis. 2018 Jan 6;66(2):261-267.
286. Brunel AS, Wojtowicz A, Lamoth F, et al. Pentraxin-3 polymorphisms and invasive mold infections in acute leukemia patients receiving intensive chemotherapy. Haematologica. 2018 Nov;103(11):e527-e530.
287. Bozza S, Campo S, Arseni B, et al. PTX3 binds MD-2 and promotes TRIF-dependent immune protection in aspergillosis. J Immunol. 2014 Sep 1;193(5):2340-8.

288. Gonçalves SM, Lagrou K, Rodrigues CS, et al. Evaluation of bronchoalveolar lavage fluid cytokines as biomarkers for invasive pulmonary aspergillosis in at-risk patients. Front Microbiol. 2017;8:2362.
289. Chorny A, Casas-Recasens S, Sintes J, et al. The soluble pattern recognition receptor PTX3 links humoral innate and adaptive immune responses by helping marginal zone B cells. J Exp Med. 2016 Sep 19;213(10):2167-85.
290. Carvalho A, Cunha C, Bistoni F, et al. Immunotherapy of aspergillosis. Clin Microbiol Infect. 2012 Feb;18(2):120-5.
291. Sainz J, Hassan L, Perez E, et al. Interleukin-10 promoter polymorphism as risk factor to develop invasive pulmonary aspergillosis. Immunol Lett. 2007 Mar 15;109(1):76-82.
292. Seo KW, Kim DH, Sohn SK, et al. Protective role of interleukin-10 promoter gene polymorphism in the pathogenesis of invasive pulmonary aspergillosis after allogeneic stem cell transplantation. Bone marrow Transplant. 2005 Dec;36(12):1089-95.
293. Cunha C, Goncalves SM, Duarte-Oliveira C, et al. IL-10 overexpression predisposes to invasive aspergillosis by suppressing antifungal immunity. J Allergy Clin Immunol. 2017 Sep;140(3):867-870 e9.
294. Potenza L, Vallerini D, Barozzi P, et al. Characterization of specific immune responses to different *Aspergillus* antigens during the course of invasive aspergillosis in hematologic patients. PloS One. 2013;8(9):e74326.
295. Wojtowicz A, Gresnigt MS, Lecompte T, et al. IL1B and DEFB1 polymorphisms increase susceptibility to invasive mold infection after solid-organ transplantation. J Infect Dis. 2014 Nov 14.
296. Lupianez CB, Canet LM, Carvalho A, et al. Polymorphisms in host immunity-modulating genes and risk of invasive aspergillosis: results from the AspBIOmics consortium. Infect Immun. 2015;84(3):643-57.
297. Merkhofer RM, Jr., O'Neill MB, Xiong D, et al. Investigation of genetic susceptibility to blastomycosis reveals interleukin-6 as a potential susceptibility Locus. mBio. 2019 Jun 18;10(3).
298. Mezger M, Steffens M, Beyer M, et al. Polymorphisms in the chemokine (C-X-C motif) ligand 10 are associated with invasive aspergillosis after allogeneic stem-cell transplantation and influence CXCL10 expression in monocyte-derived dendritic cells. Blood. 2008 Jan 15;111(2):534-6.
299. Swamydas M, Gao JL, Break TJ, et al. CXCR1-mediated neutrophil degranulation and fungal killing promote *Candida* clearance and host survival. Sci Transl Med. 2016 Jan 20;8(322):322ra10.
300. Lupianez CB, Martinez-Bueno M, Sanchez-Maldonado JM, et al. Polymorphisms within the *ARNT2* and *CX3CR1* genes are associated with the risk of developing invasive aspergillosis. Infect Immun. 2020 Mar 23;88(4).
301. Schmidt F, Thywissen A, Goldmann M, et al. Flotillin-dependent membrane microdomains are required for functional phagolysosomes against fungal infections. Cell Rep. 2020 Aug 18;32(7):108017.
302. Gonçalves SMF, A. V.; Cunha, C.; Carvalho, A. Targeting immunometabolism in host-directed therapies to fungal disease. Clin Exp Immunol 2021.
303. Shelburne SA, Ajami NJ, Chibucos MC, et al. Implementation of a pan-genomic approach to investigate holobiont-infecting microbe interaction: a case report of a leukemic patient with invasive mucormycosis. PloS One. 2015;10(11):e0139851.

304. Abdel-Rahman SM, Preuett BL. Genetic predictors of susceptibility to cutaneous fungal infections: a pilot genome wide association study to refine a candidate gene search. J Dermatol Sci. 2012 Aug;67(2):147-52.
305. Kumar V, Cheng SC, Johnson MD, et al. Immunochip SNP array identifies novel genetic variants conferring susceptibility to candidaemia. Nat Commun. 2014 Sep 8;5:4675.
306. Tian C, Hromatka BS, Kiefer AK, et al. Genome-wide association and HLA region fine-mapping studies identify susceptibility loci for multiple common infections. Nat Commun. 2017 Sep 19;8(1):599.
307. Kannambath S, Jarvis JN, Wake RM, et al. Genome-wide association study identifies novel colony stimulating factor 1 locus conferring susceptibility to cryptococcosis in human immunodeficiency VIrus-infected South Africans. Open Forum Infect Dis. 2020 Nov;7(11):ofaa489.
308. Bruno M, Matzaraki V, van de Veerdonk FL, et al. Challenges and opportunities in understanding genetics of fungal diseases: towards a functional genomics approach. Infect Immun. 2021 Jul 15;89(8):e0000521.
309. Bruno M, Dewi IMW, Matzaraki V, et al. Comparative host transcriptome in response to pathogenic fungi identifies common and species-specific transcriptional antifungal host response pathways. Comput Struct Biotechnol J. 2021;19:647-663.
310. Fairfax BP, Knight JC. Genetics of gene expression in immunity to infection. Curr Opin Immunol. 2014 Jul 28;30C:63-71.
311. Smeekens SP, Ng A, Kumar V, et al. Functional genomics identifies type I interferon pathway as central for host defense against *Candida albicans*. Nat Commun. 2013;4:1342.
312. Matzaraki V, Gresnigt MS, Jaeger M, et al. An integrative genomics approach identifies novel pathways that influence candidaemia susceptibility. PLoS One. 2017;12(7):e0180824.
313. Li Y, Oosting M, Deelen P, et al. Inter-individual variability and genetic influences on cytokine responses to bacteria and fungi. Nat Med. 2016 Aug;22(8):952-60.
314. Jaeger M, Matzaraki V, Aguirre-Gamboa R, et al. A genome-wide functional genomics approach identifies susceptibility pathways to fungal bloodstream infection in humans. J Infect Dis. 2019 Jul 31;220(5):862-872.
315. Matzaraki V, Le KTT, Jaeger M, et al. Inflammatory protein profiles in plasma of candidaemia patients and the contribution of host genetics to their variability. Front Immunol. 2021;12:662171.
316. de Vries DH, Matzaraki V, Bakker OB, et al. Integrating GWAS with bulk and single-cell RNA-sequencing reveals a role for LY86 in the anti-Candida host response. PLoS Pathog. 2020 Apr;16(4):e1008408.
317. Jaeger M, Pinelli M, Borghi M, et al. A systems genomics approach identifies SIGLEC15 as a susceptibility factor in recurrent vulvovaginal candidiasis. Sci Transl Med. 2019 Jun 12;11(496).
318. Dewi IMW, Cunha C, Jaeger M, et al. Neuraminidase and SIGLEC15 modulate the host defense against pulmonary aspergillosis. Cell Rep Med. 2021 May 18;2(5):100289.
319. Wang L, Pittman KJ, Barker JR, et al. An atlas of genetic variation linking pathogen-induced cellular traits to human disease. Cell Host Microbe. 2018 Aug 8;24(2):308-323 e6.

Chapter II

Phagosomal removal of fungal melanin reprograms macrophage metabolism to promote antifungal immunity

This chapter was published in:

Goncalves SM, Duarte-Oliveira C, Campos CF, et al. Phagosomal removal of fungal melanin reprograms macrophage metabolism to promote antifungal immunity. Nat Commun. 2020 May 8;11(1):2282.

Phagosomal removal of fungal melanin reprograms macrophage metabolism to promote antifungal immunity

Samuel M. Gonçalves[1,2], Cláudio Duarte-Oliveira[1,2], Cláudia F. Campos[1,2], Vishukumar Aimanianda[3,19], Rob ter Horst[4], Luis Leite[5], Toine Mercier[6,7], Paulo Pereira[8], Miguel Fernández-García[9], Daniela Antunes[1,2], Cláudia S. Rodrigues[1,2], Catarina Barbosa-Matos[1,2], Joana Gaifem[1,2], Inês Mesquita[1,2], António Marques[10], Nuno S. Osório[1,2], Egídio Torrado[1,2], Fernando Rodrigues[1,2], Sandra Costa[1,2], Leo AB Joosten[4], Katrien Lagrou[7,11], Johan Maertens[6,7], João F. Lacerda[8,12], António Campos Jr.[5], Gordon D. Brown[13], Axel A. Brakhage[14,15], Coral Barbas[9], Ricardo Silvestre[1,2], Frank L. van de Veerdonk[4], Georgios Chamilos[16,17], Mihai G. Netea[4,18], Jean-Paul Latgé[3,20], Cristina Cunha[1,2], Agostinho Carvalho[1,2]

[1] Life and Health Sciences Research Institute (ICVS), School of Medicine, University of Minho, 4710-057 Braga, Portugal

[2] ICVS/3B's - PT Government Associate Laboratory, Guimarães/Braga, Portugal

[3] Unité des Aspergillus, Institut Pasteur, 75015 Paris, France

[4] Department of Internal Medicine and Radboud Center for Infectious diseases (RCI), Radboud University Nijmegen Medical Centre, 6500HB Nijmegen, the Netherlands

[5] Serviço de Transplantação de Medula Óssea (STMO), Instituto Português de Oncologia do Porto, 4200-072 Porto, Portugal

[6] Department of Hematology, University Hospitals Leuven, 3000 Leuven, Belgium

[7] Department of Microbiology and Immunology, KU Leuven, 3000 Leuven, Belgium

[8] Instituto de Medicina Molecular, Faculdade de Medicina de Lisboa, 1649-028 Lisboa, Portugal

[9] Center for Metabolomics and Bioanalysis (CEMBIO), Faculty of Pharmacy, San Pablo CEU University, 28668 Madrid, Spain

[10] Serviço de Imuno-Hemoterapia, Hospital de Braga, 4710-243 Braga, Portugal

[11] Clinical Department of Laboratory Medicine, University Hospitals Leuven, 3000 Leuven, Belgium

[12] Serviço de Hematologia e Transplantação de Medula, Hospital de Santa Maria, 1649-035 Lisboa, Portugal

[13] Medical Research Council Centre for Medical Mycology at the University of Aberdeen, Aberdeen Fungal Group, Institute of Medical Sciences, Aberdeen AB25 2ZD, UK

[14] Department of Molecular and Applied Microbiology, Leibniz-Institute for Natural Product Research and Infection Biology (HKI), 07745 Jena, Germany

[15] Institute for Microbiology, Friedrich Schiller University, 07743 Jena, Germany

[16] Department of Medicine, University of Crete, 700 13 Heraklion, Greece

[17] Institute of Molecular Biology and Biotechnology, Foundation for Research and Technology, 700 13 Heraklion, Greece

[18] Department for Genomics & Immunoregulation, Life and Medical Sciences Institute (LIMES), University of Bonn, 53115 Bonn, Germany

[19] Present address: Molecular Mycology Unit, UMR2000 CNRS, Institut Pasteur, 75015 Paris, France

[20] Present address: Chinese Academy of Sciences, 100864 Beijing, China

Abstract

In response to infection, macrophages adapt their metabolism rapidly to enhance glycolysis and fuel specialized antimicrobial effector functions. Here we show that fungal melanin is an essential molecule required for the metabolic rewiring of macrophages during infection with the fungal pathogen *Aspergillus fumigatus*. Using pharmacological and genetic tools, we reveal a molecular link between calcium sequestration by melanin inside the phagosome and induction of glycolysis required for efficient innate immune responses. By remodeling the intracellular calcium machinery and impairing signaling via calmodulin, melanin drives an immunometabolic signaling axis towards glycolysis with activation of hypoxia-inducible factor 1 subunit alpha (HIF-1α) and phagosomal recruitment of mammalian target of rapamycin (mTOR). These data demonstrate a pivotal mechanism in the immunometabolic regulation of macrophages during fungal infection and highlight the metabolic repurposing of immune cells as a potential therapeutic strategy.

Keywords: *Aspergillus*; melanin; immunometabolism; glycolysis; calcium; macrophage; antifungal immunity; aspergillosis.

Introduction

The reprogramming of cellular metabolism is a fundamental mechanism through which innate immune cells meet the energetic and anabolic needs during host defense against invading pathogens [1]. Sensing of microbial ligands drives the upregulation of glycolysis, which delivers a rapid source of energy to support antimicrobial functions and the production of cytokines [2]. The enhanced glycolytic activity also directly supports cytokine expression through mechanisms that involve moonlighting activities of the enzymes themselves [3,4]. The metabolic pattern of myeloid cells activated by canonical stimuli (e.g., lipopolysaccharide, LPS) generally implies the downregulation of mitochondrial carbon metabolism and oxidative phosphorylation [5-8]. The disruption in the tricarboxylic acid cycle promotes the accumulation of mitochondrial metabolites that in turn regulate the expression of glycolytic enzymes to support inflammatory responses and antimicrobial functions [9]. This metabolic reprogramming generates lactate from glucose without further mitochondrial oxidation despite normoxic conditions, a phenotype observed in cancer cells and known as the Warburg effect [10]. It is now clear that, under conditions of microbial challenge, glucose metabolism is critically required; for example, compounds that block the metabolic shift to glycolysis [e.g., inhibitors of the mammalian target of rapamycin (mTOR) pathway or metformin] restrain cytokine production and dampen immune responses, hampering pathogen clearance [9,11-13]. Importantly however, other studies have shown that stimuli other than LPS induce up-regulation of both glycolysis and oxidative phosphorylation in immune cells [14].

The recognition of pathogen-associated molecular patterns (PAMPs) drives substantial changes in cellular metabolism and effector functions of immune cells [10]. Owing to its dynamic composition and structural plasticity, the cell wall is considered the most relevant repository for fungal PAMPs [15,16]. Exposure to β-1,3-glucan has been shown to promote the metabolic reprogramming of monocytes leading to a trained immunity phenotype characterized by enhanced cytokine production in response to heterologous secondary stimulation [11,17-19]. The requirement for the metabolic rewiring of myeloid cells was also demonstrated *in vivo*, since the pharmacological impairment of glycolysis [20] or the blockade of metabolic pathways with metformin [21] increased susceptibility of mice to systemic candidiasis. In turn, fungal pathogens have evolved intricate virulence strategies to withstanding the host immune response, by exploiting nutritional weaknesses of immune cells leading to their death [22].

Although β-1,3-glucan is a major fungal cell wall component, not much is known about the metabolic regulation of immunity to fungi other than *C. albicans* and whether other cell wall polysaccharides participate in these signaling events. Here we investigated the immunometabolic response of

macrophages to the opportunistic fungal pathogen *Aspergillus fumigatus*. This fungus can cause a wide spectrum of diseases with distinct clinical manifestations [23]. Epidemiological data has revealed that *A. fumigatus* causes >200,000 invasive infections each year in hematological patients under aggressive chemotherapy or undergoing solid organ or allogeneic stem-cell transplantation [24]. Because there are no licensed vaccines and the currently available diagnostic tests lack accuracy, mortality rates after infection are estimated above 30% [25].

Macrophages are considered critical in preventing fungal germination and tissue invasion early after infection, particularly before the influx of neutrophils [26]. One relevant mechanism is represented by the instruction of programmed necrosis in macrophages by calcineurin, which by stimulating the lateral transfer of conidia between macrophages, enables the control of fungal germination [27]. Other studies have highlighted the importance of inflammatory monocytes in experimental aspergillosis through their ability to orchestrate the conidiacidal activity of neutrophils and dendritic cells [28]. Moreover, there are several examples of genetic variants that predispose humans to aspergillosis by affecting the ability of myeloid cells to produce cytokines or exert their killing activity [29-32]. Although the fine-tuned regulation of cellular metabolism is required for the functional activity of macrophages, how these processes are orchestrated in response to *A. fumigatus* remains undefined.

Here we sought to understand the mechanisms through which infection with *A. fumigatus* rewires macrophage metabolism towards efficient innate immune responses. We show that fungal melanin is an essential PAMP required for the Warburg shift and the ensuing immunometabolic responses in macrophages. Our results define how the host is able to counter the immune inhibitory mechanisms deployed by fungal melanin in order to promote efficient antifungal immune responses required to control infection.

Methods

Ethics statement

The functional experiments involving cells isolated from the peripheral blood of healthy volunteers at Hospital of Braga, Portugal, was approved by the Ethics Subcommittee for Life and Health Sciences (SECVS) of the University of Minho, Portugal (no. 014/015). Experiments were conducted according to the principles expressed in the Declaration of Helsinki, and participants provided written informed consent.

Mice

Eight-week-old gender- and age- matched C57BL/6 mice were bred under specific-pathogen free condition and kept at the Life and Health Sciences Research Institute (ICVS) Animal Facility. Mice were fed ad libitum and kept under light/dark cycles of 12 hr, temperature of 18-25°C and humidity of 40-60%. Animal experimentation was performed following biosafety level 2 (BSL-2) protocols approved by the Institutional Animal Care and Use Committee (IACUC) of University of Minho and ethical and regulatory approvals were consented by SECVS (no. 074/016). All procedures in vivo followed the EU-adopted regulations (Directive 2010/63/EU) and were conducted according to the guidelines sanctioned by the Portuguese ethics committee for animal experimentation, Direção-Geral de Alimentação e Veterinária (DGAV).

Aspergillus strains and culture conditions

The A1163 *Δku80* [64] and B-5233 [65] strains of *A. fumigatus* were used as wild-type strains. The Δ*rodA*, Δ*pksP* and Δ*rodA/pksP* deletion mutants [43,47] and the mutant strains in the DHN-melanin biosynthetic pathway (Δ*pksP*, Δ*ayg1*, Δ*abr1*, Δ*abr2*, Δ*arp1* and Δ*arp2*) in the B-5233 background [66] were generated previously. Wild-type CBS110.46 and CBS386.75 strains with albino conidia [38] were also used, as indicated. All strains were grown on 2% malt extract agar or YAG agar for 7 days at 28 °C. The conidia were harvested from agar slants using phosphate buffer saline (PBS) (Gibco, Thermo Fisher Scientific) with 0.05 % Tween 20 (Sigma-Aldrich), followed by gentle agitation and subsequent filtration through a 40 μm pore size cell strainer (Falcon). The concentration of conidia/mL was determined by counting in a Neubauer chamber. Swollen conidia and germ tubes were obtained after incubation in Sabouraud liquid culture medium at 37 °C for 4 hr and 6 hr, respectively. Heat inactivation of conidia

was performed by incubation for 30 min at 90 °C, whereas UV inactivation was performed by exposing conidia to UV light for 3 hr.

Extraction of *A. fumigatus* melanin and conidial coating

Melanin from A1163 Δ*ku80* conidia was isolated using a combination of proteolytic (proteinase K; Sigma-Aldrich) and glycohydrolytic (Glucanex; Novo) enzymes, denaturant (guanidine thiocyanate) and hot, concentrated HCl (6 M) to treat conidia, resulting in an electron-dense layer similar in size and shape to the original conidial melanin layer but without the underlying cell components, named melanin ghosts [67]. Melanin-coated Δ*rodA/pksP* conidia were obtained by overnight coating of conidia with different concentrations of melanin ghosts, previously sonicated with pulses of 5 sec during 1 min, at room temperature (RT).

Isolation of PBMCs and generation of MDMs

Peripheral blood mononuclear cells (PBMCs) were enriched from buffy coats or whole blood by density gradient using Histopaque®-1077 (Sigma-Aldrich), washed twice in PBS and resuspended in RPMI-1640 culture medium with 2 mM glutamine (Gibco, Thermo Fisher Scientific) supplemented with 10% human serum (Sigma-Aldrich), 10 U/mL penicillin/streptomycin and 10 mM HEPES (Thermo Fisher Scientific) (cRPMI). Monocytes were isolated from PBMCs using positive magnetic bead separation with anti-$CD14^+$ coated beads (MACS Miltenyi) according to the manufacturer's instructions. Isolated monocytes were resuspended in cRPMI medium and seeded at a concentration of 1×10^6 cells/mL in 24-well and 96-well plates (Corning Inc.) and 8-well chamber slides (LAB-TEK, Thermo Fisher Scientific) for 7 days in the presence of 20 ng/mL recombinant human granulocyte macrophage colony-stimulating factor (GM-CSF, Miltenyi Biotec) or 20 ng/mL of macrophage colony-stimulating factor (M-CSF, Miltenyi Biotec). The culture medium was replaced every 3 days and acquisition of macrophage morphology was confirmed by visualization in a BX61 microscope (Olympus).

Generation of BMDMs

Bone marrow-derived macrophages (BMDMs) were obtained from femur and tibia bones of male or female 8-week-old C57BL/6 or $Hif1a^{fl/fl}$-$LysMcre^{+/+}$, hereafter referred as $HIF1^c$, mice. Briefly, bone marrow was harvested and cultured in Dulbecco's modified medium (DMEM) with 1%

penicillin/streptomycin, 1% L-glutamine and 10% FBS (Gibco, Thermo Fisher Scientific), supplemented with 20 ng/mL M-CSF (Peprotech) for 7 days at 37 °C and 5% CO_2, with the addition of 20 ng/mL of M-CSF at day 4 of differentiation. Acquisition of macrophage morphology was confirmed by visualization in a BX61 microscope (Olympus).

Cell stimulations and treatments

Unless otherwise indicated, MDMs or BMDMs (5×10^5/well in 24-well plates) were infected with *A. fumigatus* conidia at a 1:2 or 1:10 effector-to-target ratio or stimulated with 100 µg/mL of melanin ghosts or with 50, 75, 100 and 200 µg/mL 1,8-DHN for 24 hr at 37 °C and 5% CO_2. For experiments involving glucose depletion, RPMI 1640 medium without glucose (Thermo Fisher Scientific) was used. To interfere with cellular metabolism, MDMs were pre-treated for 1 hr with 5, 10 or 20 mM 2-DG, 30 µM 3PO, 500 nM 6-AN, 10 µM wortmannin or 10 nM rapamycin, and for 3 hr with 50 µM (+)-sodium L-ascorbate. For experiments involving calcium manipulation, MDMs were pre-treated for 30 min with 2 µM thapsigargin, or treated for 10 min with 25 µM W7 (all from Sigma-Aldrich) in calcium-free DMEM (Thermo Fisher Scientific) or for 1 hr with 500 µM EGTA-AM (Thermo Fisher Scientific) after infection. In some conditions, MDMs were cultured for 1 hr with calcium-free DMEM followed by the addition of 2 mM $CaCl_2$ during infection. To assess cell viability, 4 hr prior to the end of infection, 50 µL of alamarBlue™ Cell Viability Reagent (Thermo Fisher Scientific) were added to each well. Viability was assessed by the quantification of relative fluorescence units (RFU) using a Varioskan Flash fluorescent plate reader (Thermo Fisher Scientific) with a fluorescence excitation wavelength of 570 nm and an emission wavelength of 600 nm. In some experiments, viability was evaluated by flow cytometry using annexin-V/propidium iodide 6 hr after infection. In all experiments involving MDMs, data was assessed in triplicates and is shown as the mean value for each individual.

siRNA-mediated gene silencing

MDMs (5×10^4/well in 96-well plates) were incubated for 72 hr at 37°C and 5% CO_2 in Accell Delivery Media in the presence of either 1 µM STIM1 siRNA or a non-targeting siRNA control (siNC) (Dharmacon). After incubation, the transfection media was removed, and cells were infected with *A. fumigatus* conidia at a 1:10 effector-to-target ratio. Pooled replicates from three different individuals were collected after 24 hr to measure lactate secretion and cytokine production. The mRNA knockdown was confirmed by qPCR.

RNA sequencing

MDMs (5×10^5/well in 24-well plates) were infected with *A. fumigatus* conidia at a 1:2 effector-to-target ratio, and pooled replicates from three different individuals were collected after 2 and 6 hr. Uninfected MDMs were cultured in parallel as controls. Sample processing, sequencing and analysis was performed at IMGM Laboratories GmbH (Germany). Briefly, total RNA was isolated using the RNeasy Mini Kit (Qiagen) according to the manufacturer's instructions including on-column DNase digestion. Total RNA was eluted in 30 μL of RNase-free water. The quality of total RNA was analyzed with the 2100 Bioanalyzer using RNA 6000 Nano and Pico LabChip kits (Agilent Technologies). Library preparation was performed using the TruSeq® Stranded mRNA HT technology, according to the manufacturer's protocol. All single libraries were pooled into a final sequencing library with an equal DNA amount per sample. The final sequencing library generated by pooling was quantified using the highly sensitive fluorescent dye-based Qubit® dsDNA HS Assay kit (Invitrogen) before sequencing at a final concentration of 1.8 pM and with a 1% PhiX v3 control library spike-in (Illumina) on the NextSeq500 sequencing system (Illumina). For the clustering and sequencing of samples, a high output single-end 75 cycles (1×75bp SE) run was performed under the control of the NextSeq Control Software (NCS, Illumina). Quality control was carried out using NCS and Real Time Analysis 2.4.11 softwares applying the *FastQ only* pipeline. Read data were imported into the CLC Genomics Workbench (CLC bio, Qiagen) and reads were mapped against the human reference genome (GRCh37.p13) with subsequent counting and distribution of reads across genes and transcripts. The expression values were then processed to reads per kilobase million (RPKM), a normalized measure of relative abundance of transcripts [68], followed by analysis using the EdgeR Bioconductor package [69] to identify differentially expressed genes with a fold change value ≥ 2 or ≤ -2 with a false discovery rate (FDR)-corrected p-value <0.05. Heat maps were created for the most significantly represented genes of a specific functional class using the Morpheus tool (Broad Institute; https://software.broadinstitute.org/morpheus/). For pathway analysis, the annotated hallmark gene sets from the Molecular Signatures Database (MSigDB) [33] were used and enrichment analysis was performed using the Gene Ontology Biological Processes category in the Gene Ontology Consortium software (http://www.geneontology.org/).

Quantification of glucose and lactate by HPLC

After infection, supernatants were removed, centrifuged and transferred to HPLC tubes. Glucose and lactate levels were determined using a Gilson pump system (Gilson) with a 54 °C HyperREZ XP Carbohydrate H^+ 8 μM (Thermo Fisher Scientific) column and a refractive index detector (IOTA 2, Reagents). The mobile phase consisting of 0.0025 M H_2SO_4 was filtered and degasified for at least 45 min before use. Standard solutions were prepared in MilliQ water (Millipore). All data was analyzed using the Gilson Uniprot Software, version 5.11.

LC-MS/MS targeted metabolomics

MDMs (2×10^6/well, in 6-well plates) were infected with *A. fumigatus* conidia at a 1:2 effector-to-target ratio for 6 hr at 37 °C in 5% CO_2. To detach the cells, the bottom of the well was scraped lightly with a cell scraper. The resulting cell suspensions, obtained from pooled replicates from three different individuals, were centrifuged at 4 °C, the supernatant was discarded, and the resulting pellet was immediately frozen in liquid nitrogen to quickly quench the metabolism. To maximize overall metabolite yield, 280 μL of MeOH:MTBE (Methyl tert-butyl ether) (4:1, v/v) was added to the pellet, followed by three cycles of freezing/thawing in liquid nitrogen and in cold-water bath, respectively, for 10 seconds each. A sonication at 15 W for 6 min was then performed, followed by 1 min of vortexing and a centrifugation at 4 °C. From the resulting supernatant, a volume of 250 μL was carefully transferred to a new Eppendorf tube. Additionally, 280 μL of MeOH:H_2O (4:1, v/v) was added to the pellet and the same procedure above was performed. At the end, 250 μL of the resulting supernatant was mixed with the first 250 μL of supernatant. The samples were stored at -80 °C until further analysis. To perform the metabolomics analysis, standards of analytical grade (Sigma-Aldrich) were used for external calibration and adjusted to the corresponding levels in the samples. Ultrapure water, purified using a Milli-Q system (Millipore), was used for buffer preparation. Liquid chromatography-mass spectrometry (LC-MS) grade methanol and acetonitrile (both from Thermo Fisher Scientific) were used. Tributylamine (≥99.5%) (Sigma-Aldrich) stock solutions of all the standards were prepared at 1000 ppm in water and stored at -20 °C. The LC-MS/MS analyses were performed in an Agilent 1290 Infinity (Agilent Technologies) using a 1290 Infinity Binary Pump (1200 bar) and a 1260 Infinity Quaternary Pump (400 bar). The LC system was coupled to an Agilent 6460 triple quadrupole mass spectrometer using an electrospray ionization (ESI) interface working in multiple reaction monitoring (MRM) mode. The chromatographic method, the MS parameters and the

setup arrangement were based on that described by Agilent Technologies, Inc, with minor modifications. Briefly, this method uses tributylamine as an ion-pairing reagent, with buffer A composed of 97% water and 3% methanol, 10 mM tributylamine, 15 mM glacial acetic acid (VWR) and buffer B composed of 10 mM tributylamine, 15 mM glacial acetic acid, prepared in methanol. The transitions showing the highest signal to noise ratios were used for the quantification of the analytes in samples.

Mouse infection

For the *in vivo* studies, at day -3 before infection and until the end of experimental protocol, 100 mg/Kg of 2-DG was administered to mice daily via intraperitoneal route (i.p.). Control groups consisted of mice to which an equal volume of vehicle (sterile PBS) was administered. At day 0, mice were challenged with 1×10^8 live conidia of *A. fumigatus* (A1163 Δ*ku80* strain) using a noninvasive intranasal (i.n.) infection procedure upon anesthesia with 75 mg/Kg of ketamine (Ketamidor®, Ritcher Pharma) and 1 mg/Kg of medetomidine (Domtor®, Ecuphar). At 24 hr post-infection, mice were sacrificed, and the lungs were PBS-perfused and excised, excluding the trachea and major bronchi. For assessment of fungal burden, lung single-cell suspensions were serially diluted and plated on solid growth media.

Determination of systemic glucose

On the day of the experiment, mice were starved for 3-4 hr in the morning before measurements of blood glucose levels at 0 hour, by snipping the very end of the tail to collect a drop of blood in a Glucocard®+ (Arkray), which was read using the ACCU-CHEK Performa glucometer (Roche). Afterwards, mice were infected intranasally with 1×10^8 conidia of the Δ*ku80* strain with *ad libitum* access to food. After 20 hr of infection, mice were again starved for 3-4 hr before glucose measurement in the blood. The systemic glucose concentration was calculated as the glucose (mM) per gram of mice body weight.

Isolation of splenocytes

Infected animals were sacrificed at day 1 post-infection with posterior spleen excision. The excised spleen was minced into small fragments with a plunger end of a syringe and forced through a 70-μm cell strainer (Corning Inc.) Upon washing the cells with cold sterile PBS, the resulting cell pellet was resuspended in 2 mL of pre-warmed ACK lysis buffer (0.15 M NH_4Cl, 10 Mm $KHCO_3$ and 0.1 mM EDTA). Afterwards, the cells were centrifuged at 1,600 rpm for 5 min at RT. Finally, the cells were counted and adjusted to a

final concentration of 5×10^6 cells/mL of pre-warmed RPMI (Gibco, Thermo Fisher Scientific) supplemented with 10% FBS (Gibco, Thermo Fisher Scientific) and 200 µL of the cellular suspension were seeded in round bottom 96-well plates (Corning Inc.).

FACS analysis and sorting

After infection, the lungs were excised and collected in incomplete Dulbecco's Modified Eagle Medium (iDMEM) culture medium (Gibco, Thermo Fisher Scientific). Perfused lungs were chopped in small fragments and digested at 37 °C for 30 min in iDMEM culture medium containing 1 mg/mL of collagenase D (Sigma-Aldrich). Subsequently, the tissue was forced through a 70-µm cell strainer and contaminating red blood cells were lysed. Leukocytes were isolated by Percoll (GE Healthcare Bio-Sciences Ab) density gradient and finally resuspended in FACS buffer (PBS containing 2% FBS and 2 mM EDTA). To assess cell viability, cells were stained for 30 min in the dark with the Zombie Violet fluorescent dye (BioLegend) and resuspended in FACS buffer. For surface marker staining, cell suspensions were stained for 30 min on ice while protected from light with the indicated antibodies. Pellets were washed and resuspended in fresh FACS buffer prior to analysis. Gating for myeloid subpopulations in the lung was performed to analyze the composition of lung-infiltrating cells using a combination of the following antibodies: BV510 anti-mouse CD45 (clone 30-F11), BV605 anti-mouse CD11c (clone N418), PE-Cy7 anti-mouse CD11b (clone M1/70) and APC anti-mouse F4/80 (clone BM8) (all from BioLegend) [22]. Data were obtained on a BD FACS LSRII instrument (Becton Dickinson) and processed using FlowJo (Tree Star Inc). For the sorting of macrophage populations in the lung, CD45+ positive cells were isolated using positive magnetic bead separation with anti-CD45+ coated beads (MACS Miltenyi) before surface marker staining. Macrophages were sorted using a combination of the following antibodies: PerCP/Cy5.5 anti-mouse CD11c (clone N418), APC anti-mouse CD11b (clone M1/70), PE anti-mouse Siglec-F (clone E50-2440), APC-Cy7 anti-mouse Ly-6G (clone 1A8), FITC anti-mouse CD64 (clone X54-5/7.1), and PE/Cy7 anti-mouse CD45 (clone 30-F11) (from BioLegend or BD Biosciences) [70]. Data were obtained on a BD FACSAria II instrument and analyzed with the FACSDiva software (Becton Dickinson).

Measurement of ADP/ATP ratio

MDMs (1×10^5/well in 96-well plates) were infected with *A. fumigatus* conidia for 6 hr at a 1:10 effector-to-target ratio at 37°C in 5% CO_2. After infection, the ADP/ATP ratio was measured using an assay kit

(Sigma-Aldrich), according to the manufacturer's instructions. Briefly, culture medium was removed, and the ATP reagent was added to each well. Plate was incubated for 1 min at RT and luminescence was read to obtain ATP levels. After 10 min of incubation at RT, the ADP reagent was added to each well and luminescence was read. The ADP/ATP ratio was calculated by subtracting background values from ADP values and dividing the result by ATP values. Luminescence was read in a Fluoroskan FL Microplate Luminometer (Thermo Fisher Scientific).

Phagocytosis assay

To determine phagocytosis, MDMs (5×10^5/well, in 24-well plates) were infected with fluorescein isothiocyanate (FITC)-labelled conidia of *A. fumigatus* at a 1:5 effector-to-target ratio. The infection was synchronized for 30 min at 4 °C and phagocytosis was initiated by shifting the co-incubation to 37 °C at 5% CO_2 for 1 h. Phagocytosis was stopped by washing wells with PBS and extracellular conidia were stained with 0.25 mg/mL Calcofluor White (Sigma-Aldrich) for 15 min at 4 °C to avoid further ingestion. Wells were then washed twice with PBS and cells were fixed with 3.7% (v/v) formaldehyde/PBS for 15 min. The number of MDMs with ingested green conidia was enumerated by examining the slides by fluorescence microscopy (Olympus), and data were expressed as percentage of MDMs that internalized one or more conidia.

Conidiacidal activity assay

Following differentiation, MDMs (1×10^5/well, in 96-well plates) were washed twice with cRPMI medium and a suspension of *A. fumigatus* conidia was added at a 10:1 effector-to-target ratio. The cells were then incubated for 1 hr at 37 °C and 5% CO_2 to allow the internalization of conidia. Medium containing the non-ingested conidia was removed, and wells were washed twice with pre-warmed PBS. To measure the conidiacidal ability, MDMs were allowed to kill the ingested conidia for 2 hr at 37 °C in 5% CO_2. To determine the fungicidal activity of splenocytes, cells (1×10^6/well in 96-well plates) were infected with *A. fumigatus* conidia at a 1:5 effector-to-target ratio for 2 hr at 37 °C and 5% CO_2. After incubation, culture plates were snap frozen at -80 °C and thawed at 37 °C to cause cell lysis and release of ingested conidia. Serial dilutions of cell lysates were plated on solid growth media and, following a 24 hr incubation at 37 °C, the number of colony-forming units (CFUs) was enumerated and the percentage of CFU inhibition was calculated.

Measurement of ROS production

MDMs (1×10^5/well) were plated in 96-well TC-treated dark clear bottom plates (Sigma-Aldrich) and infected with live *A. fumigatus* conidia at a 1:3 effector-to-target ratio. Infections were synchronized by centrifugation at 1,000 rpm for 5 min, and then 10 μM dihydrorhodamine 123 (DHR) (Thermo Fisher Scientific) was added to each well and the production of reactive oxygen species (ROS) was measured for a 24 hr period using the Varioskan Flash fluorescent plate reader (Thermo Fisher Scientific). Excitation was performed at a wavelength of 480 nm and emission was measured at a wavelength of 528 nm.

Cytokine measurements

MDMs and BMDMs (5×10^5/well, in 24-well plates) and splenocytes (1×10^6/well, in 96-well plates) were infected with *A. fumigatus* conidia at a 1:10 effector-to-target ratio for 24 hr at 37 °C and 5% CO_2. PBMCs (5×10^5/well in 96-well plates) were infected with UV-inactivated conidia at a 1:4 effector-to-target ratio for 7 days at 37 °C and 5% CO_2. After infection, supernatants were collected and cytokine levels were quantified using ELISA MAX Deluxe Set kits (BioLegend), according to the manufacturer's instructions. Quantitative cytokine measurements were also performed on the supernatants of lung single-cell suspensions 24 hr post-infection.

RNA isolation and qRT-PCR

Total RNA from MDMs (5×10^5/well, in 24-well plates) was isolated at different time points after infection with *A. fumigatus* at a 1:10 effector-to-target ratio using the PureLink™ RNA Mini Kit (Thermo Scientific) according to the manufacturer's instructions. Total RNA from lungs was extracted using the GRS Total RNA Kit - Tissue (Grisp) at different time points after infection, according to the manufacturer's instructions. The concentration and quality of total RNA in each sample was determined by spectrophotometry using the ND-100 UV-visible light spectrophotometer (NanoDrop). One microgram of total RNA was retro-transcribed using the First-strand cDNA Synthesis Kit (Nzytech). Quantitative PCR was performed in an Applied Biosystems 7500 Fast qPCR system (Applied Biosystems, Thermo Fisher Scientific), using the PowerUp SYBR Green Master Mix (Applied Biosystems, Thermo Fisher Scientific). Data were analyzed using the 7500 Software v2.0.6 software (Applied Biosystems, Thermo Fisher Scientific). Amplification efficiencies were validated, and the expression levels of the transcripts were normalized using the *ACTB* (human), *Ubb* (mouse) and 18S (*A. fumigatus*) genes.

Western blot analysis

Human MDMs (5×10^5/well, in 24-well plates) were infected with *A. fumigatus* conidia for the indicated time points at a 1:10 effector-to-target ratio at 37 °C in 5% CO_2. After infection, cells were lysed in RIPA buffer (50 mM Tris, 250 mM NaCl, 2 mM EDTA, 1% NP-40, 10% glycerol, pH 7.2, and a mixture of protease inhibitors [Roche Molecular Biochemicals]). Cell lysis was performed at 4 °C for 30 min (with shaking) and samples were then centrifuged. The protein content was determined using the Bradford dye-binding (Bio-Rad) method. Laemmli buffer (Bio-Rad) was added to 20 μg of protein and samples were boiled and separated on a 12% SDS-PAGE gel and transferred to nitrocellulose membranes (Bio-Rad). Western blotting was performed according to manufacturer's instructions, using the following primary antibodies: rabbit anti-phospho-p70 S6 Kinase, rabbit anti-p70 S6 Kinase, rabbit anti-Akt, rabbit anti-phospho-Akt, rabbit anti-mTOR (all from Cell Signaling), mouse anti-β-actin (Abcam), all diluted 1:1000, and rabbit anti-HIF-1α antibody (Abcam) diluted 1:500. Secondary antibodies used were anti-rabbit and anti-mouse, both diluted to 1:5000. The blots were developed using chemiluminescence (SuperSignal™ West Femto Maximum Sensitivity Substrate; Thermo Fisher Scientific) and detected with ChemiDocTM XRS system (Bio-Rad). Signal intensities and quantifications were determined with the ImageLab 4.1 analysis software (Bio-Rad).

Live cell imaging

To perform live imaging of calcium, MDMs were seeded in 8 well-chamber slides (LAB-TEK, Thermo Fisher Scientific) (3×10^5/well) and loaded with 3 μM of the calcium indicator Fluo-4AM (Thermo Fisher Scientific) according to the manufacturer's protocol. Briefly, MDMs were placed in serum-free HBSS (without Ca^{2+}, $MgCl_2$ and phenol red) and loaded with Fluo-4AM for 30 min at 37 °C, 5% CO_2. Cells were then washed twice with PBS and infections with the indicated fungal strains were performed in cRPMI medium. Live cell imaging was performed on an Olympus FV1000 Plus Confocal Microscope (60× Luc Plan FL 0.70 NA objective) at 37 °C with 5 % CO_2. All analyses and processing were made using ImageJ software (Fiji). To visualize the temporal changes in calcium, raw sequences were processed and mean pixel intensity at each frame was measured. The data was first plotted as fluorescence intensity versus time (Z profile) and subsequently converted to relative scale (ΔF/F baseline). To perform imaging of HIF-1α, MDMs were seeded in 8 well-chamber slides (LAB-TEK, Thermo Fisher Scientific) (3×10^5/well) and infected for 2 hr with the indicated FITC-labelled fungal strain at 37 °C in 5% CO_2. After washing twice

with PBS, the cells were fixed with 3.7% (v/v) formaldehyde/PBS for 15 min, permeabilized with 0.3% Triton™ X-100 (Sigma-Aldrich) in PBS for 10 min, blocked with 4% BSA (Sigma-Aldrich) for 1 hr and incubated overnight with primary antibody rabbit anti-HIF-1α antibody (dilution 1:100, Abcam). MDMs were then washed twice with PBS and incubated with goat anti-Rabbit IgG (H+L) Cross-Adsorbed Secondary Antibody Alexa Fluor® 568 conjugate (dilution 1:1000, Thermo Fisher Scientific) for 1 hr at RT. Nuclei were stained with DAPI (dilution 1:1000, Thermo Fisher Scientific) for 10 min. Images were captured at 100× magnification in an Olympus FV1000 Plus Confocal microscope. HIF-1α quantification was performed using ImageJ (Fiji) and expressed as nuclear/total HIF-1α staining of at least 60 cells for each condition. For immunofluorescence imaging of mTOR on phagosomes, MDMs were seeded on coverslips pretreated with polylysine, fixed with 4% PFA for 15 min at RT following by 10 min of fixation with ice cold methanol at -20°C, washed twice with PBS, permeabilized by using 0.1% saponin (Sigma-Aldrich) and blocked for 30 min PBS with 2% BSA. After incubation with anti-mTOR antibody (dilution 1:250; Cell Signaling) for 1 hr, slides were washed twice in PBS-BSA and stained with the Alexa Fluor 555 secondary antibody (Molecular Probes), followed by DNA staining with 10 µM TOPRO-3 iodide (642/661; Invitrogen). After the washing steps, slides were mounted in Prolong Gold antifading media (Molecular Probes). Images were acquired using a laser-scanning spectral confocal microscope (TCS SP2; Leica), LCS Lite software (Leica), and a 40× Apochromat 1.25 NA oil objective using identical gain settings. A low fluorescence immersion oil (11513859; Leica) was used, and imaging was performed at room temperature. Unless otherwise stated, mean projections of image stacks were obtained using the LCS Lite software and processed with Adobe Photoshop CS2. Phagosomes surrounded by a rim of fluorescence of the indicated protein-marker were scored as positive [43,47]. At least 200 phagosomes were analyzed for each condition in two independent experiments.

Statistical analysis

The data were expressed as means ± SEM. Statistical significance of differences were determined by two-tailed Student's t-test, one-way ANOVA or two-way ANOVA with post hoc tests for multiple comparisons ($P<0.05$ was considered statistically significant). Analyses were performed in GraphPad Prism software.

Results

Macrophage metabolism is modulated by *A. fumigatus* infection

Our first aim was to investigate host cellular metabolism during the interaction of human macrophages with *A. fumigatus*. We chose two time points after infection corresponding to the early transcriptional events following phagocytosis (2 hr) and the initial phases of fungal escape by germination (6 hr). RNA-seq analysis revealed substantial changes in the macrophage transcriptome after 2 hr of infection, encompassing 1,187 differentially expressed genes relative to uninfected controls (Fig. 1a). The number of differentially expressed genes decreased markedly at 6 hr to a total of 83, indicating that the bulk of transcriptional changes occurred early after infection. Enrichment analysis demonstrated that pathways involved in cytokine production and signalling, response to inflammatory stimuli, and immune cell differentiation were overrepresented in the upregulated genes after 2 hr of infection (Fig. 1b). In accordance with the low number of differentially expressed genes detected 6 hr after infection, genes involved in the negative regulation of transcription and DNA binding were enriched in the downregulated pathways.

A targeted analysis of the differentially expressed genes after 2 hr of infection using hallmark gene sets from the Molecular Signatures Database [33] revealed a substantial upregulation of genes involved in glycolysis, but not oxidative phosphorylation (Fig. 1c). The commitment of macrophages towards glycolysis was reflected by the upregulation of the glucose transporters *SLC2A1* (*GLUT1*) and *SLC2A6* (*GLUT6*), the key glycolytic regulator 6-phosphofructose-2-kinase/fructose-2,6-bisphosphatase 3 (*PFKFB3*), and hypoxia-inducible factor 1 subunit alpha (*HIF1A*). In contrast, thioredoxin-interacting protein (*TXNIP*), which encodes a redox sensor that suppresses glucose uptake and metabolism [34], was instead downregulated. These results were consistent with a skewing of infected macrophages towards an M1 inflammatory phenotype characterized by the upregulation of several proinflammatory cytokines, including *IL1B*, *TNF* and *IL6*.

Gene expression analysis using a more detailed time course of infection demonstrated that induction of glycolytic genes such as *GLUT1*, hexokinase 2 (*HK2*) and *PFKFB3* initiated early after the challenge and was sustained throughout infection (Fig. 1d). *Glut1* and several glycolytic enzymes were also induced in the lungs of mice as early as day 1 and until day 3 after fungal infection (Fig. 1e). The transcriptional induction of glycolysis was confirmed by the increased secretion of lactate and glucose consumption by human macrophages throughout the infection, an effect that was dependent on the multiplicity of infection

(Fig. 1f), but was not influenced by the differentiating stimulus (Supplementary Fig. 1a). Fungal infection also elicited an increased ADP/ATP balance (Fig. 1g). To gain further insight into the metabolites produced along the glycolytic pathway, we performed a targeted analysis of metabolic pathways after 6 hr of infection using liquid chromatography tandem-mass spectrometry (LC-MS/MS). In these conditions, increased levels of most glycolytic intermediates were detected, namely fructose-6-phosphate, dihydroxyacetone phosphate, glyceraldehyde-3-phosphate and pyruvate (Fig. 1h).

The metabolic rewiring of macrophages during infection commits them to glucose metabolism for survival, and this phenotype is exploited by *C. albicans* to trigger cell death by depleting glucose levels [22]. In contrast, human macrophages infected with *A. fumigatus* did not display a significant loss of viability, even after 24 hr of infection (Supplementary Fig. 1b). Likewise, the total number of macrophages in the lungs of infected mice also remained intact after infection (Supplementary Fig. 1c). Further supporting the lack of macrophage death due to competition for glucose, expression of fungal glycolytic enzymes, including ATP-dependent 6-phosphofructokinase (*pfkA*) and hexokinase-1 (*hxkA*), was not significantly modulated during infection (Supplementary Fig. 1d), a finding in line with the negligible amount of lactate measured during fungal culture (Supplementary Fig. 1e). These results reveal the glycolytic reprogramming of macrophages in response to *A. fumigatus*, while highlighting different metabolic strategies across fungal genera to survive and thrive during infection.

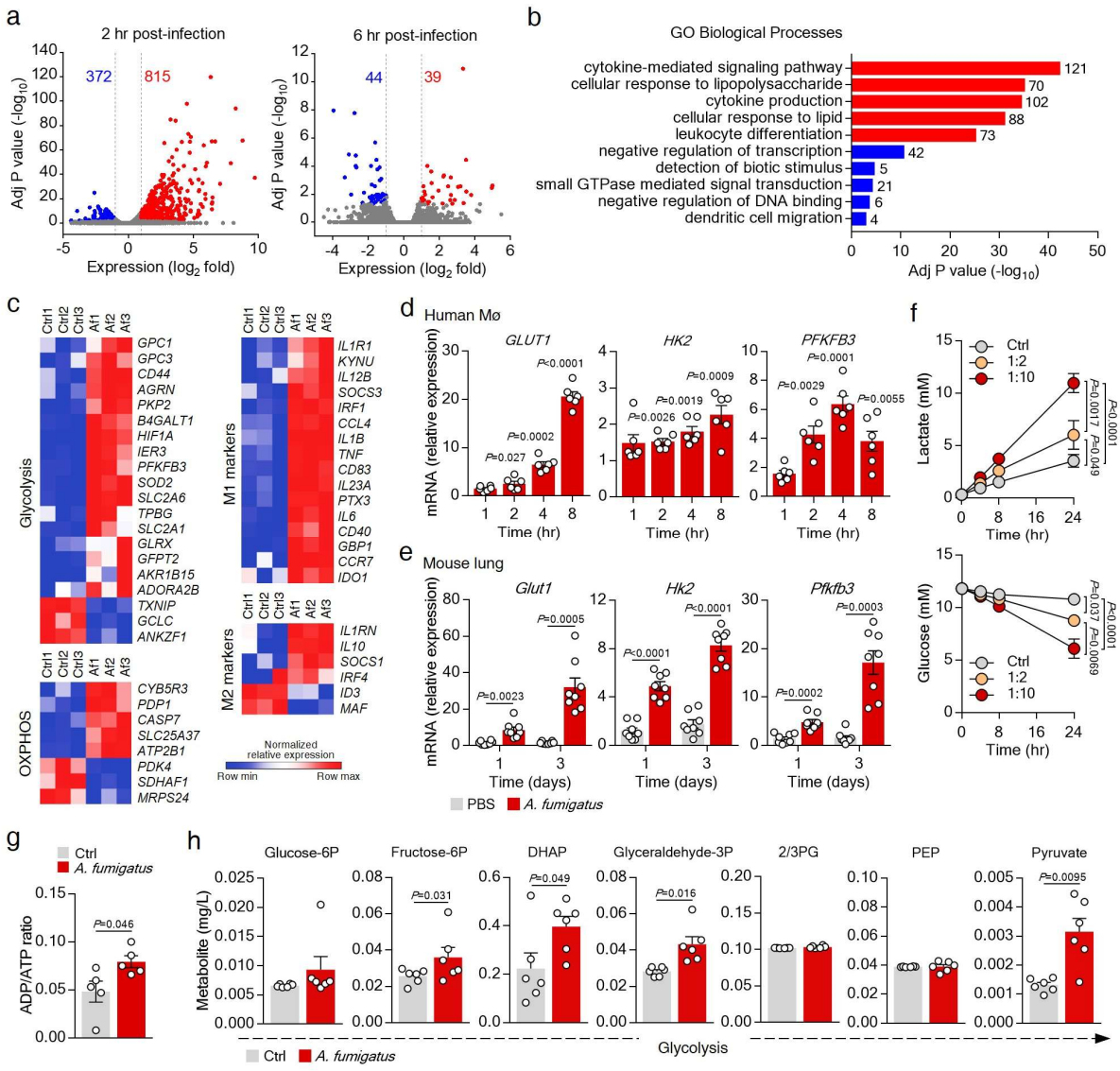

Figure 1. *A. fumigatus* induces glycolysis in macrophages. (a) Transcriptome analysis of human macrophages infected with *A. fumigatus* for 2 or 6 hr. Numbers indicate genes with differential expression, up- (red) or down-regulated (blue) in infected relative to uninfected cells. (b) Pathway analysis of up- (red) or down-regulated (blue) genes 2 hr after infection. Genes were categorized into the most represented pathways in which the gene products are involved. (c) Transcriptional profiles of macrophages left untreated (Ctrl) or infected with *A. fumigatus* (Af) for 2 hr (n=3). Expression of genes is presented as centered and scaled $\log_2$ fluorescence intensity (blue and red keys) grouped by product function. (d) mRNA expression of *GLUT1*, *HK2* and *PFKFB3* in macrophages infected for 1, 2, 4 or 8 hr relative to uninfected cells (n=6). (e) mRNA expression of *Glut1*, *Hk2* and *Pfkfb3* in mouse lungs sampled 1 or 3 days after infection (n=8, representative of three independent experiments). (f) Lactate secretion and glucose consumption by macrophages left untreated or infected at 1:2 or 1:10 for 24 hr (n=6). (g) ADP/ATP ratio (n=5) and (h) targeted metabolomics (n=6) in macrophages left untreated or infected for

6 hr. Data are expressed as mean values ± SEM; P values were calculated using Student's two-tailed t test or two-way ANOVA with Tukey's multiple comparisons test.

Glycolysis is required for immune responses to *A. fumigatus*

Production of proinflammatory cytokines, phagocytosis and killing are major effector functions of macrophages during infection with *A. fumigatus* [16]. We tested therefore how the inhibition of glycolysis using 2-deoxyglucose (2-DG), a competitive inhibitor of hexokinase, affected these processes. We confirmed that the treatment with 2-DG decreased lactate secretion by infected macrophages in a dose-dependent manner (Fig. 2a), without affecting cellular viability (Supplementary Fig. 2a). Likewise, macrophages cultured in glucose-deprived media or media containing galactose, impairing the glycolytic flux, were also unable to secrete lactate during infection (Supplementary Fig. 2b). Upon treatment with 2-DG (Fig. 2b) or using media without glucose or with galactose (Supplementary Fig. 2c), macrophages displayed an impaired conidiacidal activity, which was in line with the decreased production of reactive oxygen species (Fig. 2c). The phagocytic ability instead remained intact (Fig. 2d), a finding supported by data showing that phagocytosis relies on oxidative phosphorylation [14]. In addition, treatment of macrophages with 2-DG (Fig. 2e) or the use of glucose-deprived media (Supplementary Fig. 2d) impaired the production of proinflammatory cytokines, including IL-1β, TNF and IL-6, after 24 hr of infection. The production of adaptive cytokines by PBMCs, such as IFNγ and IL-17A, detected after 7 days of infection, was also compromised following the blockade of glycolysis (Supplementary Fig. 2e).

Since the blockade of hexokinase by 2-DG might also affect the pentose phosphate pathway (PPP), we evaluated lactate secretion by macrophages treated with 3-(3-pyridinyl)-1-(4-pyridinyl)-2-propen-1-one (3PO), a selective inhibitor of PFKFB3, and 6-aminonicotinamide (6-AN), an inhibitor of the 6-phosphogluconate dehydrogenase enzyme from the PPP. In these conditions, we confirmed an impaired lactate secretion (Fig. 2f) and cytokine production (Supplementary Fig. 2f) using 3PO, but not 6-AN. To gain further insight into lung microenvironment-associated effects on glycolysis, we measured lactate secretion by murine alveolar macrophages after infection (Fig. 2g and Supplementary Fig. 2g). The results showed an induction of lactate secretion, an effect that was abrogated following treatment with 2-DG. Collectively, these data highlight the critical requirement for glycolysis to host defense mechanisms in response to *A. fumigatus*.

Because our results pointed to a pivotal role of glucose metabolism in antifungal host defense, we next validated this requirement in a mouse model of pulmonary aspergillosis, in which immunocompetent animals were treated with 2-DG or PBS prior to infection (Fig. 2h). In line with the activation of glucose metabolism, we detected systemic hypoglycemia in mice after the challenge (Supplementary Fig. 2h). Blocking glycolysis rendered mice more susceptible to infection, as revealed by the increased fungal burden in the lungs 1 day after infection (Fig. 2h), a finding that did not involve loss of viability of alveolar macrophages (Supplementary Fig. 2i). In addition, the levels of cytokines in lung homogenates from 2-DG-treated mice were significantly lower than those from mock-treated animals (Fig. 2i). Consistently, the production of cytokines after restimulation of splenocytes from 2-DG-treated mice (Fig. 2j) and their conidiacidal activity (Fig. 2k) was also impaired. Taken together, these data confirm that glucose metabolism plays a central role in the induction of host responses to *A. fumigatus in vivo*.

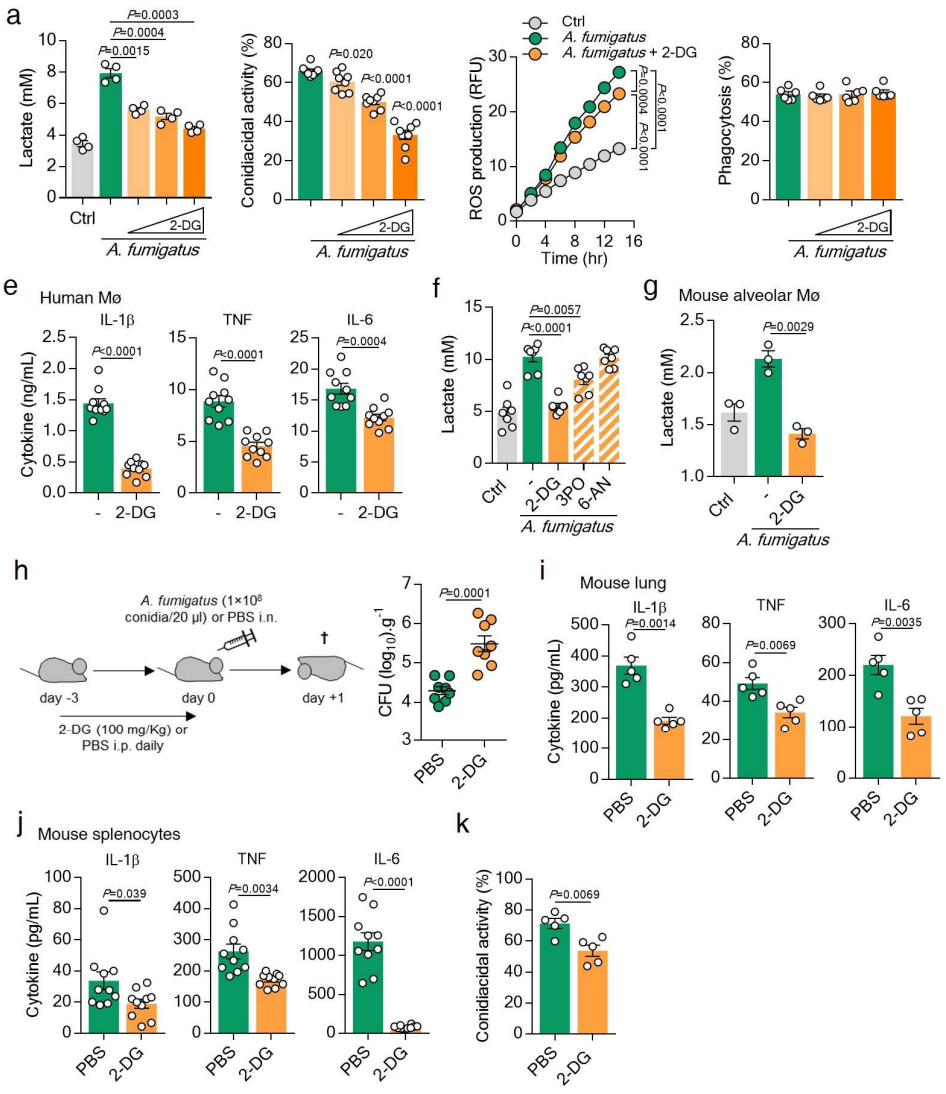

Figure 2. Glycolysis is required for antifungal immune responses. (a) Lactate secretion (n=4) and (b) conidiacidal activity (n=8) of macrophages left untreated (Ctrl) or infected with *A. fumigatus* for 24 or 3 hr respectively, without or with 5, 10 or 20 mM 2-DG (n=4). (c) ROS production by macrophages left untreated or infected for 24 hr without or with 10 mM 2-DG (n=8). (d) Phagocytosis of macrophages infected for 1 hr without or with 5, 10 or 20 mM 2-DG (n=6). (e) Production of IL-1β, TNF and IL-6 by macrophages infected for 24 hr without or with 10 mM 2-DG (n=10). (f) Lactate secretion by macrophages left untreated (Ctrl) or infected with *A. fumigatus* for 24 hr without or with 10 mM 2-DG, and 30 µM 3PO or 500 nM 6-AN (n=7). (g) Lactate secretion by mouse alveolar macrophages left untreated (Ctrl) or infected for 24 hr without or with 10 mM 2-DG (n=3). (h) Experimental setup for glycolysis inhibition in vivo during infection. Fungal burden (log_{10}) per g of lung tissue was determined in PBS- or 2-DG-treated mice after 1 day of infection (n=8, representative of three independent experiments). (i) Levels of IL-1β, TNF and IL-6 in lung homogenates of PBS- or 2-DG-treated mice after 1 day of infection (n=5). (j) Production of IL-1β, TNF and IL-6 and (k) conidiacidal activity of mouse splenocytes isolated

from PBS- or 2-DG-treated mice and restimulated for 24 (n=10) or 2 hr (n=5), respectively. Data are expressed as mean values ± SEM; P values were calculated using Student's two-tailed t test or two-way ANOVA with Tukey's multiple comparisons test.

Induction of host glycolysis depends on fungal melanin

To identify the mechanism(s) underlying the activation of glycolysis during infection, we compared lactate secretion by macrophages challenged with different fungal morphotypes for 24 hr. Secretion of lactate was higher when stimulation involved dormant conidia compared to swollen conidia or germ tubes (Fig. 3a). We hypothesized that the fungal molecule(s) inducing glycolysis were present on dormant conidia but were mostly lost after germination. Rodlet and melanin, made up of hydrophobic protein RodA and polymerized 1,8-dihydroxynaphthalene (DHN), respectively, form the outermost layer of dormant conidia and are both removed during germination [35]. To test their contribution, we assessed lactate secretion after infection with dormant conidia of the Δ*rodA* mutant devoid of the surface rodlet layer [36] or the Δ*pksP* mutant lacking the polyketide synthase responsible for the initial step in DHN-melanin biosynthesis [37]. Infection with Δ*rodA* conidia induced lactate secretion (Fig. 3b) and glucose consumption (Supplementary Fig. 3a) to an extent comparable to that measured for the parental strain Δ*ku80*, whereas Δ*pksP* or Δ*rodA/pksP* conidia failed to efficiently trigger this metabolic reprogramming. Macrophages infected with Δ*pksP* conidia also displayed decreased mRNA levels of glycolysis-related genes (Fig. 3c). Collectively, these findings are consistent with a critical role for fungal melanin in reprogramming macrophage metabolism during infection.

To determine at which stage the putative ligand(s) inducing glycolysis were synthesized in the pathway, we screened deletion mutants in the enzymes required to catalyze each step for their ability to activate glycolysis. We confirmed that lactate secretion was severely affected throughout the entire DHN-melanin biosynthetic pathway (Supplementary Fig. 3b), suggesting that fully mature melanin particles, and not the heptaketide naphthopyrone synthesized by PksP alone, is required for the metabolic reprogramming. The requisite role for melanin in the activation of glycolysis was confirmed by similar defective levels of lactate secreted by macrophages infected with the albino strains of *A. fumigatus* CBS 110.46 and CBS 386.75 [38] (Fig. 3d). To elucidate whether melanin pigments that differ from DHN-melanin could also activate glycolysis, we infected macrophages with *A. nidulans* whose melanin differs

from that of *A. fumigatus* [39]. In these conditions, lactate secretion occurred to a degree similar to that induced by the Δ*ku80* strain of *A. fumigatus* (Fig. 3e).

Because the recently identified melanin receptor MelLec could be involved in melanin-induced activation of glycolysis, we stimulated macrophages with 1,8-DHN, polymerization of which leads to melanin biosynthesis, and that contains the conserved naphthalene-diol unit recognized by MelLec [32]. We observed that the levels of lactate secreted by macrophages stimulated with 1,8-DHN were significantly lower than those after infection with the Δ*ku80* strain (Fig. 3f), suggesting that recognition of 1,8-DHN melanin and signalling via MelLec is, to a large extent, dispensable for the activation of glycolysis. In support of this, infection of bone marrow-derived macrophages (BMDMs), which lack expression of MelLec [32], with Δ*pksP* conidia also induced lower concentrations of secreted lactate (Supplementary Fig. 3c). Moreover, human macrophages carrying the loss-of-function rs2306894 variant in MelLec displayed comparable levels of lactate secreted after infection to that of wild-type cells (Supplementary Fig. 3d).

To directly link the presence of melanin on the conidial surface and activation of glycolysis, we stimulated macrophages with melanin ghosts alone or added together with Δ*pksP* conidia. Strikingly, none of these conditions significantly induced lactate secretion (Fig. 3g), a finding suggesting the need for melanin to be actively shed or removed during conidial germination to activate glycolysis. Indeed, only live, but not heat-killed or UV-inactivated, conidia triggered lactate secretion by macrophages (Fig. 3h), a finding highly suggestive of a cell wall remodelling associated with melanin release. To further test this, we performed functional complementation experiments using live dormant Δ*rodA*/*pksP* conidia (allowing enhanced adhesion due to removal of the hydrophobic layer) coated with purified fragments of melanin isolated from *A. fumigatus* conidia. The ability of the Δ*rodA*/*pksP* strain to induce lactate secretion was rescued by the melanin coating in a dose-dependent manner (Fig. 3i), a finding supported by the increase in the mRNA expression of glycolytic genes (Fig. 3j). In line with the link between glycolysis and cytokine production, infection with melanin-coated live Δ*rodA*/*pksP* conidia also reverted the defective production of proinflammatory cytokines (Fig. 3k). The same experimental approach using inactivated conidia was instead unable to restore lactate secretion to normal levels (Supplementary Fig. 3e). These results demonstrate that the active intracellular removal of melanin is required for the reprogramming of glucose metabolism in macrophages.

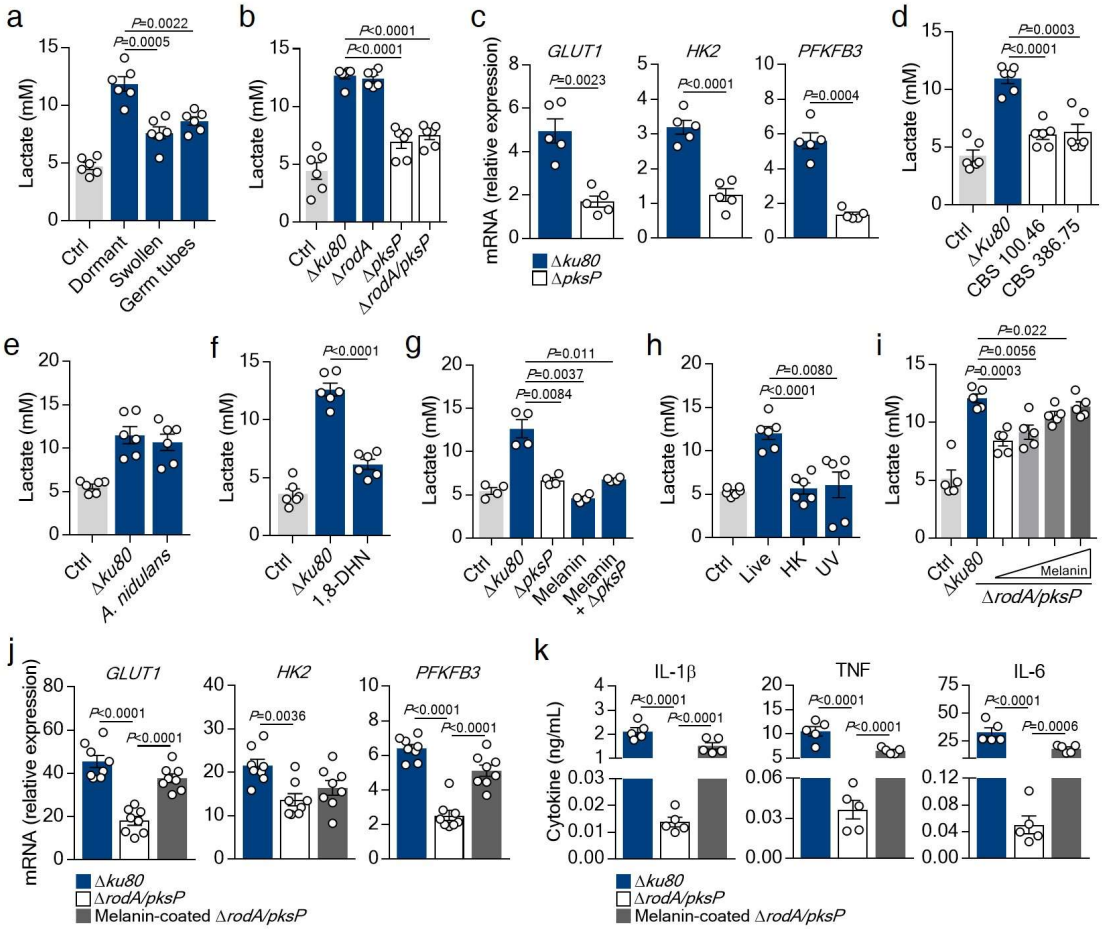

Figure 3. Intracellular removal of fungal melanin induces glucose metabolism. (a) Lactate secretion by macrophages left untreated (Ctrl) or infected with dormant or swollen conidia, or germ tubes of *A. fumigatus* for 24 hr (n=6). (b) Lactate secretion by macrophages left untreated (Ctrl) or infected with dormant conidia from the parental Δ*ku80* strain or the cell wall mutants Δ*rodA*, Δ*pksP* or Δ*rodA/pksP* for 24 hr (n=6). (c) mRNA expression of *GLUT1*, *HK2* and *PFKFB3* in macrophages infected with Δ*ku80* or Δ*pksP* strains for 2 hr relative to uninfected cells (n=5). (d) Lactate secretion by macrophages left untreated (Ctrl) or infected with the albino CBS 100.46 and 386.75 strains of *A. fumigatus* (n=6), (e) the WG355 strain of *A. nidulans* (n=6), (f) 1,8-DHN (n=6) or (g) the Δ*pksP* strain, DHN-melanin, or DHN-melanin added together with Δ*pksP* conidia (n=4) for 24 hr. Infection with Δ*ku80* conidia was used as control. (h) Lactate secretion by macrophages left untreated (Ctrl) or infected with live, heat-killed (HK) or UV-inactivated (UV) conidia for 24 hr (n=5). (i) Lactate secretion by macrophages infected with the Δ*ku80*, Δ*rodA/pksP* or the Δ*rodA/pksP* strain coated with 100, 300, and 600 μg/mL of DHN-melanin for 24 hr (n=5). (j) mRNA expression of *GLUT1*, *HK2* and *PFKFB3* (n=8) and (k) production of IL-1β, TNF and IL-6 (n=5) by macrophages infected with the Δ*ku80*, Δ*rodA/pksP* or the melanin-coated Δ*rodA/pksP* strain for 2 or 24 hr, respectively, relative to uninfected cells (n=8). Data are expressed as mean values ± SEM; P values were calculated using Student's two-tailed t test or one-way ANOVA with Tukey's multiple comparisons test.

Fungal melanin rewires host metabolism via mTOR and HIF-1α

The metabolic reprogramming of myeloid cells toward glycolysis is driven by the activation of mTOR, an intracellular sensor that functions as a master regulator of glucose metabolism [40]. Consistent with this, the transcriptome of human macrophages after 2 hr of infection with *A. fumigatus* was markedly enriched in genes involved in mTOR signaling (Fig. 4a). The activation of the mTOR pathway during infection was confirmed by the enhanced phosphorylation of the p70S6 kinase, a downstream target of the mTORC1 complex (Fig. 4b and Supplementary Fig. 4a). Remarkably, Δ*pksP* conidia failed to elicit a significant increase in p-p70S6K, indicating that melanin is required for the induction of mTOR signaling. Because mTOR activation is often mediated by the intermediary activation of the phosphatidylinositol-4,5-bisphosphate 3-kinase (PI3K)/Akt pathway [41], we assessed phosphorylation of Akt in the same conditions. Similar to mTOR, the levels of p-Akt were increased during infection with Δ*ku80* conidia, but less when the Δ*pksP* strain was used (Fig. 4b and Supplementary Fig. 4b). As these results suggest a coupled activation of Akt/mTOR and glycolysis, we next investigated the causality between these two processes during infection. Inhibiting this pathway with rapamycin (mTOR) (Fig. 4c) or wortmannin (Akt) (Supplementary Fig. 4c) during infection with Δ*ku80* conidia impaired the ability of macrophages to reprogram their metabolism, leading to lower levels of secreted lactate. Along the same line, blocking mTOR (Fig. 4d) or Akt (Supplementary Fig. 4d) impaired the production of cytokines after infection.

Based on evidence that mTOR-mediated induction of glycolysis requires activation of HIF-1α and stimulation of glycolytic enzymes [42], we next assessed the expression of HIF-1α in infected macrophages. We found higher amounts of HIF-1α accumulated in the nucleus of cells infected with the Δ*ku80* than the Δ*pksP* strain (Fig. 4e and Supplementary Fig. 4e), a finding indicating a melanin-dependent induction of HIF-1α-mediated gene expression. Likewise, HIF-1α was more abundant in lysates from macrophages infected with Δ*ku80* conidia (Supplementary Fig. 4f), and a similar profile was determined for *HIF1A* mRNA (Supplementary Fig. 4g). To further investigate the link between activation of HIF-1α and the metabolic reprogramming of macrophages, we assessed the impact of HIF-1α deficiency in response to infection using BMDMs from wild-type (C57BL/6) and myeloid-restricted HIF-1α-deficient (HIF1^{c}) mice. In contrast to wild-type BMDMs, the ability of melanin to induce lactate secretion was lost in HIF1^{c} cells (Fig. 4f), a finding recapitulated in human macrophages upon treatment with ascorbate, a co-factor for the hydrolases that negatively regulate HIF-1α (Supplementary Fig. 4h). Production of the proinflammatory cytokine IL-1β, known to be transcriptionally regulated by HIF-1α [9], was also impaired in HIF1^{c} BMDMs (Fig. 4g), a finding in line with the lower levels of cytokines produced

by human macrophages treated with ascorbate (Supplementary Fig. 4i). In support of the link between fungal melanin and mTOR/HIF-1α signaling, infection of macrophages with melanin-coated live Δ*rodA/pksP* conidia restored both p-p70S6K (Fig. 4h) and HIF-1α translocation to the nucleus (Fig. 4e) to levels comparable to those obtained after infection with the Δ*ku80* strain. Taken together, these results suggest that signalling via mTOR and HIF-1α is required for the melanin-mediated activation of glycolysis in macrophages.

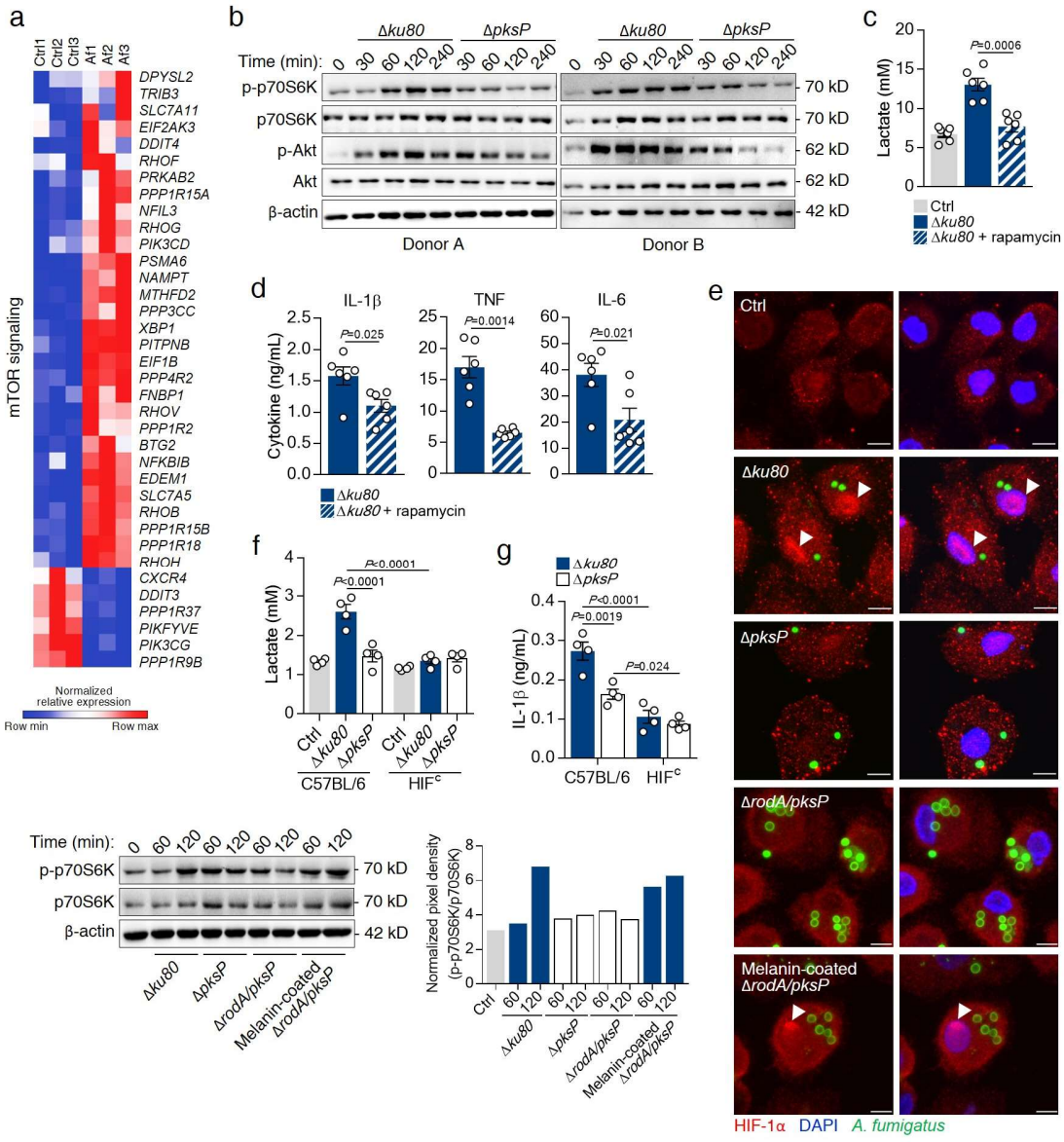

Figure 4. mTOR and HIF-1α reprogram metabolism in response to *A. fumigatus*. (a) Transcriptional profiles of macrophages left untreated (Ctrl) or infected with *A. fumigatus* (Af) for 2 hr (n=3). Expression of genes is presented as centered and scaled $\log_2$ fluorescence intensity (blue and red keys). (b) Total and p-p70S6K and total and p-Akt in macrophages infected with the Δ*ku80* or Δ*pksP* strains for 4 hr (representative of three

independent experiments, with β-actin used as loading control). (c) Lactate secretion and (d) production of IL-1β, TNF and IL-6 by macrophages left untreated (Ctrl) or infected with the Δ*ku80* strain for 24 hr without or with 10 mM rapamycin (n=6). (e) Expression of HIF-1α in macrophages left untreated or infected with the Δ*ku80*, Δ*rodA/pksP* or the melanin-coated Δ*rodA/pksP* strain for 2 hr (representative of three independent experiments). The white arrows indicate accumulation in the nuclei of macrophages. Scale bars, 100 μm. (f) Lactate secretion and (g) production of IL-1β by BMDMs from C57BL/6 and HIF1^{c} mice left untreated (Ctrl) or infected with the Δ*ku80* or Δ*pksP* strains for 24 hr (n=4). (h) Levels of total and p-p70S6K in macrophages left untreated (Ctrl) or infected with the Δ*ku80*, Δ*pksP,* Δ*rodA/pksP* or melanin-coated Δ*rodA/pksP* strains for 3 hr (representative of three independent experiments, with β-actin used as loading control). The pixel density of the p-p70S6K/p70S6K ratio was normalized to β-actin. Data are expressed as mean values ± SEM; P values were calculated using Student's two-tailed t test or one-way ANOVA with Tukey's multiple comparisons test.

Remodeling of calcium signaling enables host glycolysis

Since the ability of fungal melanin to sequester calcium inside the phagosome is a major inhibitory mechanism of intracellular signalling pathways [43], we evaluated the contribution of calcium signalling to macrophage metabolism during infection. In line with the interference of fungal melanin with calcium responses, live imaging of macrophages preloaded with the calcium indicator Fluo4-AM revealed that infection with Δ*pksP* or Δ*rodA/pksP*, but not Δ*ku80* conidia, triggered a sustained accumulation of cytosolic calcium early after infection (Fig. 5a-b and Supplementary Fig. 5a). Importantly, stimulation of macrophages with live Δ*rodA/pksP* conidia coated with purified melanin abrogated cytosolic calcium flux in a similar fashion to the Δ*ku80* strain, confirming melanin as a master regulator of calcium-mediated responses. This effect was dependent on fungal viability since stimulation with inactivated Δ*rodA/pksP* conidia or melanin ghosts instead failed to promote cytosolic calcium accumulation (Supplementary Fig. 5b).

To ascertain the specific contribution of melanin-mediated regulation of calcium signalling to host cellular metabolism, we next performed calcium depletion and signaling inhibition during infection and evaluated the induction of glycolysis. Strikingly, the depletion of extracellular calcium sources had no effect on calcium signalling and metabolism after infection with Δ*pksP* conidia (Fig. 5c). In contrast, incubation with the cell-permeable EGTA-AM further inhibited calcium responses to Δ*pksP* conidia, suggesting that intracellular calcium sources regulate the metabolic reprogramming. Because calcium concentrations in different subcellular compartments exert distinct functional effects [44], we performed

the depletion of endoplasmic reticulum (ER) calcium stores with thapsigargin, a sarco/ER calcium ATPase (SERCA) inhibitor, during infection. Upon inhibiting SERCA, the impaired ability of macrophages to secrete lactate in response to infection with Δ*pksP* conidia was rescued (Fig. 5d). To further differentiate store depletion versus calcium entry, we evaluated lactate secretion following calcium supplementation. In these conditions, cells infected with the Δ*pksP* conidia still failed to upregulate lactate levels (Fig. 5e). In addition, we silenced stromal-interacting molecule 1 (STIM1), a calcium sensor essential for calcium store depletion-triggered calcium influx [45] (Supplementary Fig. 5c). The inhibition of STIM1 also did not alter the profile of lactate secretion by macrophages infected with the Δ*ku80* or Δ*pksP* strains (Fig. 5f). Together, these observations indicate that ER calcium stores, independently of calcium entry, regulate intracellular signaling pathways, which are required for the activation of glucose metabolism by fungal melanin.

To gain further insight into the calcium-induced signaling pathways mediating activation of glycolysis by melanin, we next tested whether calcium/calmodulin (CaM) signaling was involved. We treated macrophages with W7, a specific CaM antagonist, and assessed the levels of lactate secretion after infection. In these conditions, macrophages infected with the Δ*pksP* strain displayed increased levels of secreted lactate (Fig. 5g), a finding in accordance with the upregulation of glycolytic genes (Supplementary Fig. 5d) and indicating that the inhibition of calcium/CaM signaling by melanin is required for the transcriptional induction of glycolysis. To further illustrate the regulation of immunometabolic signaling by fungal melanin, we next evaluated the influence of calcium signaling on mTOR expression. In line with the impaired phosphorylation of the mTOR target p70S6 kinase (Fig. 4b), mTOR expression was also decreased during infection with Δ*pksP* conidia, a defect that was rescued by the CaM antagonist W7 (Supplementary Fig. 5e). Because melanin blocks CaM recruitment to conidia-containing phagosomes [43], we next assessed mTOR recruitment to the phagosome. Macrophages infected with the Δ*pksP* strain displayed a lower percentage of $mTOR^+$ phagosomes when compared to cells infected with Δ*ku80* conidia (Fig. 5h-i). Importantly however, mTOR recruitment was restored following CaM inhibition, a finding implying a direct link between melanin-mediated restraining of calcium signaling and activation of mTOR and the downstream metabolic reprogramming of macrophages. Furthermore, macrophages infected with Δ*pksP* conidia and treated with either thapsigargin or W7 displayed an enhanced ability to produce cytokines (Fig. 5j). Collectively, these results highlight a mechanism whereby the inhibition of calcium/CaM signaling enables efficient immunometabolic responses.

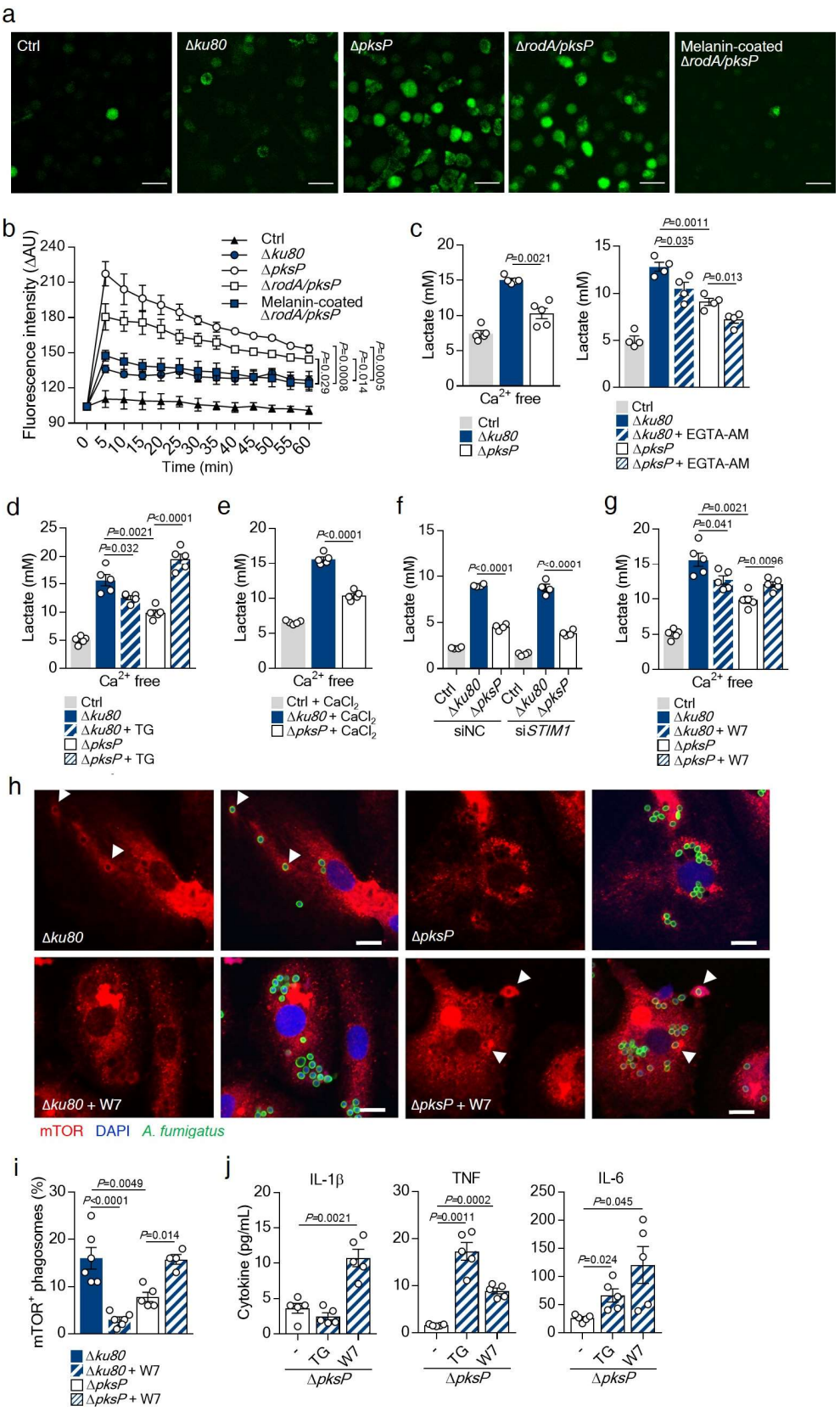

Figure 5. Calcium signaling regulates glucose metabolism in response to *A. fumigatus*. (a) Micrographs of macrophages preloaded with Fluo-4-AM and left untreated (Ctrl) or infected with the Δ*ku80*, Δ*pksP*, Δ*rodA/pksP* or melanin-coated Δ*rodA/pksP* strains for 15 min (representative of three independent experiments).

Scale bars, 35 μm. (b) Quantification of FLUO-4-AM fluorescence in 5 min intervals for 1 hr and expressed as the difference in arbitrary units (ΔAU) between infected and uninfected cells. (c) Lactate secretion by macrophages left untreated (Ctrl) or infected with the Δ*ku80* or Δ*pksP* strains for 24 hr using calcium-free medium (n=5) or 500 μM EGTA-AM (n=4). (d) Lactate secretion by macrophages left untreated (Ctrl) or infected in calcium-free medium for 24 hr and in the presence of 2 μM thapsigargin (TG) (n=5) or (e) 2 mM $CaCl_2$ (n=5). (f) Lactate secretion by macrophages left untreated (Ctrl) or infected and silenced with a *STIM1* siRNA (si*STIM1*) (n=4). A scrambled siRNA was used as negative control (siNC). (g) Lactate secretion by macrophages left untreated (Ctrl) or infected for 24 hr in the presence of 25 μM W7 (n=5). (h) Immunofluorescent staining for mTOR and (i) quantification of $mTOR^+$ phagosomes in infected macrophages, without or with 25 μM W7 for 2 hr (representative of two independent experiments). The white arrows indicate the recruitment of mTOR to the phagosome. Scale bars, 10 μm. Data on quantification was determined by analyzing at least 200 phagosomes. (j) Production of IL-1β, TNF and IL-6 by macrophages infected with the Δ*pksP* strain for 24 hr without or with 2 μM TG or 25 μM W7 (n=5). Data are expressed as mean values ± SEM; P values were calculated using Student's two-tailed t test or one-way ANOVA and two-way ANOVA with Tukey's multiple comparisons test.

Discussion

The metabolic reprogramming of innate immune cells is required to generate protective inflammation and drive antimicrobial defenses [12,20,46]. We establish fungal melanin as an essential PAMP required for the induction of glycolysis in macrophages and the resulting antifungal immune responses. DHN-melanin is a major determinant of the fungal interaction with the innate immune system [35], endowing *A. fumigatus* with the ability to survive killing by phagocytes, namely by blocking phagosome biogenesis [43,47] and acidification of phagolysosomes [48], and preventing phagocyte apoptosis [49]. We now show that the host has in turn evolved strategies to counter the inhibitory mechanisms deployed by melanin, by sensing its removal during intracellular swelling or cell wall remodeling inside the phagosome and using these signals to rewire cellular metabolism and promote antifungal immune responses.

The innate immune system is equipped to respond to the expression of virulence factors from fungi [16]. The identification of the MelLec receptor, which recognizes DHN-melanin and activates antifungal defenses, highlights the evolution of the receptor repertoire in innate cells towards the efficient recognition of fungal melanin [32]. Because the induction of glycolysis by melanin, but not MelLec expression, is evolutionarily conserved between human and murine macrophages, MelLec appears to be largely redundant for their metabolic reprogramming. Instead, the germination associated with the active removal of melanin in live fungi within the phagosome is required for host cells to reorient their metabolism towards protection. As such, melanin can be considered a vita-PAMP, molecules expressed by viable pathogens that are sensed by the host to weigh the intensity of specific antimicrobial responses [50]. It is noteworthy that the bacterial vita-PAMP cyclic-di-adenosine monophosphate triggers stress-mediated autophagy to restrain phagocyte death [51], and these molecular pathways are also well-known targets for the action of melanin during infection [47]. How is the outer layer of the cell wall remodeled to shed melanin during germination and which signals are generated remains unclear. Could there be an intracellular receptor other than MelLec involved in melanin recognition? It is possible, since fungal ligands, namely β-(1,3)-glucan, directly activate the inflammasome upon their release during infection [52], and melanin could behave analogously. In fact, both the metabolic reprogramming of macrophages and inflammasome activation [53] rely exclusively on infection by live conidia, and melanin particles have been occasionally detected in the cytosol of infected cells (Chamilos, unpublished), raising the intriguing possibility that inflammasome activation and induction of glycolysis in macrophages are molecular events coupled via melanin-mediated signaling.

The recognition of β-1,3-glucan from the cell wall is required for the metabolic reprogramming of myeloid cells in response to *C. albicans* [11,20]. Surface exposure of β-1,3-glucan on *A. fumigatus* appears instead largely redundant for macrophage glycolysis given its broad expression on the surface of albino conidia [47]. Our data nevertheless suggests a minor contribution from signals other than melanin. Whether these include other cell wall polysaccharides or fungal-derived products requires further investigation. The differential activation of glucose metabolism upon exposure of host cells to distinct fungal PAMPs also reflects important differences in the outcome of the host-fungus interaction. In certain cases, fungi can hijack nutritional weaknesses of host cells that are a direct consequence of immunometabolic shifts to their own benefit; the terminal commitment of macrophages to glycolysis after infection with *C. albicans* is subverted by the efficient shift of fungal metabolism to rapidly deplete glucose and trigger cell death [22]. Because of lacking nutrients in the lung microenvironment, *A. fumigatus* resorts to different strategies to survive, which include the cross-pathway control system and degradation of proteins to acquire amino acids and the glyoxylate cycle to produce carbohydrates from lipids available at the site of infection [54]. In contrast to *C. albicans*, the metabolic reprogramming of macrophages in response to *A. fumigatus* represents instead an advantageous mechanism of host defence, highlighting the immunometabolic repurposing of immune cells towards enhanced glycolysis as an attractive therapeutic strategy in aspergillosis.

Despite the remarkable differences in the nature of the fungal ligands and the mechanisms through which these deliver signals required to induce glycolysis, the pathways that are activated in response to different fungal pathogens appear to converge on a common signaling axis involving mTOR and HIF-1α. This pathway represents a major signaling hub that regulates metabolic changes underlying trained immunity in myeloid cells in response to β-1,3-glucan [11,17-19]. Although trained immunity induced by melanin has not been explored, we provide evidence that this pigment is endowed with the ability to regulate mTOR and HIF-1α signaling. Our findings are supported by proteomics of conidia-containing phagolysosomes [55], in which melanin was revealed as a major regulator of mTOR activator/regulator (LAMTOR), a member of the Ragulator/LAMTOR complex known to regulate mTOR [56]. Importantly, mTOR suppresses factor inhibiting HIF-1 (FIH-1), a negative regulator of HIF-1α [57], and FIH-1 may represent one central node congregating mTOR and HIF-1α signaling towards the activation of glycolysis in response to infection. Myeloid HIF-1α has been shown to be required for protection against aspergillosis, a phenotype attributed to impaired chemokine production and enhanced neutrophil apoptosis, resulting in a net decrease of neutrophil numbers [58]. Because HIF-1α also regulated cytokine

production and the metabolic activity of human dendritic cells infected with *A. fumigatus* [59], it may deliver broader implications to antifungal immunity, with consequences to different cell types and involving distinct effector mechanisms.

What are the molecular signals that bridge melanin removal and the mTOR/HIF-1α axis culminating with the metabolic reprogramming of macrophages? We demonstrate that the immunometabolic reprogramming induced by *A. fumigatus* depends on calcium sequestration inside the phagosome by melanin which in turn triggers glycolysis-promoting signals. Calcium-mediated regulation of glycolysis has been known for several decades; for example, calcium overload was observed concomitantly to glycolytic inhibition in heart tissue [60], whereas calcium depletion promoted increased levels of glycolytic intermediates in cerebral cortex slices [61]. We demonstrate that calcium/CaM signalling orchestrates mTOR recruitment to the phagosome, an effect directly regulated by fungal melanin. Phagosome and entotic vacuole fission depend on mTOR localization to vacuolar membranes surrounding engulfed cells [62] and, likewise, we propose that the subcellular redistribution of mTOR to melanin-containing phagosomes is required for its activation. Because the spatial organization of mTOR is coordinated through a variety of sensors and regulators that converge on Rag GTPases [63], the phagosomal regulation of LAMTOR by melanin [55] suggests similar mechanisms during fungal infection, in line with the ability of melanized conidia to inhibit phagosomal recruitment of CaM and prevent the specialized autophagy pathway LC3-associated phagocytosis (LAP) [43]. By deploying melanin, the fungus promotes calcium sequestration inside the phagosome and inhibits the recruitment of LAPosome machinery components, including the NADPH oxidase and CaM, to block LAP and avoid elimination [43,47]. Our data demonstrates that melanin, by blocking the activation of LAP, contributes to fungal persistence within the phagosome, allowing conidial germination and removal of melanin, providing the necessary signals to redirect macrophage metabolism towards glycolysis and efficient fungal clearance.

Our study provides mechanistic insights into the interplay between *A. fumigatus* and the glucose metabolism of immune cells. It has however limitations, such as the likely involvement of metabolic pathways other than glycolysis in the activation of antifungal immunity. Cellular metabolism consists of highly interconnected pathways that feed into each other and it is challenging, if not at all impossible, to analyze them in an entirely independent way. Nevertheless, our results suggest a dominant role for glycolysis and represent a promising first step toward the elucidation of the metabolic profiles involved in the activation of antifungal immunity . Current therapeutic limitations and concerns over the emergence of antifungal resistance are inspiring the search for novel host-directed therapies. Understanding how

metabolic networks coordinate immune cell function may lead to innovative therapeutic approaches or metabolic adjuncts to reorient host cells towards immune protection against infection.

Acknowledgements

This work was supported by the Northern Portugal Regional Operational Programme (NORTE 2020), under the Portugal 2020 Partnership Agreement, through the European Regional Development Fund (FEDER) (NORTE-01-0145-FEDER-000013), the Fundação para a Ciência e Tecnologia (FCT) (SFRH/BD/136814/2018 to S.M.G., SFRH/BD/141127/2018 to C.D.O., PD/BD/137680/2018 to D.A., IF/00474/2014 to N.S.O., IF/01390/2014 to E.T., IF/00959/2014 to S.C., IF/00021/2014 to R.S., PTDC/SAU-SER/29635/2017 and CEECIND/04601/2017 to C.C., and CEECIND/03628/2017 to A.C.), the Institut Mérieux (Mérieux Research Grant 2017 to C.C.), and the European Society of Clinical Microbiology and Infectious Diseases (ESCMID Research Grant 2017 to A.C.). M.G.N. was supported by a Spinoza grant of the Netherlands Organization for Scientific Research. A.A.B. was supported by the Deutsche Forschungsgemeinschaft Collaborative Research Center/Transregio TR124 FungiNet (project A1). G.D.B. was funded by the Wellcome Trust (102705), the MRC Centre for Medical Mycology and the University of Aberdeen (MR/N006364/1).

Author contributions

S.M.G. designed the study, performed experiments and data analysis, and wrote the manuscript. C.D.O., C.F.C. and I.M. performed the animal experiments, V.A. prepared fungal components, D.A. and G.C. performed confocal microscopy, C.S.R. performed HPLC measurements, and C.B.M., J.G., S.C. performed flow cytometry and cell sorting experiments, and G.C. performed the live recording of calcium levels. N.S.O. analyzed RNA-seq data and M.F.G. and C.B. performed targeted metabolomics. A.M. supervised the collection of samples from healthy donors. R.t.H., L.L., T.M., P.P., E.T., F.R., L.A.B.J., K.L., J.M., J.F.L., A.C.J. and R.S. analyzed data and contributed to the manuscript. G.D.B., A.A.B. and G.C. contributed to the manuscript. F.L.v.d.V., M.G.N., J.P.L., C.C. and A.C. designed the study and wrote the manuscript.

Supplementary Information

Supplementary Figure 1

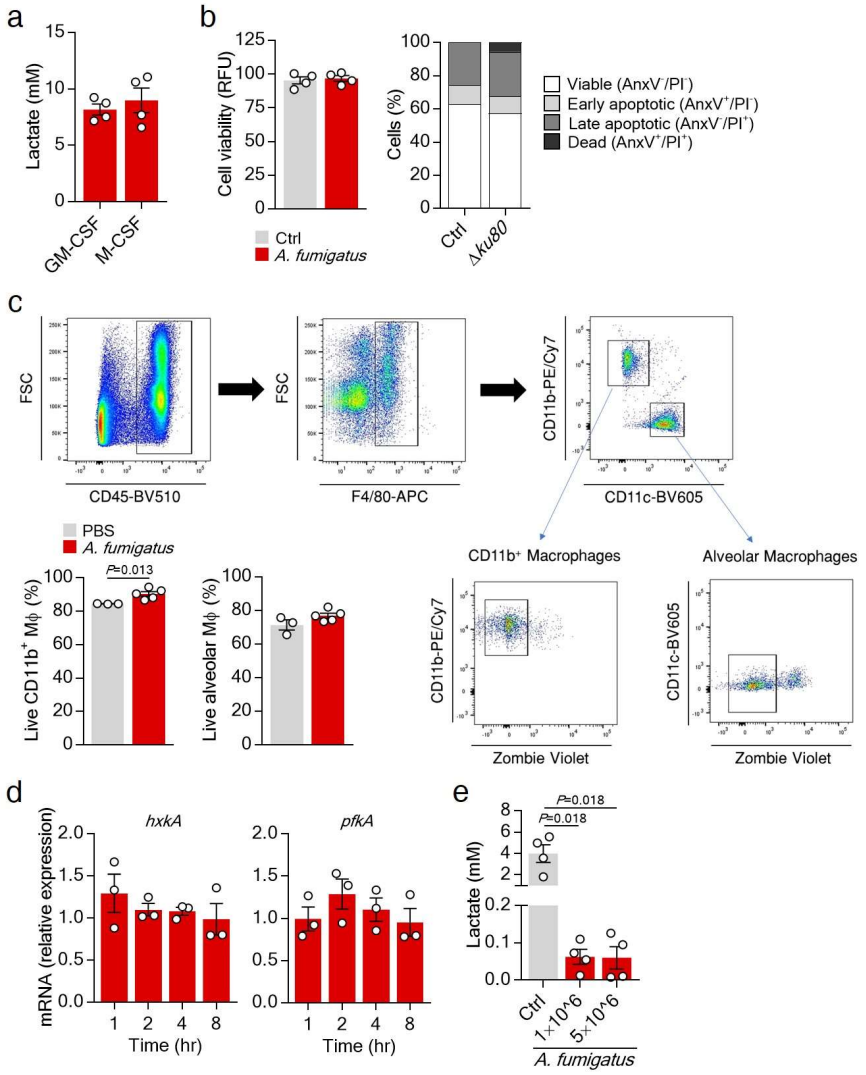

Supplementary Figure 1 | *A. fumigatus* induces the metabolic shift of macrophages during infection. (a) Lactate secretion by macrophages differentiated from monocytes using GM-CSF or M-CSF and infected with *A. fumigatus* for 24 hr (n=4). (b) Cell viability of macrophages left untreated (Ctrl) or infected for 24 hr and determined using AlamarBlue, expressed as relative fluorescence units (RFU) (n=4), or using annexin-V/PI staining, expressed as percentage (%) of cells (n=2). (c) Flow cytometry analysis of lung cells from C57BL/6 mice after 1 day of infection with *A. fumigatus* or following a mock challenge (PBS). Leukocytes were gated by size using forward and side scatter and then on live single cells (by propidium iodide exclusion). The pan-leukocyte marker CD45 identified leukocytes, whereas macrophages were further defined as F4/80^{+}CD11b^{+}CD11c^{-} (plots are representative of three independent experiments). Viability was determined using the Zombie Violet dye. Results

are expressed as the percentage (%) of viable cells. (d) mRNA expression of *hxkA* and *pfkA* from *A. fumigatus* during infection of macrophages for 1, 2, 4 or 8 hr relative to the fungus alone (n=3). (e) Lactate secretion by macrophages left untreated (Ctrl) or by conidia of *A. fumigatus* alone cultured in vitro at two different concentrations for 24 hr (n=4). Data are expressed as mean values ± SEM; P values were calculated by Student's two-tailed t test.

Supplementary Figure 2

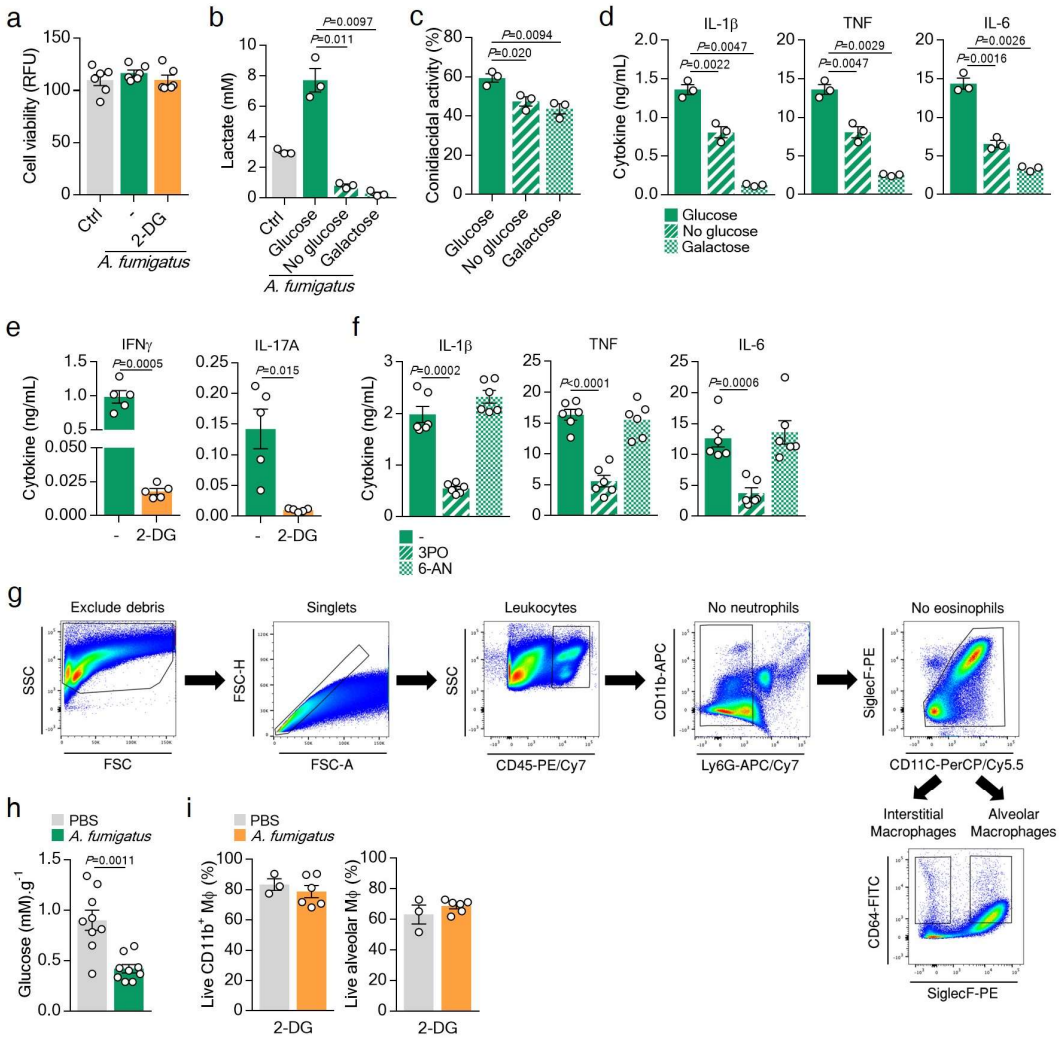

Supplementary Figure 2 | Glycolysis is required for immune responses to *A. fumigatus*. (a) Cell viability (relative fluorescence units, RFU) of macrophages left untreated (Ctrl) or infected with *A. fumigatus* for 24 hr without or with 10 mM 2-DG (n=6). (b) Lactate secretion by macrophages either left untreated (Ctrl) or infected for 24 hr in the presence or absence of glucose or using galactose-supplemented media (n=3). (c) Conidiacidal activity and (d) production of IL-1β, TNF and IL-6 by macrophages infected for 3 or 24 hr, respectively, in the presence or absence of glucose or using galactose-supplemented media (n=3). (e) Production of IFNγ and IL-17A by PBMCs stimulated with inactivated conidia for 7 days without or with 10 mM 2-DG (n=5). (f) Production of IL-

1β, TNF and IL-6 by macrophages infected for 24 hr, without or with 10 mM 2-DG, 30 μM 3PO and 500 nM 6-AN (n=6). (g) Gating strategy employed for FACS-based sorting of alveolar macrophages from naïve mice. (h) Levels of glucose determined in the blood of mice after 1 day of infection (n=9, representative of one out of three independent experiments). (i) Viability of $CD11b^{+}$ and alveolar macrophages (%) in the lungs of 2-DG-treated mice after 1 day of infection with *A. fumigatus* (n=6) or following a mock challenge (PBS). Data are expressed as mean values ± SEM; P values were calculated using Student's two-tailed t test.

Supplementary Figure 3

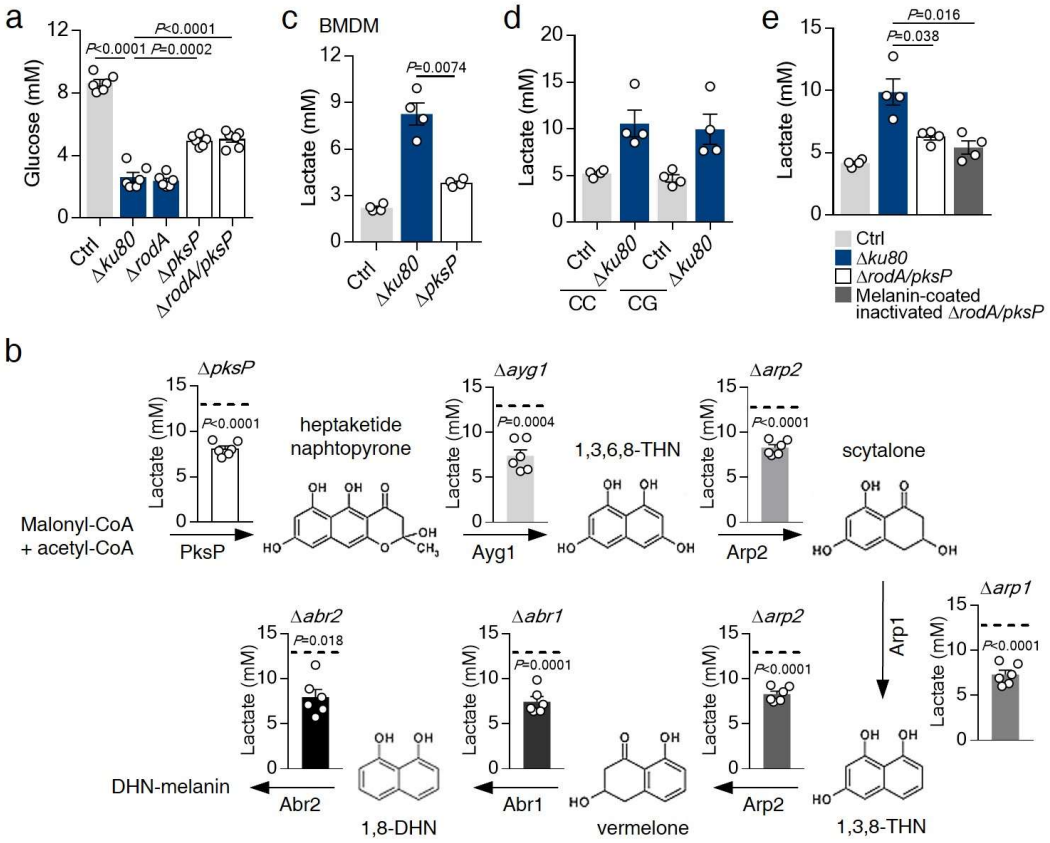

Supplementary Figure 3 | Fungal melanin induces host glucose metabolism. (a) Glucose consumption by macrophages left untreated (Ctrl) or infected with the Δ*ku80*, Δ*rodA*, Δ*pksP* or Δ*rodA/pksP* strains of *A. fumigatus* for 24 hr (n=6). (b) Lactate secretion by macrophages infected with deletion mutants in the genes along the biosynthetic pathway of DHN-melanin for 24 hr (n=6). The dotted line represents the levels of secreted lactate determined upon infection with the B-5233 parental strain. The different compounds synthesized at each step along the biosynthetic pathways are illustrated. (c) Lactate secretion by BMDMs from C57BL/6 mice infected with the Δ*ku80* or Δ*pksP* strains for 24 hr (n=4). (d) Lactate secretion by macrophages isolated from carriers with

distinct genotypes of the Gly26Ala SNP in MelLec and infected for 24 hr (n=4). (e) Lactate secretion by macrophages infected with live conidia of the Δ*ku80* or Δ*rodA/pksP* strains, or UV-inactivated conidia of the Δ*rodA/pksP* strain coated with 600 μg/mL of DHN-melanin for 24 hr (n=4). Data are expressed as mean values ± SEM; P values were calculated using Student's two-tailed t test.

Supplementary Figure 4

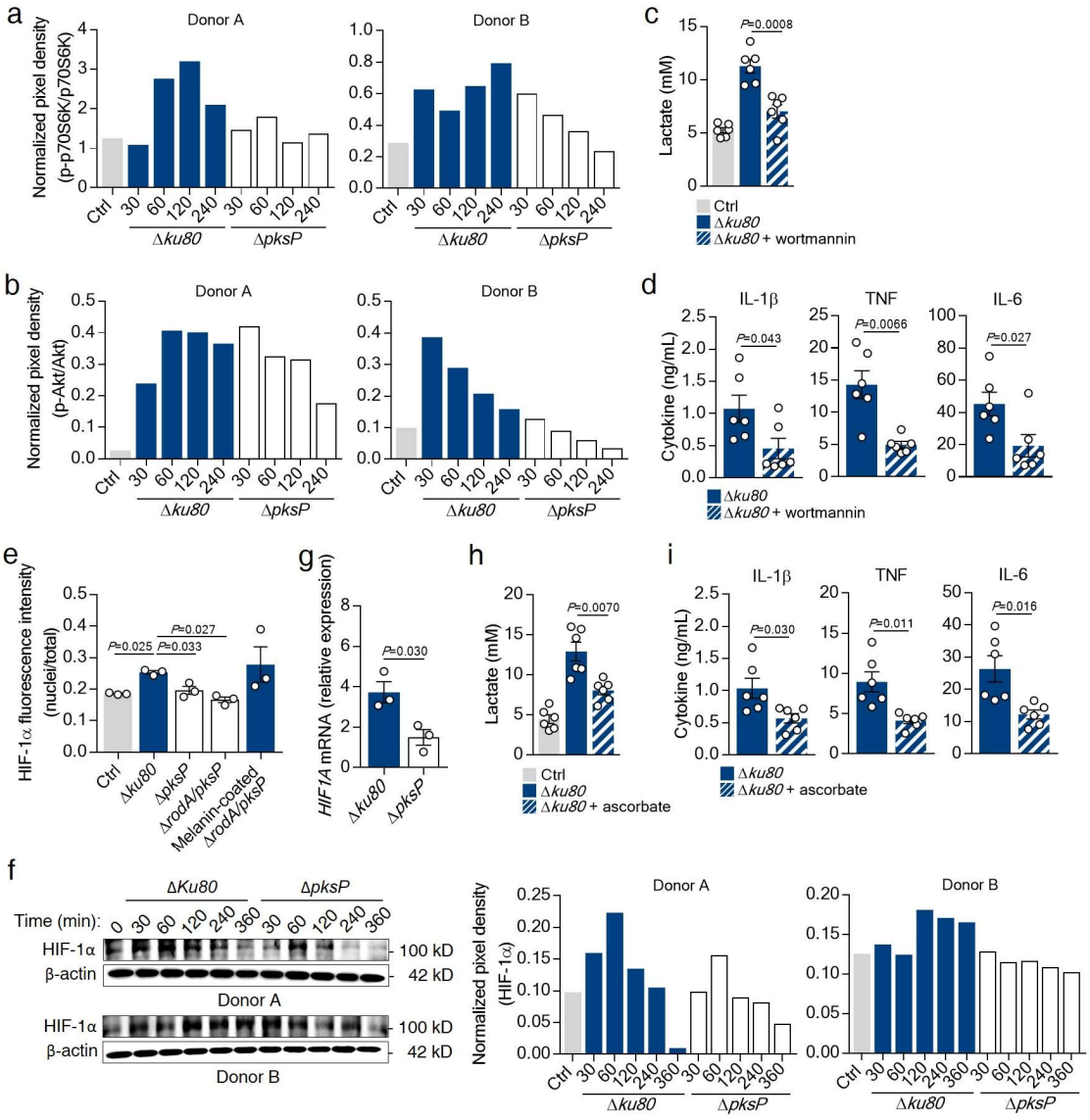

Supplementary Fig. 4 | *A. fumigatus* induces the metabolic shift of macrophages via mTOR and HIF-1α. (a) Densitometric analysis of the p-70S6K/p70S6K ratio and (b) the p-Akt/Akt ratio, both normalized to β-actin, in macrophages infected with the Δ*ku80* or Δ*pksP* strains for 4 hr, with β-actin used as loading control (n=2). (c) Lactate secretion and (d) production of IL-1β, TNF and IL-6 by macrophages infected with the Δ*ku80* strain for 24 hr without or with 10 μM wortmannin (n=6). (e) Expression of HIF-1α in macrophages left untreated

(Ctrl) or infected with the Δ*ku80*, Δ*rodA/pksP* or the melanin-coated Δ*rodA/pksP* strain for 2 hr (n=3). Results are expressed as fluorescence intensity (nuclear/total fluorescence) of at least 60 cells for each condition. (f) Levels of total HIF-1α in macrophages infected with the Δ*ku80* or Δ*pksP* strains for 6 hr. The densitometric analysis was performed by comparing the pixel density of the HIF-1α/β-actin ratio (n=2). (g) mRNA expression of *HIF1A* in macrophages infected with the Δ*ku80* or Δ*pksP* strains for 2 hr relative to uninfected cells (n=3). (h) Lactate secretion and (i) production of IL-1β, TNF and IL-6 by macrophages infected with the Δ*ku80* strain for 24 hr without or with 50 μM (+)-sodium L-ascorbate (n=6). Data are expressed as mean values ± SEM; P values were calculated using Student's two-tailed t test.

Supplementary Figure 5

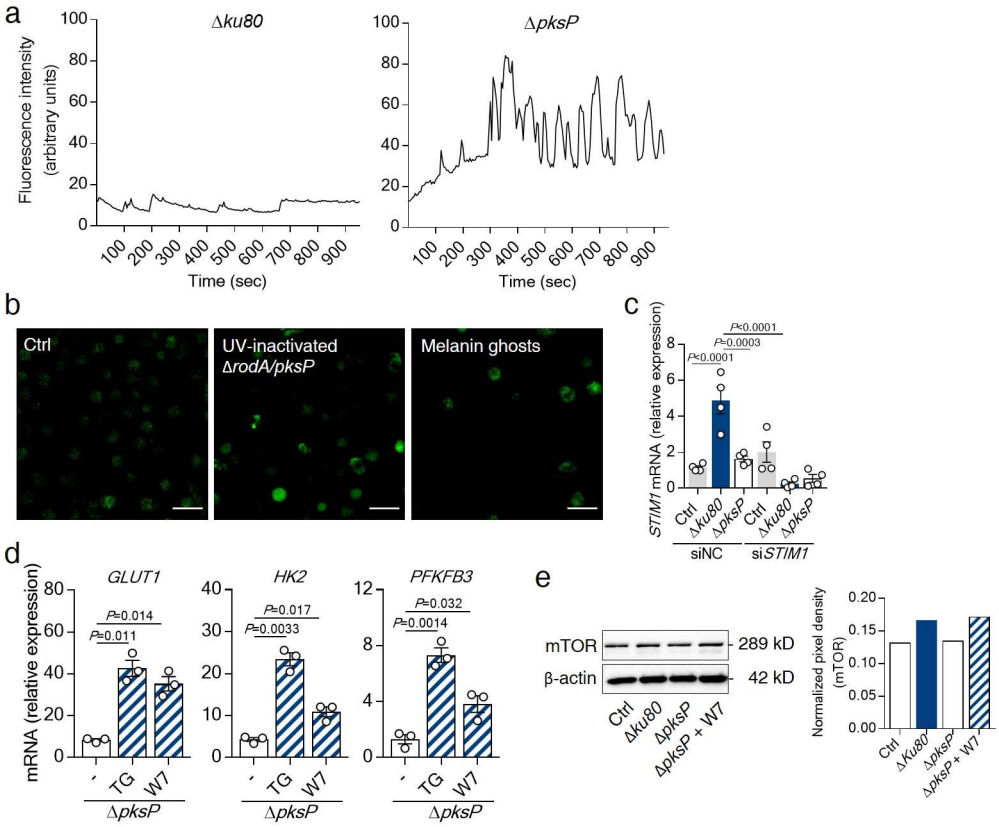

Supplementary Figure 5 | Inhibition of calcium signaling enables host glucose metabolism in response to *A. fumigatus*. (a) Representative patterns of cytosolic calcium spikes in macrophages preloaded with the calcium indicator Fluo-4-AM and infected with the Δ*ku80* or Δ*pksP* strains. (b) Micrographs of macrophages preloaded with the calcium indicator Fluo-4-AM and left untreated (Ctrl) or stimulated with UV-inactivated Δ*rodA/pksP* conidia or melanin ghosts for 15 min (representative of three independent experiments). Scale bars, 35 μm. (c) mRNA expression of *STIM1* in macrophages left uninfected (Ctrl) or infected and silenced

with a *STIM1* siRNA (si*STIM1*) (n=4). A scrambled siRNA was used as negative control (siNC). (d) mRNA expression of *GLUT1*, *HK2* and *PFKFB3* in macrophages infected with the Δ*pksP* strain for 2 hr relative to uninfected cells without or with 2 μM TG or 25 μM W7 (n=3). (e) Total mTOR in macrophages infected for 2 hr with the Δ*ku80*, Δ*pksP* or Δ*pksP* strains with 25 μM W7, with β-actin used as loading control (representative of two independent experiments). The pixel density of mTOR was normalized to β-actin. Data are expressed as mean values ± SEM; P values were calculated using Student's two-tailed t test or one-way ANOVA with Tukey's multiple comparisons test.

Supplementary Table 1. List of primers.

Primer name		**Primer sequence (5´-3´)**
hACTB	Forward	CTTCCAGCCTTCCTTCCTGG
	Reverse	ATTGCCAGGGTACATGGTGG
hGLUT1	Forward	ACTCATGACCATCGCGCTAG
	Reverse	GGACCCTGGCTGAAGAGTTC
hHK2	Forward	TTGACCAGGAGATTGACATGGG
	Reverse	CAACCGCATCAGGACCTCA
hPFKFB3	Forward	ATTGCGGTTTTCGATGCCAC
	Reverse	GCCACAACTGTAGGGTGGT
hHIF1A	Forward	GCTTTAACTTTGCTGGCCCC
	Reverse	TTTTCGTTGGGTGAGGGGAG
hSTIM1	Forward	GTCACAGTGAGAAGGCGACA
	Reverse	TGTGGATGTTACGGACTGCC
mUbb	Forward	TGGCTATTAATTATTCGGTCTGGAT
	Reverse	GCAAGTGGCTAGAGTGCAGAGTAA
mGlut1	Forward	CACTGTGGTGTCGCTGTTTG
	Reverse	AAAGATGGCCACGATGCTCA
mHk2	Forward	CACCCTACAGCAGCTGTGAA
	Reverse	TCTCCATCTCCACCCTCTGG
mPfkfb3	Forward	TGTCCAGCAGAGGCAAGAAG
	Reverse	TCTCGTTGAGTGCCTTCCAC
af18S	Forward	ATGGCCGTTCTTAGTTGGTG
	Reverse	GAGCCGATAGTCCCCCTAAG
afhxkA	Forward	TGACCACTTCGTCAAGGAGC

	Reverse	GGCAGATATCGAAGCCTCCC
afpfkA	Forward	TTGACTTCCTGCGGGAGAAC
	Reverse	CCTTGGCCTCCTCCTTGAAG

References

1. O'Neill LA, Pearce EJ. Immunometabolism governs dendritic cell and macrophage function. J Exp Med. 2016 Jan 11;213(1):15-23.
2. Van den Bossche J, O'Neill LA, Menon D. Macrophage immunometabolism: where are we (going)? Trends Immunol. 2017 Jun;38(6):395-406.
3. Millet P, Vachharajani V, McPhail L, et al. GAPDH binding to TNF-alpha mRNA contributes to posttranscriptional repression in monocytes: a novel mechanism of communication between inflammation and metabolism. J Immunol. 2016 Mar 15;196(6):2541-51.
4. Palsson-McDermott EM, Curtis AM, Goel G, et al. Pyruvate kinase M2 regulates Hif-1alpha activity and IL-1beta induction and is a critical determinant of the warburg effect in LPS-activated macrophages. Cell Metabol. 2015 Jan 6;21(1):65-80.
5. Jha AK, Huang SC, Sergushichev A, et al. Network integration of parallel metabolic and transcriptional data reveals metabolic modules that regulate macrophage polarization. Immunity. 2015 Mar 17;42(3):419-30.
6. Lampropoulou V, Sergushichev A, Bambouskova M, et al. Itaconate links inhibition of succinate dehydrogenase with macrophage metabolic remodeling and regulation of inflammation. Cell Metabol. 2016 Jul 12;24(1):158-66.
7. Mills EL, Kelly B, Logan A, et al. Succinate dehydrogenase supports metabolic repurposing of mitochondria to drive Inflammatory macrophages. Cell. 2016 Oct 6;167(2):457-470 e13.
8. Van den Bossche J, Baardman J, Otto NA, et al. Mitochondrial dysfunction prevents repolarization of inflammatory macrophages. Cell Rep. 2016 Oct 11;17(3):684-696.
9. Tannahill GM, Curtis AM, Adamik J, et al. Succinate is an inflammatory signal that induces IL-1beta through HIF-1alpha. Nature. 2013 Apr 11;496(7444):238-42.
10. Stienstra R, Netea-Maier RT, Riksen NP, et al. Specific and complex reprogramming of cellular metabolism in myeloid cells during innate immune responses. Cell Metabol. 2017 Jul 5;26(1):142-156.
11. Cheng SC, Quintin J, Cramer RA, et al. mTOR- and HIF-1alpha-mediated aerobic glycolysis as metabolic basis for trained immunity. Science. 2014 Sep 26;345(6204):1250684.
12. Lachmandas E, Beigier-Bompadre M, Cheng SC, et al. Rewiring cellular metabolism via the AKT/mTOR pathway contributes to host defence against *Mycobacterium tuberculosis* in human and murine cells. Eur J Immunol. 2016 Nov;46(11):2574-2586.
13. Wickersham M, Wachtel S, Wong Fok Lung T, et al. Metabolic stress drives keratinocyte defenses against *Staphylococcus aureus* infection. Cell Rep. 2017 Mar 14;18(11):2742-2751.
14. Lachmandas E, Boutens L, Ratter JM, et al. Microbial stimulation of different Toll-like receptor signalling pathways induces diverse metabolic programmes in human monocytes. Nat Microbiol. 2016 Dec 19;2:16246.
15. Netea MG, Joosten LA, van der Meer JW, et al. Immune defence against *Candida* fungal infections. Nat Rev Immunol. 2015 Oct;15(10):630-42.
16. van de Veerdonk FL, Gresnigt MS, Romani L, et al. *Aspergillus fumigatus* morphology and dynamic host interactions. Nat Rev Microbiol. 2017 Nov;15(11):661-674.
17. Arts RJ, Novakovic B, Ter Horst R, et al. Glutaminolysis and fumarate accumulation integrate immunometabolic and epigenetic programs in trained immunity. Cell Metabol. 2016 Dec 13;24(6):807-819.
18. Bekkering S, Arts RJW, Novakovic B, et al. Metabolic induction of trained immunity through the mevalonate pathway. Cell. 2018 Jan 11;172(1-2):135-146 e9.

19. Dominguez-Andres J, Novakovic B, Li Y, et al. The itaconate pathway is a central regulatory node linking innate immune tolerance and trained immunity. Cell Metabol. 2018 Oct 1.
20. Dominguez-Andres J, Arts RJW, Ter Horst R, et al. Rewiring monocyte glucose metabolism via C-type lectin signaling protects against disseminated candidiasis. PLoS Pathog. 2017 Sep;13(9):e1006632.
21. Cheng SC, Scicluna BP, Arts RJ, et al. Broad defects in the energy metabolism of leukocytes underlie immunoparalysis in sepsis. Nat Immunol. 2016 Apr;17(4):406-13.
22. Tucey TM, Verma J, Harrison PF, et al. Glucose homeostasis is important for immune cell viability during *Candida* challenge and host survival of systemic fungal Infection. Cell Metabol. 2018 May 1;27(5):988-1006 e7.
23. Segal BH. Aspergillosis. N Engl J Med. 2009 Apr 30;360(18):1870-84.
24. Brown GD, Denning DW, Gow NA, et al. Hidden killers: human fungal infections. Sci Transl Med. 2012 Dec 19;4(165):165rv13.
25. Maertens JA, Raad, II, Marr KA, et al. Isavuconazole versus voriconazole for primary treatment of invasive mould disease caused by *Aspergillus* and other filamentous fungi (SECURE): a phase 3, randomised-controlled, non-inferiority trial. Lancet. 2016 Feb 20;387(10020):760-9.
26. Herbst S, Shah A, Mazon Moya M, et al. Phagocytosis-dependent activation of a TLR9-BTK-calcineurin-NFAT pathway co-ordinates innate immunity to *Aspergillus fumigatus*. EMBO Mol Med. 2015 Mar;7(3):240-58.
27. Shah A, Kannambath S, Herbst S, et al. Calcineurin orchestrates lateral transfer of *Aspergillus fumigatus* during macrophage cell death. Am J Respir Crit Care Med. 2016 Nov 1;194(9):1127-1139.
28. Espinosa V, Jhingran A, Dutta O, et al. Inflammatory monocytes orchestrate innate antifungal immunity in the lung. PLoS Pathog. 2014 Feb;10(2):e1003940.
29. Cunha C, Di Ianni M, Bozza S, et al. Dectin-1 Y238X polymorphism associates with susceptibility to invasive aspergillosis in hematopoietic transplantation through impairment of both recipient- and donor-dependent mechanisms of antifungal immunity. Blood. 2010 Dec 9;116(24):5394-402.
30. Cunha C, Goncalves SM, Duarte-Oliveira C, et al. IL-10 overexpression predisposes to invasive aspergillosis by suppressing antifungal immunity. J Allergy Clin Immunol. 2017 Sep;140(3):867-870 e9.
31. Gresnigt MS, Cunha C, Jaeger M, et al. Genetic deficiency of NOD2 confers resistance to invasive aspergillosis. Nat Commun. 2018 6;9(1):2636.
32. Stappers MHT, Clark AE, Aimanianda V, et al. Recognition of DHN-melanin by a C-type lectin receptor is required for immunity to *Aspergillus*. Nature. 2018 Mar 15;555(7696):382-386.
33. Liberzon A, Birger C, Thorvaldsdottir H, et al. The molecular signatures database (MSigDB) hallmark gene set collection. Cell Syst. 2015 Dec 23;1(6):417-425.
34. Parikh H, Carlsson E, Chutkow WA, et al. TXNIP regulates peripheral glucose metabolism in humans. PLoS Med. 2007 May;4(5):e158.
35. Latge JP, Beauvais A, Chamilos G. The cell wall of the human fungal pathogen *Aspergillus fumigatus*: biosynthesis, organization, immune response, and virulence. Annu Rev Microbiol. 2017 Sep 8;71:99-116.
36. Aimanianda V, Bayry J, Bozza S, et al. Surface hydrophobin prevents immune recognition of airborne fungal spores. Nature. 2009 Aug 27;460(7259):1117-21.

37. Jahn B, Koch A, Schmidt A, et al. Isolation and characterization of a pigmentless-conidium mutant of *Aspergillus fumigatus* with altered conidial surface and reduced virulence. Infect Immun. 1997 Dec;65(12):5110-7.
38. Sarfati J, Diaquin M, Debeaupuis JP, et al. A new experimental murine aspergillosis model to identify strains of *Aspergillus fumigatus* with reduced virulence. Nihon Ishinkin Gakkai Zasshi. 2002;43(4):203-13.
39. Langfelder K, Streibel M, Jahn B, et al. Biosynthesis of fungal melanins and their importance for human pathogenic fungi. Fungal Genet Biol. 2003 Mar;38(2):143-58.
40. Duvel K, Yecies JL, Menon S, et al. Activation of a metabolic gene regulatory network downstream of mTOR complex 1. Mol Cell. 2010 Jul 30;39(2):171-83.
41. Dibble CC, Cantley LC. Regulation of mTORC1 by PI3K signaling. Trends Cell Biol. 2015 Sep;25(9):545-55.
42. Majumder PK, Febbo PG, Bikoff R, et al. mTOR inhibition reverses Akt-dependent prostate intraepithelial neoplasia through regulation of apoptotic and HIF-1-dependent pathways. Nat Med. 2004 Jun;10(6):594-601.
43. Kyrmizi I, Ferreira H, Carvalho A, et al. Calcium sequestration by fungal melanin inhibits calcium-calmodulin signalling to prevent LC3-associated phagocytosis. Nat Microbiol. 2018 Jul;3(7):791-803.
44. Raffaello A, Mammucari C, Gherardi G, et al. Calcium at the center of cell signaling: interplay between endoplasmic reticulum, mitochondria, and lysosomes. Trends Biochem Sci. 2016 Dec;41(12):1035-1049.
45. Liou J, Kim ML, Heo WD, et al. STIM is a Ca^{2+} sensor essential for Ca^{2+}-store-depletion-triggered Ca2+ influx. Curr Biol. 2005 Jul 12;15(13):1235-41.
46. Howard NC, Marin ND, Ahmed M, et al. *Mycobacterium tuberculosis* carrying a rifampicin drug resistance mutation reprograms macrophage metabolism through cell wall lipid changes. Nat Microbiol. 2018 Oct;3(10):1099-1108.
47. Akoumianaki T, Kyrmizi I, Valsecchi I, et al. *Aspergillus* cell wall melanin blocks LC3-associated phagocytosis to promote pathogenicity. Cell Host Microbe. 2016 Jan 13;19(1):79-90.
48. Thywissen A, Heinekamp T, Dahse HM, et al. Conidial dihydroxynaphthalene melanin of the human pathogenic fungus *Aspergillus fumigatus* interferes with the host endocytosis pathway. Front Microbiol. 2011;2:96.
49. Volling K, Thywissen A, Brakhage AA, et al. Phagocytosis of melanized *Aspergillus* conidia by macrophages exerts cytoprotective effects by sustained PI3K/Akt signalling. Cell Microbiol. 2011 Aug;13(8):1130-48.
50. Ugolini M, Sander LE. Dead or alive: how the immune system detects microbial viability. Curr Opin Immunol. 2018 Oct 23;56:60-66.
51. Moretti J, Roy S, Bozec D, et al. STING senses microbial viability to orchestrate stress-mediated autophagy of the endoplasmic reticulum. Cell. 2017 Nov 2;171(4):809-823 e13.
52. Briard B, Karki R, Malireddi RKS, et al. Fungal ligands released by innate immune effectors promote inflammasome activation during *Aspergillus fumigatus* infection. Nat Microbiol. 2018 Dec 3.
53. Karki R, Man SM, Malireddi RK, et al. Concerted activation of the AIM2 and NLRP3 inflammasomes orchestrates host protection against *Aspergillus* infection. Cell Host Microbe. 2015 Mar 11;17(3):357-68.
54. Willger SD, Grahl N, Cramer RA, Jr. *Aspergillus fumigatus* metabolism: clues to mechanisms of in vivo fungal growth and virulence. Med Mycol. 2009;47 Suppl 1:S72-9.

55. Schmidt H, Vlaic S, Kruger T, et al. Proteomics of *Aspergillus fumigatus* conidia-containing phagolysosomes identifies processes governing immune evasion. Mol Cell Proteomics. 2018 Jun;17(6):1084-1096.
56. Scheffler JM, Sparber F, Tripp CH, et al. LAMTOR2 regulates dendritic cell homeostasis through FLT3-dependent mTOR signalling. Nat Commun. 2014 Oct 22;5:5138.
57. Sakamoto T, Weng JS, Hara T, et al. Hypoxia-inducible factor 1 regulation through cross talk between mTOR and MT1-MMP. Mol Cell Biol. 2014 Jan;34(1):30-42.
58. Shepardson KM, Jhingran A, Caffrey A, et al. Myeloid derived hypoxia inducible factor 1-alpha is required for protection against pulmonary *Aspergillus fumigatus* infection. PLoS Pathog. 2014 Sep;10(9):e1004378.
59. Fliesser M, Morton CO, Bonin M, et al. Hypoxia-inducible factor 1alpha modulates metabolic activity and cytokine release in anti-*Aspergillus fumigatus* immune responses initiated by human dendritic cells. Int J Med Microbiol. 2015 Dec;305(8):865-73.
60. Corretti MC, Koretsune Y, Kusuoka H, et al. Glycolytic inhibition and calcium overload as consequences of exogenously generated free radicals in rabbit hearts. J Clin Invest. 1991 Sep;88(3):1014-25.
61. Takagaki G. Control of aerobic glycolysis and pyruvate kinase activity in cerebral cortex slices. J Neurochem. 1968 Sep;15(9):903-16.
62. Krajcovic M, Krishna S, Akkari L, et al. mTOR regulates phagosome and entotic vacuole fission. Mol Biol Cell. 2013 Dec;24(23):3736-45.
63. Shen K, Sabatini DM. Ragulator and SLC38A9 activate the Rag GTPases through noncanonical GEF mechanisms. Proc Natl Acad Sci U S A. 2018 Sep 18;115(38):9545-9550.
64. da Silva Ferreira ME, Kress MR, Savoldi M, et al. The akuB(KU80) mutant deficient for nonhomologous end joining is a powerful tool for analyzing pathogenicity in *Aspergillus fumigatus*. Eukaryot Cell. 2006 Jan;5(1):207-11.
65. Tsai HF, Washburn RG, Chang YC, et al. *Aspergillus fumigatus* arp1 modulates conidial pigmentation and complement deposition. Mol Microbiol. 1997 Oct;26(1):175-83.
66. Tsai HF, Wheeler MH, Chang YC, et al. A developmentally regulated gene cluster involved in conidial pigment biosynthesis in *Aspergillus fumigatus*. J Bacteriol. 1999 Oct;181(20):6469-77.
67. Bayry J, Beaussart A, Dufrene YF, et al. Surface structure characterization of A*spergillus fumigatus* conidia mutated in the melanin synthesis pathway and their human cellular immune response. Infect Immun. 2014 Aug;82(8):3141-53.
68. Mortazavi A, Williams BA, McCue K, et al. Mapping and quantifying mammalian transcriptomes by RNA-Seq. Nat Methods. 2008 Jul;5(7):621-8.
69. Robinson MD, McCarthy DJ, Smyth GK. edgeR: a Bioconductor package for differential expression analysis of digital gene expression data. Bioinformatics. 2010 Jan 1;26(1):139-40.
70. Misharin AV, Morales-Nebreda L, Mutlu GM, et al. Flow cytometric analysis of macrophages and dendritic cell subsets in the mouse lung. Am J Respir Cell Mol Biol. 2013 Oct;49(4):503-10.

Chapter III

Genetic variation in PFKFB3 impairs antifungal immunometabolic responses and predisposes to invasive pulmonary aspergillosis

This chapter was published in:

Goncalves SM, Antunes D, Leite L, et al. Genetic variation in PFKFB3 impairs antifungal immunometabolic responses and predisposes to invasive pulmonary aspergillosis. mBio. 2021 Jun 29;12(3):e0036921.

Genetic variation in PFKFB3 impairs antifungal immunometabolic responses and predisposes to invasive pulmonary aspergillosis

Samuel M. Gonçalves[1,2], Daniela Antunes[1,2], Luis Leite[3], Toine Mercier[4,5], Rob ter Horst[6], Joana Vieira[7], Eduardo Espada[7], Carlos Pinho Vaz[3], Rosa Branca[3], Fernando Campilho[3], Fátima Freitas[8], Dário Ligeiro[9], António Marques[10], Frank L. van de Veerdonk[6], Leo AB Joosten[6], Katrien Lagrou[5,11], Johan Maertens[4,5], Mihai G. Netea[6,12], João F. Lacerda[7,13], António Campos Jr.[3], Cristina Cunha[1,2], Agostinho Carvalho[1,2]

[1] Life and Health Sciences Research Institute (ICVS), School of Medicine, University of Minho, Braga, Portugal

[2] ICVS/3B's - PT Government Associate Laboratory, Guimarães/Braga, Portugal

[3] Serviço de Transplantação de Medula Óssea (STMO), Instituto Português de Oncologia do Porto, Porto, Portugal

[4] Department of Hematology, University Hospitals Leuven, Leuven, Belgium

[5] Department of Microbiology, Immunology and Transplantation, KU Leuven, Leuven, Belgium

[6] Department of Internal Medicine and Radboud Center for Infectious diseases (RCI), Radboud University Nijmegen Medical Centre, Nijmegen, the Netherlands

[7] Serviço de Hematologia e Transplantação de Medula, Hospital de Santa Maria, Lisboa, Portugal

[8] Instituto Português do Sangue e Transplantação, IP, Porto, Portugal

[9] Instituto Português do Sangue e Transplantação, IP, Lisboa, Portugal

[10] Serviço de Imuno-Hemoterapia, Hospital de Braga, Braga, Portugal

[11] Clinical Department of Laboratory Medicine and National Reference Center for Mycosis, University Hospitals Leuven, Leuven, Belgium

[12] Department for Genomics & Immunoregulation, Life and Medical Sciences Institute (LIMES), University of Bonn, Bonn, Germany

[13] Instituto de Medicina Molecular, Faculdade de Medicina da Universidade de Lisboa, Lisboa, Portugal

Abstract

Activation of immune cells in response to fungal infection involves the reprogramming of their cellular metabolism to support antimicrobial effector functions. Although metabolic pathways such as glycolysis are known to represent critical regulatory nodes in antifungal immunity, it remains undetermined whether these are differentially regulated at interindividual level. In this study, we identify a key role for 6-phosphofructo-2-kinase/fructose-2,6-bisphosphatase 3 (PFKFB3) in the immunometabolic responses to *Aspergillus fumigatus*. A genetic association study performed in 439 recipients of allogeneic hematopoietic stem cell transplantation (HSCT) and corresponding donors revealed that the donor, but not recipient, rs646564 variant in the *PFKFB3* gene increased the risk of invasive pulmonary aspergillosis (IPA) after transplantation. The risk genotype impaired the expression of PFKFB3 by human macrophages in response to fungal infection, which was correlated with a defective activation of glycolysis and the ensuing antifungal effector functions. In patients with IPA, the risk genotype was associated with lower concentrations of cytokines in the bronchoalveolar lavage. Collectively, these findings demonstrate the important contribution of genetic variation in *PFKFB3* to the risk of IPA in patients undergoing HSCT, and support its inclusion in prognostic tools to predict the risk of fungal infection in this clinical setting.

Importance

The fungal pathogen *Aspergillus fumigatus* can cause severe and life-threatening forms of infection in immunocompromised patients. Activation of glycolysis is essential for innate immune cells to mount effective antifungal responses. In this study, we report the contribution of genetic variation in the key glycolytic activator 6-phosphofructo-2-kinase/fructose-2,6-bisphosphatase 3 (PFKFB3) to the risk of invasive pulmonary aspergillosis (IPA) after allogeneic hematopoietic stem-cell transplantation. The *PFKFB3* genotype associated with increased risk of infection was correlated with an impairment of the antifungal effector functions of macrophages in vitro and in patients with IPA. This work highlights the clinical relevance of genetic variation in *PFKFB3* to the risk of IPA and supports its integration in risk stratification and preemptive measures for patients at high-risk of IPA

Keywords

Immunometabolism, PFKFB3, *Aspergillus*, Invasive Pulmonary Aspergillosis, Stem-cell transplantation, Single Nucleotide Polymorphism, Macrophage, Antifungal immunity

Introduction

Recent advances in medicine and the introduction of broad-spectrum antibiotics has prompted an increasing incidence of invasive fungal infections, particularly among hematological patients with chemotherapy or patients undergoing solid organ or allogeneic hematopoietic stem-cell transplantation (HSCT) [1]. Invasive pulmonary aspergillosis (IPA) is a major cause of mortality in these clinical settings, with rates estimated between 20 and 30% [2,3], but that can reach 80% when infection involves azole-resistant strains [4]. The clinical relevance of these infections is further emphasized by limitations in available tests for the diagnosis of IPA. The development of more effective medical interventions is therefore an urgent need that demands an improved understanding of the pathogenesis of IPA.

The reprogramming of immune cell metabolism is acknowledged as a crucial event required for mounting protective immune responses against fungal pathogens [5]. During infection, innate immune cells, e.g., monocytes and macrophages, rewire their energy metabolism from oxidative phosphorylation to glycolysis to rapidly and efficiently support antimicrobial functions, such as phagocytosis and production of inflammatory mediators [6]. The critical role of glucose metabolism during infection is further supported by experimental evidence demonstrating that its blockade dampens the immune response and hampers the clearance of selected bacterial and fungal pathogens [7-11]. In turn, pathogens have also developed complex virulence strategies to exploit and subvert the metabolic requirements of immune cells to their benefit [12,13].

The recognition of pathogen-associated molecular patterns (PAMPs) drives substantial changes in cellular metabolism and effector functions of immune cells [14]. The fungal cell wall contains a considerable diversity of PAMPs, including β-1,3-glucan, melanin, and chitin [15,16], capable of promoting the metabolic and functional reprogramming of immune cells. For example, stimulation of monocytes with β-1,3-glucan promotes metabolic and epigenetic changes underlying the acquisition of a "trained immunity" phenotype characterized by enhanced cytokine production in response to heterologous secondary stimulation [7,17-20]. More recently, the removal of fungal melanin within the phagosomal compartment of macrophages was established as the activating signal required for the induction of glucose metabolism in immune cells during infection with *Aspergillus fumigatus* [8].

The upregulation of glycolytic enzymes upon infection also directly supports cytokine expression through mechanisms that involve "moonlighting" activities [21,22]. The 6-phosphofructo-2-kinase/fructose-2,6- bisphosphatase 3 (PFKFB3) enzyme is a master regulator of the glycolytic pathway [23]. By orchestrating the balance between the synthesis and degradation of fructose-2,6-bisphosphate,

it acts as an allosteric activator of 6-phophofructo-1-kinase, the rate-limiting enzyme in glycolysis [24]. As a result of its glycolysis-promoting activity, PFKFB3 has been shown to coordinate antiviral effector functions of macrophages [25] and to be highly expressed in myeloid cells from critically ill COVID-19 patients [26]. Also, PFKFB3 has been shown to be a target of the zinc fingers and homeoboxes 2 (ZHX2) transcription factor and, as a result, to accelerate disease progression in models of sepsis [27].

Since the risk of infection varies considerably even among patients with comparable immune dysfunction and predisposing clinical factors, susceptibility to IPA is thought to depend largely on genetic predisposition [28-32]. However, the potential involvement of variation in genes involved in glucose metabolism during the development of IPA has never been addressed. Here, we describe the association of genetic variation in *PFKFB3* with an increased risk for developing IPA in HSCT patients, as the result of a defective metabolic reprogramming and downstream antifungal effector functions of macrophages. Collectively, our results pinpoint a novel genetic factor regulating metabolic responses in immune cells and provide support for risk stratification and preventive measures aimed at a more effective management of IPA.

Methods

Ethics statement

Approval for the IFIGEN study was obtained from the SECVS (no. 125/014), the Ethics Committee for Health of the Instituto Português de Oncologia - Porto, Portugal (no. 26/015), the Ethics Committee of the Lisbon Academic Medical Center, Portugal (no. 632/014), and the National Commission for the Protection of Data, Portugal (no. 1950/015). The FUNBIOMICS study was approved by SECVS (no. 126/2014) and the Ethics Committee of the University Hospitals of Leuven, Belgium. The Human Functional Genomics Project (HFGP) study was approved by the Ethical Committee of Radboud University Nijmegen, the Netherlands (no. 42561.091.12). Experiments were conducted according to the principles expressed in the Declaration of Helsinki, and participants provided written informed consent. The functional experiments involving cells isolated from the peripheral blood of healthy volunteers at the Hospital of Braga, Portugal, was approved by the Ethics Subcommittee for Life and Health Sciences (SECVS) of the University of Minho, Portugal (no. 014/015).

Population cohort

The functional experiments were performed in healthy individuals of Western European ancestry recruited at Hospital de Braga, Braga, Portugal, and in the 500FG cohort from the HFGP, which comprises 534 Dutch healthy individuals of Western European ancestry. The genetic association study with IPA was performed in a total of 460 hematological patients of European ancestry undergoing allogeneic HSCT at Instituto Português de Oncologia, Porto, and at Hospital de Santa Maria, Lisbon was enrolled in the IFIGEN study between 2009 and 2015. Of these, 439 had available donor and recipient DNA samples and patient-level data. The demographic and clinical characteristics of the patients are summarized in Table 1. Ninety-one cases of probable/proven IPA were identified according to the standard criteria from the European Organization for Research and Treatment of Cancer/Mycology Study Group (EORTC/MSG) [42]. Twenty-one patients were excluded from the study based on the “possible” classification of infection.

Table 1. Baseline characteristics of transplant recipients enrolled in the study.

Variables	IPA (n=91)	No IPA (n=348)	P value
Age at transplantation, no (%)			
≤20 years	13 (14.3)	69 (19.8)	0.264
21 – 40 years	23 (25.3)	101 (29.0)	
>40 years	55 (60.4)	178 (51.2)	
Gender, no (%)			
Female	38 (41.8)	150 (43.1)	0.859
Male	53 (58.2)	198 (56.9)	
Underlying disease, no. (%)			
Acute leukemia	49 (53.8)	179 (51.5)	0.115
Lymphoproliferative diseases	14 (15.4)	69 (19.8)	
Myelodysplastic/myeloproliferative diseases	13 (14.3)	30 (8.6)	
Chronic myeloproliferative diseases	7 (7.7)	20 (5.7)	
Aplastic anemia	6 (6.6)	17 (4.9)	
Other	2 (2.2)	33 (9.5)	
Transplantation type, no. (%)			
Matched, related	34 (37.4)	169 (48.6)	0.037
Matched, unrelated	33 (36.3)	81 (23.3)	
Mismatched, related	0 (0.0)	7 (2.0)	
Mismatched, unrelated	24 (26.4)	91 (26.2)	
Graft source, no. (%)			
Peripheral blood	80 (87.9)	287 (82.5)	0.506
Bone-marrow	10 (11.0)	53 (15.2)	
Cord blood	1 (1.1)	8 (2.3)	
Disease stage, no. (%)			
First complete remission	49 (53.8)	188 (54.0)	0.800
Second or subsequent remission, or relapse	13 (14.3)	59 (17.0)	
Active disease	29 (31.9)	101 (29.0)	
Conditioning regimen, no (%)			
RIC	68 (74.7)	228 (65.5)	0.091
Myeloablative	23 (25.3)	120 (34.5)	
CMV serostatus of donor and recipient, no. (%)			

D-/R+ or D+/R+	80 (87.9)	313 (89.9)	0.504
D-/R- or D+/R-	11 (12.1)	35 (10.1)	
Duration of neutropenia, mean days (range)†	13.1 (8 – 39)	13.5 (5 – 35)	0.460
Acute GVHD, no. (%)			
No GVHD or grades I – II	63 (69.2)	302 (86.8)	0.0002
Grades III – IV	28 (30.8)	46 (13.2)	
Antifungal prophylaxis, no. (%)‡			
Fluconazole	42 (46.2)	117 (33.6)	0.002
Posaconazole	26 (28.6)	107 (30.8)	
Other	9 (9.9)	14 (4.0)	
None or unknown	14 (15.4)	110 (31.6)	

Twenty-one patients with "possible" IPA were excluded. Lymphoproliferative diseases included cases of chronic lymphocytic leukemia, multiple myeloma, and B- and T-cell lymphomas. Chronic myeloproliferative diseases included cases of chronic myelogenous leukemia and primary myelofibrosis. Other diseases included cases of idiopathic medullar aplasia, lymphohistiocytosis, hemoglobinopathies and paroxysmal nocturnal hemoglobinuria. RIC, reduced intensity conditioning; CMV, cytomegalovirus; D, donor; R, recipient; GVHD, graft-versus-host-disease. †Neutropenia was defined as $\leq 0.5\times10^9$ cells/L. ‡Other antifungals used in prophylaxis included voriconazole, liposomal amphotericin B, itraconazole and caspofungin. P values were calculated by Fisher's exact probability t-test or Student's t-test for continuous variables.

SNP selection and genotyping

Genomic DNA was isolated from whole blood using the QIAcube automated system (Qiagen). SNPs were selected based on their putative role as cytokine QTLs in the HFGP study and on their ability to tag surrounding variants with a pairwise correlation coefficient r^2 of at least 0.80 and a minor allele frequency ≥5% using publicly available sequencing data from the Pilot 1 of the 1000 Genomes Project for the CEU population. Genotyping of rs674430 and rs646564 SNPs in *PFKFB3* was performed using KASPar assays (LGC Genomics) in an Applied Biosystems 7500 Fast Real-Time PCR system (Thermo Fisher Scientific), according to the manufacturer's instructions. The DNA samples of individuals from the 500FG cohort were genotyped using the commercially available chip Illumina HumanOmniExpressExome-8 v1.0. Quality control and imputation were performed as described [43].

Cytokine QTL mapping

Following the generation of genotype and cytokine data, cytokine QTLs were mapped as described [43]. Briefly, concentrations of human cytokines were determined using specific commercial ELISA kits (PeliKine Compact, or R&D Systems), per the manufacturer's instructions. Cytokine QTLs were identified by log-transforming raw cytokine levels and mapping them to genotype data using a linear regression model with age, gender and cell counts as covariates.

Generation of monocyte-derived macrophages

Buffy coats from healthy donors were obtained after written informed consent. Briefly, peripheral blood mononuclear cells (PBMCs) were enriched from buffy coats by density gradient using Histopaque®-1077 (Sigma-Aldrich). Cells present in the enriched mononuclear fraction were washed twice in PBS and resuspended in RPMI-1640 culture medium with 2 mM glutamine (Thermo Fisher Scientific) supplemented with 10% human serum (Sigma-Aldrich), 10 U/mL penicillin/streptomycin, and 10 mM HEPES (Thermo Fisher Scientific). Monocytes were then separated using positive magnetic bead separation with anti-$CD14^+$ coated beads (MACS Miltenyi) according to the manufacturer's instructions. To evaluate the purity of the isolated monocyte population, 5×10^5 cells were stained with a BV 650 anti-human CD14 (clone M5E2) antibody for 30 min at 4°C. Cell viability was assessed by staining with Zombie Green fluorescent dye (BioLegend) for 30 min at 4°C. Pellets were washed and resuspended in FACS buffer (PBS containing 2% FBS and 2mM EDTA) prior to analysis. Data were obtained on a BD FACS LSRII instrument (Becton Dickinson), and processed using FlowJo (Tree Star Inc). The obtained $CD14^+$ populations displayed a purity higher than 94%, and with more than 97% viable cells. Isolated monocytes were then resuspended in complete RPMI medium and seeded at a concentration of 1×10^6 cells/mL in 24-well and 96-well plates (Corning Inc.) for 7 days in the presence of 20 ng/mL of recombinant human granulocyte-macrophage colony-stimulating factor (GM-CSF, Miltenyi Biotec). Acquisition of macrophage morphology was confirmed by visualization in a BX61 microscope (Olympus, Tokyo, Japan).

Stimulation of MDMs

Unless otherwise indicated, monocyte-derived macrophages (MDMs) (5×10^5/well in 24-well plates) were either left untreated or stimulated with live conidia of *A. fumigatus* at a 1:5 or 1:10 effector-to-target ratio,

respectively, for 24 hr at 37 °C and 5% CO_2. In some conditions, MDMs were pre-treated for 4 hr with 30 μM of 3-(3-pyridinyl)-1-(4-pyridinyl)-2-propen-1-one (3PO) to inhibit PFKFB3 activity. In all experiments, data were assessed in triplicates and are shown as the mean value for each individual.

Quantification of glucose and lactate by HPLC

After infection, supernatants were removed, centrifuged, and transferred to HPLC tubes. Glucose and lactate levels were determined using a Gilson pump system (Gilson) with a 54 °C HyperREZ XP Carbohydrate H^+ 8 μM (Thermo Fisher Scientific) column and a refractive index detector (IOTA 2, Reagents). The mobile phase consisting of 0.0025 M H_2SO_4 was filtered and degasified for at least 45 min before use. Standard solutions were prepared in MilliQ water (Millipore). All data were analyzed using the Gilson Uniprot Software, version 5.11.

Phagocytosis assay

To evaluate phagocytosis, MDMs (5×10^5/well, in 24-well plates) were infected with fluorescein isothiocyanate (FITC)-labeled conidia of *A. fumigatus* at a 1:5 effector-to-target ratio. The infection was synchronized for 30 min at 4 °C and phagocytosis was initiated by shifting the co-incubation to 37 °C at 5% CO_2 for 1 hr. Phagocytosis was stopped by washing wells with PBS and extracellular conidia were stained with 0.25 mg/mL Calcofluor White (Sigma-Aldrich) for 15 min at 4 °C to avoid further ingestion. After washing wells twice with PBS, cells were fixed with 3.7% (v/v) formaldehyde/PBS for 15 min. The number of MDMs with ingested green conidia was enumerated by examining the slides by fluorescence microscopy (Olympus), and data were expressed as the percentage of MDMs that internalized one or more conidia.

Conidiacidal activity assay

Following differentiation, MDMs (1×10^5/well, in 96-well plates) were stimulated with live *A. fumigatus* conidia at a 10:1 effector-to-target ratio for 1 hr at 37 °C and 5% CO_2, to allow the internalization of conidia. Medium containing the non-ingested conidia was removed, and wells were washed twice with PBS. To measure the conidiacidal activity, MDMs were allowed to eliminate the internalized conidia for 2 hr at 37 °C in 5% CO_2. After incubation, culture plates were snap-frozen at -80 °C and thawed at 37 °C to cause cell lysis and release of ingested conidia. Serial dilutions of cell lysates were plated on solid

growth media and, following a 24 hr incubation at 37 °C, the number of colony-forming units (CFUs) was enumerated and the percentage of CFU inhibition was calculated.

Measurement of ROS production

MDMs (5×10^5/well, in 24-well plates) were infected with live *A. fumigatus* conidia at a 1:5 effector-to-target ratio for 4 hr at 37 °C and 5% CO_2. After infection, the culture medium was removed, and cells were trypsinized for 10 min at 37 °C. Then, cells were collected and centrifuged for 5 min at 2,000 rpm. Finally, each pellet was resuspended in 10 μM dihydroethidium (cytosolic ROS) or 5 μM Mitosox (mitochondrial ROS) (Thermo Fisher Scientific), and cells were then incubated for 30 min at 37 °C, protected from light. Data were obtained on a BD FACS LSRII instrument (Becton Dickinson) and processed using FlowJo (Tree Star Inc)

ELISA

MDMs (5×10^5/well in 24-well plates) were infected with *A. fumigatus* conidia at a 1:5 or 1:10 effector-to-target ratio, respectively, for 24 hr at 37 °C and 5% CO_2. After infection, supernatants were collected and cytokine levels were quantified using ELISA MAX Deluxe Set kits (BioLegend), according to the manufacturer's instructions. Cytokine measurements in BAL samples were performed using the Human Premixed Multi-Analyte Kit (R&D Systems), according to the manufacturer's instructions.

Western blot analysis

MDMs (5×10^5/well, in 24-well plates) were infected with *A. fumigatus* conidia for 2 hr at a 1:10 effector-to-target ratio at 37 °C in 5% CO_2. After infection, cells were lysed in RIPA buffer (50 mM Tris, 250 mM NaCl, 2 mM EDTA, 1% NP-40, 10% glycerol, pH 7.2, and a mixture of protease inhibitors [Roche Molecular Biochemicals]). Cell lysis was performed at 4 °C for 30 min (with shaking) and samples were then centrifuged. The protein content was determined using the Bradford dye-binding (Bio-Rad) method. Laemmli buffer (Bio-Rad) was added to 20 μg of protein and samples were boiled and separated on a 12% SDS-PAGE gel and transferred to nitrocellulose membranes (Bio-Rad). Western blotting was performed according to the manufacturer's instructions, using the following primary antibodies: rabbit anti-PFKFB3 and mouse anti-β-actin, both from Abcam and diluted 1:1000. Secondary antibodies used

were anti-rabbit (Thermo Fisher Scientific) and anti-mouse (Bio-Rad), both diluted to 1:5000. The blots were developed using chemiluminescence (SuperSignal™ West Femto Maximum Sensitivity Substrate; Thermo Fisher Scientific) and detected with ChemiDoc™ XRS system (Bio-Rad). Signal intensities and quantifications were determined with the ImageLab 4.1 analysis software (Bio-Rad).

BAL fluid collection

BAL specimens were collected as previously described [33]. Briefly, specimens were collected using a flexible fiberoptic bronchoscope following local anesthesia with 2% lidocaine (Xylocaine), when infection was clinically suspected. Samples were obtained by instillation of a pre-warmed 0.9% sterile saline solution (20 mL twice). The sampling area was determined based on the localization of the lesion on chest imaging (X-ray or computed tomography scan). BAL specimens with comparable recovery rates were used. All samples were stored at -80 °C until use.

Statistical analysis

The probability of IPA according to *PFKFB3* genotypes was determined using the cumulative incidence method and compared using Gray's test [44]. Cumulative incidences at 24 months were computed with the *cmprsk* package for R version 2.10.1 [45], with censoring of data at the date of last follow-up visit and relapse and death as competing events. All clinical and genetic variables achieving a P-value ≤0.15 in the univariate analysis were entered one by one in a pairwise model together and kept in the final model if they remained significant ($P<0.05$). Multivariate analysis was performed using the subdistribution regression model of Fine and Gray with the *cmprsk* package for R [46]. Data obtained in functional assays were expressed as mean ± SEM. Unpaired Student's t-test with Bonferroni's adjustment and 2-tailed Mann-Whitney rank-sum test were used to determine statistical significance ($P<0.05$).

Results

The *PFKFB3* locus influences cytokine production during fungal infection

We have recently demonstrated that activation of glycolysis is required for effective immune responses against *A. fumigatus* [8]. We, therefore, examined whether variation in genes involved in the glycolytic pathway affected host responses to fungal infection. To do so, we tested the association of common SNPs (minor allele frequency, ≥5%) in relevant candidate genes with differential cytokine production after fungal stimulation of PBMCs from healthy individuals of the 500FG cohort in the Human Functional Genomics Project (HFGP).

We identified a total of 107 cQTLs in three genes involved in glucose metabolism, namely *PFKFB3*, *HK2,* and *AKT1* (Table S1). Although these were not different at a genome-wide level, several strong cQTLs were identified in *PFKFB3* displaying an uncorrected P-value <0.05. We next assessed linkage disequilibrium (LD) between the SNPs in *PFKFB3* (Fig. S1) and identified rs674430 and rs646564 to represent suitable candidates tagging the largest LD blocks influencing the production of multiple cytokines (Table S1). Specifically, the rs674430 SNP was associated with a genotype-dependent effect on the production of TNF (overall P=0.012) and IL-6 (overall P=0.013) by PBMCs after 24 hr of infection (Fig. 1A), whereas the rs646564 SNP influenced IFN-γ (overall P=0.011) and IL-22 (overall P=0.016) produced by cells stimulated for 7 days (Fig. 1B). Collectively, these findings suggest genetic variation in *PFKFB3* as an important regulator of cytokine production in response to *A. fumigatus* infection.

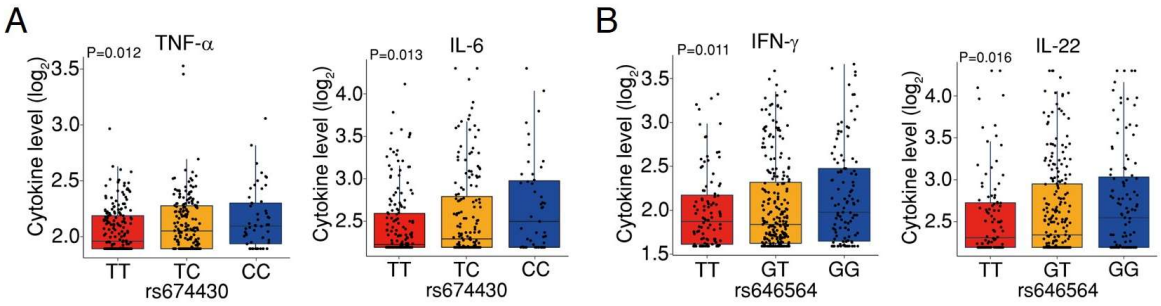

Figure 1. The *PFKFB3* locus influences the production of cytokines by PBMCs. (A) Levels (log2) of TNF and IL-6 according to rs674430 genotypes, and (B) IFNγ and IL-22 according to rs646564 genotypes detected after stimulation of PBMCs from the 500FG cohort with *A. fumigatus* for 24 hr or 7 days, respectively. Data are expressed as mean values ± SEM. Overall P-values were determined using a linear regression model with age and gender as covariates.

Genetic variation at the *PFKFB3* locus increases the risk of IPA after HSCT

Because of the critical role of SNPs in *PFKFB3* in regulating cytokine production, we next investigated the relationship between genetic variants at this locus and susceptibility to IPA in a disease-relevant context. We, therefore, assessed the cumulative incidence of IPA in patients from the IFIGEN cohort undergoing allogeneic HSCT (Table 1) according to recipient or donor *PFKFB3* genotypes at the rs674430 or rs646564 SNPs. Our results demonstrate that the donor, but not the recipient, rs646564 was associated with an increased risk of IPA after transplantation (Fig. 2A). The cumulative incidence of IPA for donor rs646564 was 31% for TT (P=0.02), 23% for GT (P=0.21), and 18% for GG genotypes (reference), respectively. In contrast, no significant association with the risk of IPA was detected for rs6744330 (Fig. 2B). In a multivariate model accounting for patient age and gender, hematological malignancy, type of transplantation, conditioning regimen, development of acute graft-versus-host-disease (GVHD) grade III-IV and antifungal prophylaxis, the donor TT genotype conferred a 2.7-fold increased risk of developing IPA (P=0.0017) (Table 2). These results highlight genetic variation at the *PFKFB3* locus in the donor compartment as a critical risk factor regulating susceptibility to IPA after HSCT.

Table 2. Multivariate analysis of the association between rs646564 in *PFKFB3* and risk of IPA.

Genetic/clinical variables	n=439	
	Adjusted HR† (95% CI)	P value
Donor TT at rs646564	2.72 (1.46 - 5.06)	0.0017
aGVHD III-IV	3.84 (1.46 - 10.1)	0.062

GVHD, graft-versus-host-disease; HR, hazard ratio; CI, confidence interval. Multivariate analyses were based on the subdistribution regression model of Fine and Gray in the discovery study and on conditional logistic regression in the confirmation study and meta-analysis. †Hazard ratios were adjusted for patient age and gender, hematological malignancy, type of transplantation, conditioning regimen, development of acute GVHD grade III-IV and antifungal prophylaxis. Only the variables remaining significant after adjustment are shown.

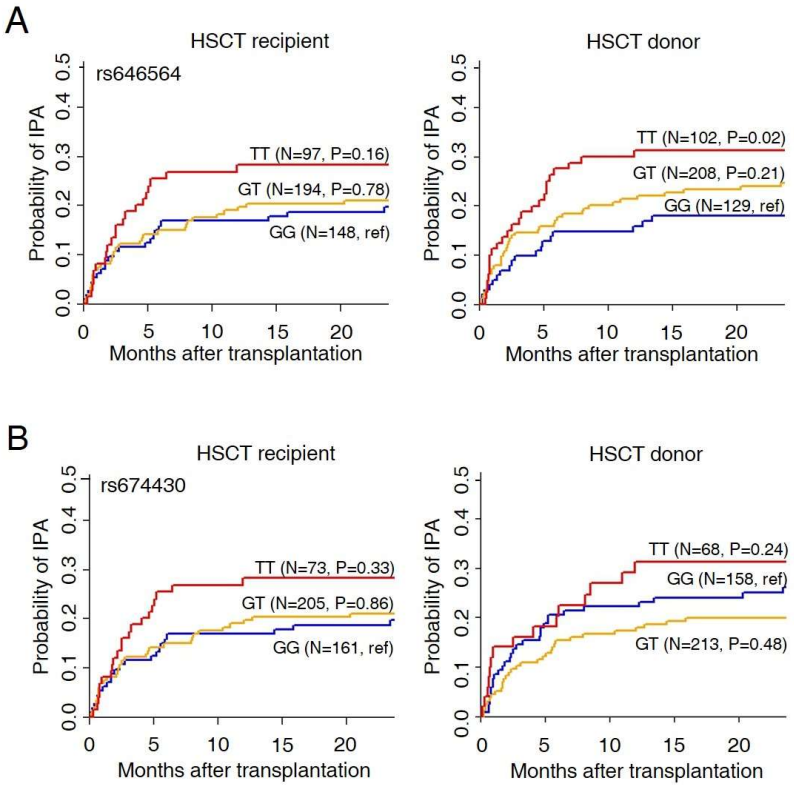

Figure 2. Genetic variation in *PFKFB3* influences the risk of IPA. Cumulative incidence of IPA in 439 eligible HSCT recipients from the IFIGEN cohort according to the recipient or donor *PFKFB3* genotypes at (A) rs646564 and (B) rs674430. Data were censored at 24 months, and relapse and death were competing events. P values are for Gray's test.

The rs646564 SNP impairs PFKFB3-mediated activation of glycolysis

To understand the mechanisms through which rs646564 might impact the metabolic homeostasis of immune cells and contribute to antifungal immune responses, we next assessed the expression of PFKFB3 in macrophages from healthy donors carrying different rs646564 genotypes after infection with *A. fumigatus*. In line with its enhanced transcriptional activity [8], the expression of the PFKFB3 protein was also increased early after infection (Fig. 3A). However, induction of PFKFB3 was instead markedly impaired in macrophages carrying the TT genotype compared to cells from GG carriers. The treatment with 3-(3-pyridinyl)-1-(4-pyridinyl)-2-propen-1-one (3PO), despite its role as a selective inhibitor of PFKFB3, also promoted a slight decrease in the expression of PFKFB3 (Fig. 3B). In line with its impact on PFKFB3 expression, the rs646564 SNP was found to significantly impair glucose consumption by both unstimulated and 24 hr-infected macrophages with the TT genotype (Fig. 3C). Macrophages from TT carriers also secreted lower amounts of lactate than cells with the GG genotype in the same conditions

(Fig. 3D), a finding ultimately pointing to a defective activation of the glycolytic pathway in carriers of the T allele. In support of these findings, inhibition of PFKFB3 with 3PO resulted in similar effects to those of the TT genotype on lactate secretion (Fig. 3D), although not glucose consumption (Fig. 3C). These results demonstrate that the rs646564 SNP contributes to IPA by compromising the efficient activation of glycolysis by macrophages in response to fungal infection.

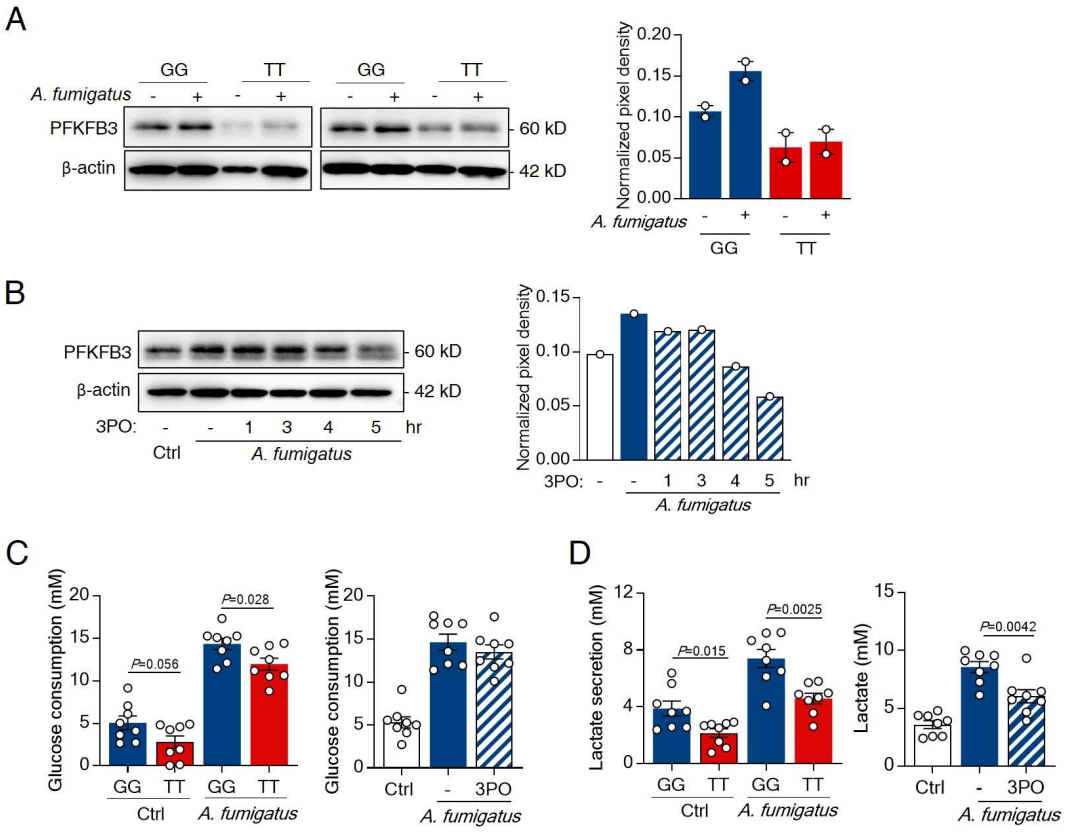

Figure 3. The rs646564 SNP in *PFKFB3* inhibits the activation of glycolysis in macrophages. Expression of PFKFB3 in macrophages infected with *A. fumigatus* for 2 hr (A) according to different rs646564 genotypes or (B) following treatment with 3PO (representative of three independent experiments). The pixel density of the PFKFB3 was normalized to β-actin. (C) Glucose consumption and (D) lactate secretion by macrophages left untreated or infected with *A. fumigatus* for 24 hr, according to different rs646564 genotypes or following treatment with 3PO. Data are expressed as mean values ± SEM.

The rs646564 SNP compromises antifungal effector functions of macrophages

To mount a protective immune response during infection with *A. fumigatus*, effector functions of macrophages such as the production of proinflammatory cytokines, phagocytosis, and killing activity are required [16]. We tested therefore how the impairment of glycolysis driven by the rs646564 SNP in

PFKFB3 might affect these antifungal mechanisms. Besides influencing the production of the adaptive cytokines IFN-γ and IL-22 (Fig. 1B), the TT genotype also impaired the secretion of proinflammatory cytokines, but not IL-10, by macrophages after 24 hr of infection (Fig. 4A), a finding illustrating likely distinct regulatory mechanisms mediated by rs646564 across cell types. A comparable defect in cytokine secretion by infected macrophages was also observed after the pharmacological inhibition of PFKFB3 (Fig. 4A). In addition, the conidiacidal activity of macrophages from TT carriers was also significantly decreased compared to cells with the GG genotype (Fig. 4B), an effect that could, at least in part, be explained by the impaired production of reactive oxygen species (ROS) by TT macrophages after infection with *A. fumigatus* (Fig. 4C). Likewise, the conidiacidal activity (Fig. 4B) was also similarly impaired upon treatment with 3PO. In contrast, the phagocytic ability of macrophages was not compromised in either the presence of the TT genotype or 3PO-treated macrophages (Fig. 4D). These results confirm a critical role for PFKFB3 in the induction and regulation of antifungal effector functions of macrophages in response to *A. fumigatus*.

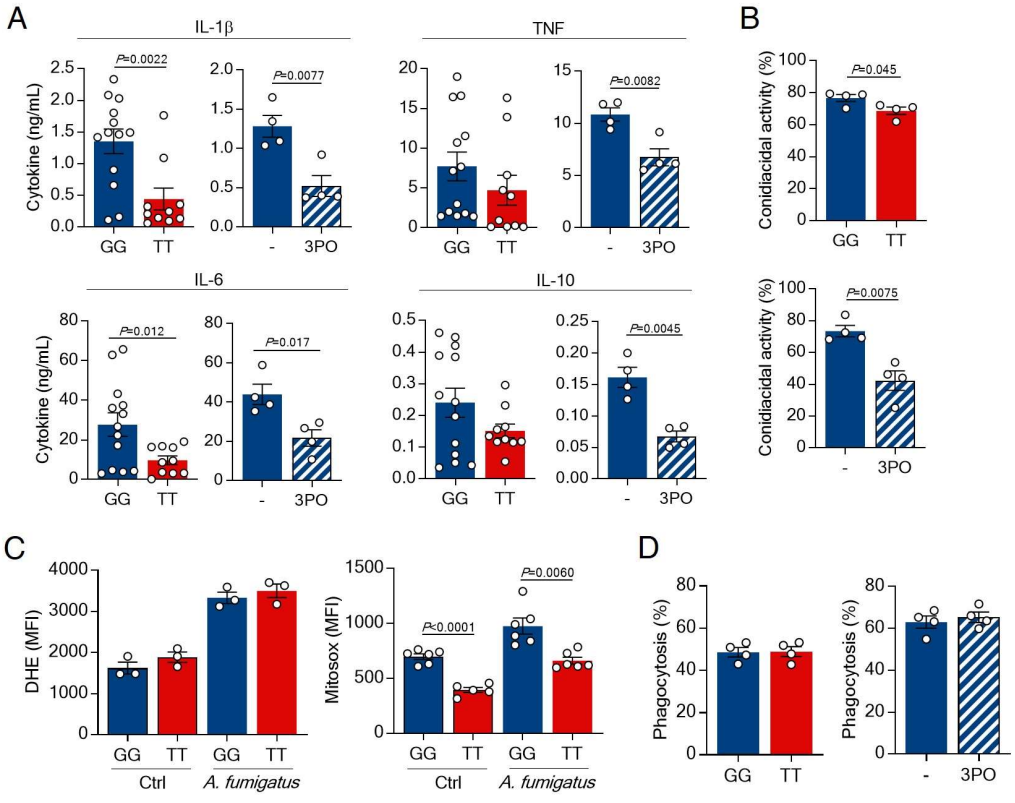

Figure 4. Antifungal effector mechanisms of macrophages are impaired by the rs646564 SNP in *PFKFB3*. (A) Production of IL-1β, TNF, IL-6, and IL-10 by macrophages infected with *A. fumigatus* for 24 hr according to different rs646564 genotypes or following treatment with 3PO. (B) Conidiacidal activity of macrophages according to different rs646564 genotypes or following treated with 3PO. (C) Production of cytosolic

ROS (left) and mitochondrial ROS (right) by macrophages infected with *A. fumigatus* for 4 hr according to different rs646564 genotypes or following treatment with 3PO. Data are expressed as mean fluorescence intensity (MFI). (D) Phagocytosis of macrophages according to different rs646564 genotypes or following treatment with 3PO. Data are expressed as mean values ± SEM.

Genetic variation at *PFKFB3* locus regulates the alveolar cytokine profile in IPA

To examine whether the rs646564 SNP also regulated cytokine production in IPA patients, we next profiled the concentration of relevant cytokines in bronchoalveolar lavage (BAL) samples collected from patients enrolled in the FUNBIOMICS study at diagnosis of fungal infection [33]. We found that the alveolar concentrations of IL-1β and IL-6 were lower among patients carrying the TT genotype than GG carriers (Fig. 5A). In line with their regulation by the rs646564 SNP in PBMCs (Fig. 1B), production of T cell-derived cytokines was also influenced, with lower concentrations of IL-17A and IL-22 being detected in samples from TT compared to GG carriers (Fig 5B). Collectively, these findings illustrate a critical link between genetic variation in the glycolytic pathway and the activation of immune responses in patients with IPA, and may explain the association with susceptibility to infection.

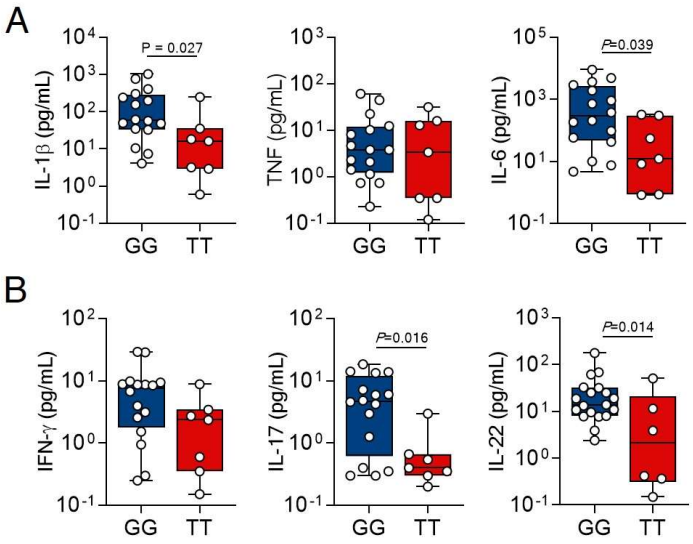

Figure 5. PFKFB3 regulates cytokine production in IPA. Levels of (A) IL-1β, TNF, and IL-6, and (B) IFNγ, IL-17, and IL-22 in BAL samples from patients diagnosed with IPA (n, GG=16; TT=7). Data are expressed as mean values ± SEM.

Discussion

Several factors are known to predispose to fungal disease, particularly in immunocompromised and severely ill patients, but these alone fail to explain the development of infection in all affected patients. Several studies have reported an expanding number of common SNPs associated with the development of IPA in patients at-risk [28,30]. Based on their validation across independent cohorts [32], the most robust markers for IPA identified to date include well-known components of the immune response to *A. fumigatus*, such as the soluble pattern recognition molecule pentraxin-3 (PTX3) [29,32] and the C-type lectin receptor dectin-1 [31,34]. However, no evidence disclosing a relevant contribution of the host genetic profile to the immunometabolic responses activated in response to *A. fumigatus* has been disclosed thus far. We now demonstrate that genetic variation in *PFKFB3* contributes to IPA via molecular mechanisms influencing the metabolic homeostasis of immune cells and the signals that orchestrate cytokine production and fungal clearance.

To counter fungal infection, myeloid cells undergo metabolic reprogramming via distinct mechanisms whereby enhanced glycolysis fuels antimicrobial effector functions required for effective clearance of the pathogen [8,19]. A key step in the regulation of the glycolytic pathway is the PFKFB3-mediated control of the levels of the fructose-2,6-bisphosphate metabolite. Our data disclose a genetic variant associated with defective activation of PFKFB3 following fungal infection. These results are in line with previous reports demonstrating that the genetic inactivation of PFKFB3 in murine cells was shown to disrupt glycolysis and innate defenses against other infections such as infection by the respiratory syncytial virus [25]. Likewise, the defective induction of PFKFB3 in T cells from rheumatoid arthritis patients was reported to drive a hypoglycolytic phenotype, impairing ATP generation, the redox balance, and the production of ROS. In contrast, overexpression of PFKFB3 in patient T cells enhances the glycolytic flux and protects cells from excessive apoptosis [35]. These findings highlight PFKFB3 as a critical regulatory node at the interface of metabolism and immunity.

We demonstrate that the activation of PFKFB3 is critical for the regulation of cytokine production and antifungal effector functions in macrophages. The activation of the NLRP3 inflammasome in macrophages and the subsequent release of IL-1β have been found to modulate glycolysis via PFKFB3 [36]. Importantly, genetic variation in PFKFB3 is correlated with differential production of IL-1β after fungal infection, suggesting the existence of bidirectional signaling events, in which PFKFB3 may also be able to regulate the activation of the NLRP3 inflammasome to drive the production of IL-1β. Endothelial PFKFB3 expression was also found to be increased after TNF treatment [37], and IL-6 was reported to enhance

glycolysis in mouse embryonic fibroblasts and human cell lines by upregulating PFKFB3 expression [38]. These results suggest the existence of a reciprocal regulation between production of pro-inflammatory cytokines and PFKFB3 activation. However, the crosstalk between these mechanisms occurs remains unclear. Recent reports highlight that, although the activity of PFKFB3 as a major regulator of glycolysis occurs mostly in the cytosol, it is also able to mediate glycolysis-independent nuclear roles [27]. This suggests that PFKFB3 can, directly or indirectly, modulate and interact with the NF-κB pathway, to regulate inflammatory responses.

PFKFB3 has a largely detrimental role in supporting cancer cell growth, by promoting glycolysis, cell cycle progression, and angiogenesis [39]. In this sense, and although the inactivation of PFKFB3 is regarded as a promising therapeutic opportunity across several types of cancer [24,40], we hypothesize that the balanced induction of this enzyme specifically in immune cells may instead represent a valuable strategy benefiting patients suffering from IPA, especially those harboring loss-of-function SNPs in *PFKFB3*. Accordingly, the activation of PFKFB3 has been shown to accelerate disease progression in models of sepsis [27]. In this context, the inhibition of PFKFB3 could be therapeutically exploited to dampen the pathogenic activation of glycolysis and, therefore, it is not surprising that such approaches have been shown to alleviate sepsis-related acute lung injury by suppressing inflammatory responses and the apoptosis of alveolar epithelial cells [41].

Current limitations in the management of fungal diseases, as well as concerns over the emergence of antifungal resistance, are inspiring the search for novel host-directed therapies. Our expanded understanding of how metabolic networks coordinate immune cell function and how specific genetic signatures influence immunometabolic responses and regulate susceptibility to fungal disease is opening new horizons towards personalized medical interventions based on individual genomics. The renewed interest in immunometabolism is expected to improve our understanding of how these signaling networks coordinate immune cell function, ultimately paving the way towards innovative therapeutic approaches involving adjuvant immunotherapy to reorient host cells towards immune protection in the context of fungal infections.

Acknowledgments

This work was supported by the Fundação para a Ciência e Tecnologia (FCT) (PTDC/SAU-SER/29635/2017, PTDC/MED-GEN/28778/2017, UIDB/50026/2020 and UIDP/50026/2020), the Northern Portugal Regional Operational Programme (NORTE 2020), under the Portugal 2020 Partnership Agreement, through the European Regional Development Fund (ERDF) (NORTE-01-0145-FEDER-000039), the Institut Mérieux (Mérieux Research Grant 2017), the European Society of Clinical Microbiology and Infectious Diseases (ESCMID Research Grant 2017), the European Union's Horizon 2020 research and innovation programme under grant agreement no. 847507, and the "la Caixa" Foundation (ID 100010434) and FCT under the agreement LCF/PR/HR17/52190003. Individual support was provided by FCT (SFRH/BD/136814/2018 to SMG, PD/BD/137680/2018 to DA, CEECIND/04058/2018 to CC, and CEECIND/03628/2017 to AC). MGN was supported by an ERC Advanced Grant and a Spinoza Grant of the Netherlands Organization for Scientific Research.

Author contributions

Conception and design: SMG, CC, AC. Collection of clinical specimens and acquisition of patient-level data: LL, TM, JV, EE, CPV, RB, FC, FF, DL, AM KL, JM, JFL, AC Jr. Acquisition of functional data: SMG, DA, RtH. Analysis and interpretation of data: SMG, DA, RtH, FLvdV, LABJ, MGN, CC, AC. Drafting or revising of the manuscript: SMG, CC, AC. Final approval of manuscript: SMG, DA, LL, TM, RtH, JV, EE, CPV, RB, FC, FF, DL, AM, FLvdV, LABJ, KL, JM, MGN, JFL, AC Jr, CC, AC.

Supplementary Information

Supplementary Figure 1

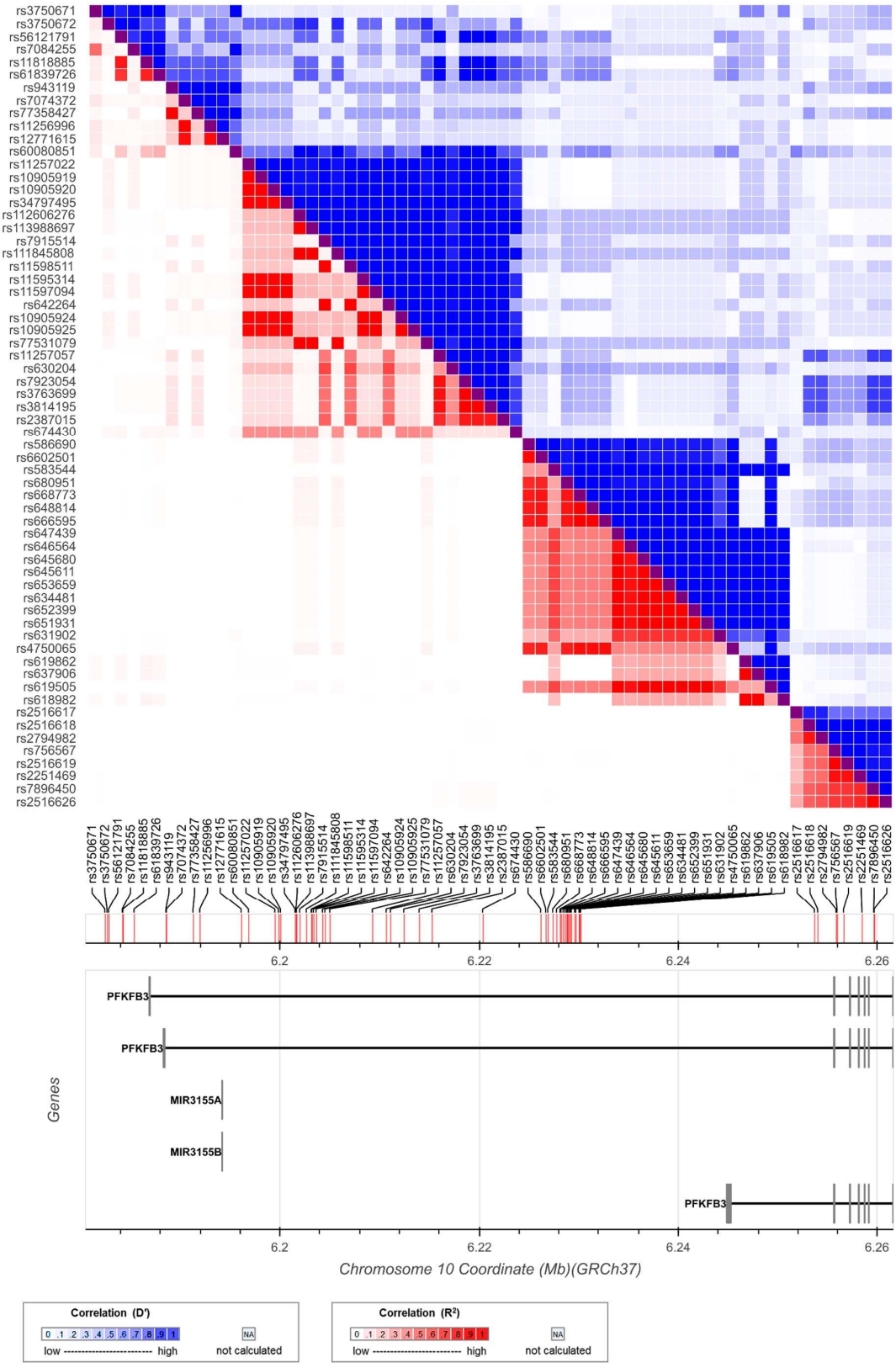

Supplementary Figure 1 | Linkage disequilibrium structure of the *PFKFB3* gene. The localization of the *PFKFB3* SNPs was obtained from the human genome assembly GRCh37 (hg19) and is indicated with vertical lines. The dbSNP reference numbers are indicated for each SNP. Blue colors refer to r^2 and red colors refer to D'. The intensity of the coloration reflects the degree of LD.

Supplementary Table.1 Analysis of cytokine QTLs in PBMCs stimulated with *A. fumigatus*.

Stimulation	SNP	Gene Name	Cytokine	p-value	chr_name	chrom_start	ensembl_gene_stable_id
A. fumigatus conidia_PBMC_24h	rs7084255	*PFKFB3*	IL6	0,0009	10	6184167	ENSG00000170525
A. fumigatus conidia_PBMC_24h	rs7923054	*PFKFB3*	TNFA	0,0009	10	6211087	ENSG00000170525
A. fumigatus conidia_PBMC_24h	rs3763699	*PFKFB3*	TNFA	0,0009	10	6212428	ENSG00000170525
A. fumigatus conidia_PBMC_24h	rs3814195	*PFKFB3*	TNFA	0,0009	10	6213960	ENSG00000170525
A. fumigatus conidia_PBMC_24h	rs2387015	*PFKFB3*	TNFA	0,0017	10	6215257	ENSG00000170525
A. fumigatus conidia_PBMC_24h	rs77358427	*PFKFB3*	TNFA	0,0022	10	6191272	ENSG00000170525
A. fumigatus conidia_PBMC_24h	rs11257057	*PFKFB3*	TNFA	0,0024	10	6209274	ENSG00000170525
A. fumigatus conidia_PBMC_24h	rs2516617	*PFKFB3*	TNFA	0,0028	10	6253651	ENSG00000170525
A. fumigatus conidia_PBMC_24h	rs2516618	*PFKFB3*	TNFA	0,0032	10	6253983	ENSG00000170525
A. fumigatus conidia_PBMC_24h	rs943119	*PFKFB3*	TNFA	0,0034	10	6188543	ENSG00000170525
A. fumigatus conidia_PBMC_24h	rs2794982	*PFKFB3*	TNFA	0,0038	10	6255838	ENSG00000170525
A. fumigatus conidia_PBMC_7days	rs646564	*PFKFB3*	IFNy	0,0108	10	6228598	ENSG00000170525
A. fumigatus conidia_PBMC_24h	rs674430	*PFKFB3*	TNFA	0,0116	10	6220360	ENSG00000170525
A. fumigatus conidia_PBMC_7days	rs634481	*PFKFB3*	IL22	0,0118	10	6229002	ENSG00000170525
A. fumigatus conidia_PBMC_24h	rs674430	*PFKFB3*	IL6	0,0125	10	6220360	ENSG00000170525
A. fumigatus conidia_PBMC_24h	rs7084255	*PFKFB3*	TNFA	0,013	10	6184167	ENSG00000170525
A.fumigatus conidia_PBMC_7days	rs653659	*PFKFB3*	IL22	0,0132	10	6228878	ENSG00000170525
A. fumigatus conidia_PBMC_7days	rs645611	*PFKFB3*	IL22	0,0132	10	6228824	ENSG00000170525
A. fumigatus conidia_PBMC_7days	rs645680	*PFKFB3*	IL22	0,0132	10	6228777	ENSG00000170525
A. fumigatus conidia_PBMC_7days	rs652399	*PFKFB3*	IL22	0,0136	10	6229127	ENSG00000170525
A. fumigatus conidia_PBMC_7days	rs651931	*PFKFB3*	IL22	0,0138	10	6229235	ENSG00000170525
A. fumigatus conidia_PBMC_7days	rs634481	*PFKFB3*	IFNy	0,0145	10	6229002	ENSG00000170525
A. fumigatus conidia_PBMC_7days	rs619505	*PFKFB3*	IL22	0,0154	10	6230059	ENSG00000170525
A. fumigatus conidia_PBMC_7days	rs646564	*PFKFB3*	IL22	0,0157	10	6228598	ENSG00000170525
A.fumigatus conidia_PBMC_7days	rs56121791	*PFKFB3*	IFNy	0,0158	10	6182796	ENSG00000170525
A. fumigatus conidia_PBMC_7days	rs583544	*PFKFB3*	IFNy	0,017	10	6226889	ENSG00000170525

A. fumigatus conidia_PBMC_24h	rs13405909	*HK2*	TNFA	0,0172	2	75067136	ENSG00000159399
A. fumigatus conidia_PBMC_7days	rs3750671	*PFKFB3*	IFNy	0,0174	10	6182423	ENSG00000170525
A. fumigatus conidia_PBMC_24h	rs2422043	*HK2*	TNFA	0,0176	2	75065463	ENSG00000159399
A. fumigatus conidia_PBMC_7days	rs61839726	*PFKFB3*	IFNy	0,0179	10	6185344	ENSG00000170525
A. fumigatus conidia_PBMC_7days	rs653659	*PFKFB3*	IFNy	0,0181	10	6228878	ENSG00000170525
A. fumigatus conidia_PBMC_7days	rs645611	*PFKFB3*	IFNy	0,0181	10	6228824	ENSG00000170525
A. fumigatus conidia_PBMC_7days	rs645680	*PFKFB3*	IFNy	0,0181	10	6228777	ENSG00000170525
A. fumigatus conidia_PBMC_7days	rs652399	*PFKFB3*	IFNy	0,0184	10	6229127	ENSG00000170525
A. fumigatus conidia_PBMC_7days	rs651931	*PFKFB3*	IFNy	0,0185	10	6229235	ENSG00000170525
A. fumigatus conidia_PBMC_7days	rs619505	*PFKFB3*	IFNy	0,0197	10	6230059	ENSG00000170525
A. fumigatus conidia_PBMC_24h	rs3771798	*HK2*	TNFA	0,02	2	75064392	ENSG00000159399
A. fumigatus conidia_PBMC_24h	rs3821308	*HK2*	TNFA	0,02	2	75077232	ENSG00000159399
A. fumigatus conidia_PBMC_24h	rs4852351	*HK2*	TNFA	0,0212	2	75122513	ENSG00000159399
A. fumigatus conidia_PBMC_24h	rs3771793	*HK2*	TNFA	0,0214	2	75065900	ENSG00000159399
A. fumigatus conidia_PBMC_24h	rs3821311	*HK2*	TNFA	0,0215	2	75066153	ENSG00000159399
A. fumigatus conidia_PBMC_7days	rs619862	*PFKFB3*	IL22	0,0229	10	6230028	ENSG00000170525
A. fumigatus conidia_PBMC_7days	rs637906	*PFKFB3*	IL22	0,0231	10	6230041	ENSG00000170525
A. fumigatus conidia_PBMC_7days	rs618982	*PFKFB3*	IL22	0,0233	10	6230178	ENSG00000170525
A. fumigatus conidia_PBMC_7days	rs11818885	*PFKFB3*	IFNy	0,0234	10	6184232	ENSG00000170525
A. fumigatus conidia_PBMC_24h	rs2516626	*PFKFB3*	TNFA	0,0235	10	6259657	ENSG00000170525
A. fumigatus conidia_PBMC_24h	rs3750671	*PFKFB3*	IL6	0,0251	10	6182423	ENSG00000170525
A. fumigatus conidia_PBMC_7days	rs680951	*PFKFB3*	IFNy	0,0252	10	6227382	ENSG00000170525
A. fumigatus conidia_PBMC_24h	rs112606276	*PFKFB3*	IL6	0,0255	10	6201604	ENSG00000170525
A. fumigatus conidia_PBMC_24h	rs113988697	*PFKFB3*	IL6	0,0256	10	6201651	ENSG00000170525
A. fumigatus conidia_PBMC_24h	rs111845808	*PFKFB3*	IL6	0,0259	10	6202630	ENSG00000170525
A. fumigatus conidia_PBMC_24h	rs34797495	*PFKFB3*	IL6	0,0263	10	6201513	ENSG00000170525
A. fumigatus conidia_PBMC_24h	rs77531079	*PFKFB3*	IL6	0,0277	10	6204990	ENSG00000170525
A. fumigatus conidia_PBMC_24h	rs4853071	*HK2*	TNFA	0,028	2	75124882	ENSG00000159399
A. fumigatus conidia_PBMC_7days	rs6602501	*PFKFB3*	IFNy	0,0281	10	6226689	ENSG00000170525
A. fumigatus conidia_PBMC_24h	rs7896450	*PFKFB3*	TNFA	0,0281	10	6259627	ENSG00000170525
A. fumigatus conidia_PBMC_24h	rs4241265	*HK2*	TNFA	0,0282	2	75124299	ENSG00000159399
A. fumigatus conidia_PBMC_24h	rs4443024	*HK2*	TNFA	0,0282	2	75124037	ENSG00000159399
A. fumigatus conidia_PBMC_24h	rs12151815	*HK2*	TNFA	0,0283	2	75124698	ENSG00000159399

A. fumigatus conidia_PBMC_24h	rs4549114	*HK2*	TNFA	0,0284	2	75125369	ENSG00000159399
A.fumigatus conidia_PBMC_7days	rs586690	*PFKFB3*	IFNy	0,0285	10	6226172	ENSG00000170525
A. fumigatus conidia_PBMC_24h	rs656489	*HK2*	TNFA	0,0296	2	75060099	ENSG00000159399
A. fumigatus conidia_PBMC_7days	rs647439	*PFKFB3*	IL22	0,0297	10	6228413	ENSG00000170525
A. fumigatus conidia_PBMC_24h	rs2602350	*HK2*	TNFA	0,0303	2	75057778	ENSG00000159399
A. fumigatus conidia_PBMC_24h	rs619850	*HK2*	TNFA	0,0303	2	75059013	ENSG00000159399
A. fumigatus conidia_PBMC_24h	rs673585	*HK2*	TNFA	0,0303	2	75057589	ENSG00000159399
A. fumigatus conidia_PBMC_24h	rs670083	*HK2*	TNFA	0,0306	2	75056725	ENSG00000159399
A. fumigatus conidia_PBMC_24h	rs672707	*HK2*	TNFA	0,0306	2	75057360	ENSG00000159399
A. fumigatus conidia_PBMC_24h	rs657209	*HK2*	TNFA	0,031	2	75056218	ENSG00000159399
A. fumigatus conidia_PBMC_7days	rs3771788	*HK2*	IL22	0,0313	2	75076789	ENSG00000159399
A. fumigatus conidia_PBMC_24h	rs4443023	*HK2*	TNFA	0,0314	2	75123170	ENSG00000159399
A. fumigatus conidia_PBMC_24h	rs2516619	*PFKFB3*	TNFA	0,0321	10	6256592	ENSG00000170525
A. fumigatus conidia_PBMC_24h	rs756567	*PFKFB3*	TNFA	0,0324	10	6255931	ENSG00000170525
A. fumigatus conidia_PBMC_24h	rs11257022	*PFKFB3*	IL6	0,0344	10	6199485	ENSG00000170525
A. fumigatus conidia_PBMC_24h	rs10905919	*PFKFB3*	IL6	0,0345	10	6199853	ENSG00000170525
A. fumigatus conidia_PBMC_24h	rs10905920	*PFKFB3*	IL6	0,0346	10	6200045	ENSG00000170525
A. fumigatus conidia_PBMC_7days	rs1545523	*HK2*	IL22	0,0346	2	75089569	ENSG00000159399
A.fumigatus conidia_PBMC_7days	rs60080851	*PFKFB3*	IFNy	0,0347	10	6196839	ENSG00000170525
A. fumigatus conidia_PBMC_7days	rs61839726	*PFKFB3*	IL22	0,0353	10	6185344	ENSG00000170525
A. fumigatus conidia_PBMC_24h	rs12771615	*PFKFB3*	TNFA	0,0359	10	6196110	ENSG00000170525
A. fumigatus conidia_PBMC_24h	rs2251469	*PFKFB3*	TNFA	0,0363	10	6258433	ENSG00000170525
A. fumigatus conidia_PBMC_24h	rs11595314	*PFKFB3*	IL6	0,0364	10	6203188	ENSG00000170525
A. fumigatus conidia_PBMC_7days	rs668773	*PFKFB3*	IFNy	0,0367	10	6227759	ENSG00000170525
A. fumigatus conidia_PBMC_24h	rs11597094	*PFKFB3*	IL6	0,0367	10	6203361	ENSG00000170525
A. fumigatus conidia_PBMC_24h	rs10905924	*PFKFB3*	IL6	0,0377	10	6204266	ENSG00000170525
A. fumigatus conidia_PBMC_7days	rs631902	*PFKFB3*	IL22	0,0379	10	6229574	ENSG00000170525
A. fumigatus conidia_PBMC_24h	rs7915514	*PFKFB3*	TNFA	0,0379	10	6201973	ENSG00000170525
A. fumigatus conidia_PBMC_24h	rs642264	*PFKFB3*	TNFA	0,0384	10	6203627	ENSG00000170525
A. fumigatus conidia_PBMC_24h	rs10905925	*PFKFB3*	IL6	0,0384	10	6204506	ENSG00000170525
A. fumigatus conidia_PBMC_24h	rs3771773	*HK2*	TNFA	0,0389	2	75089454	ENSG00000159399
A. fumigatus conidia_PBMC_24h	rs11598511	*PFKFB3*	TNFA	0,0392	10	6203152	ENSG00000170525
A. fumigatus conidia_PBMC_24h	rs11256996	*PFKFB3*	TNFA	0,0397	10	6191945	ENSG00000170525

A. fumigatus conidia_PBMC_24h	rs10496195	*HK2*	TNFA	0,0411	2	75074932	ENSG00000159399
A. fumigatus conidia_PBMC_24h	rs7074372	*PFKFB3*	TNFA	0,0421	10	6188591	ENSG00000170525
A. fumigatus conidia_PBMC_24h	rs2087173	*HK2*	TNFA	0,0429	2	75122760	ENSG00000159399
A. fumigatus conidia_PBMC_24h	rs630204	*PFKFB3*	TNFA	0,0438	10	6210655	ENSG00000170525
A.fumigatus conidia_PBMC_7days	rs647439	*PFKFB3*	IFNy	0,0443	10	6228413	ENSG00000170525
A. fumigatus conidia_PBMC_7days	rs4750065	*PFKFB3*	IFNy	0,0444	10	6229689	ENSG00000170525
A. fumigatus conidia_PBMC_7days	rs648814	*PFKFB3*	IFNy	0,0449	10	6228118	ENSG00000170525
A. fumigatus conidia_PBMC_7days	rs3771781	*HK2*	IL22	0,0461	2	75085163	ENSG00000159399
A. fumigatus conidia_PBMC_7days	rs666595	*PFKFB3*	IFNy	0,0461	10	6228226	ENSG00000170525
A. fumigatus conidia_PBMC_7days	rs583544	*PFKFB3*	IL22	0,0474	10	6226889	ENSG00000170525
A. fumigatus conidia_PBMC_24h	rs3750672	*PFKFB3*	IL6	0,0499	10	6182642	ENSG00000170525

References

1. Brown GD, Denning DW, Gow NA, et al. Hidden killers: human fungal infections. Sci Transl Med. 2012 Dec 19;4(165):165rv13.
2. Herbrecht R, Patterson TF, Slavin MA, et al. Application of the 2008 definitions for invasive fungal diseases to the trial comparing voriconazole versus amphotericin B for therapy of invasive aspergillosis: a collaborative study of the mycoses study group (MSG 05) and the european organization for research and treatment of cancer infectious diseases group. Clin Infect Dis. 2015 Mar 1;60(5):713-20.
3. Maertens JA, Raad, II, Marr KA, et al. Isavuconazole versus voriconazole for primary treatment of invasive mould disease caused by *Aspergillus* and other filamentous fungi (SECURE): a phase 3, randomised-controlled, non-inferiority trial. Lancet. 2016 Feb 20;387(10020):760-9.
4. van der Linden JW, Snelders E, Kampinga GA, et al. Clinical implications of azole resistance in *Aspergillus fumigatus*, the Netherlands, 2007-2009. Emerg Infect Dis. 2011 Oct;17(10):1846-54.
5. Weerasinghe H, Traven A. Immunometabolism in fungal infections: the need to eat to compete. Curr Opin Microbiol. 2020 Aug 8;58:32-40.
6. Van den Bossche J, O'Neill LA, Menon D. Macrophage immunometabolism: where are we (going)? Trends Immunol. 2017 Jun;38(6):395-406.
7. Cheng SC, Quintin J, Cramer RA, et al. mTOR- and HIF-1alpha-mediated aerobic glycolysis as metabolic basis for trained immunity. Science. 2014 Sep 26;345(6204):1250684.
8. Goncalves SM, Duarte-Oliveira C, Campos CF, et al. Phagosomal removal of fungal melanin reprograms macrophage metabolism to promote antifungal immunity. Nat Commun. 2020 May 8;11(1):2282.
9. Lachmandas E, Beigier-Bompadre M, Cheng SC, et al. Rewiring cellular metabolism via the AKT/mTOR pathway contributes to host defence against *Mycobacterium tuberculosis* in human and murine cells. Eur J Immunol. 2016 Nov;46(11):2574-2586.
10. Tannahill GM, Curtis AM, Adamik J, et al. Succinate is an inflammatory signal that induces IL-1beta through HIF-1alpha. Nature. 2013 Apr 11;496(7444):238-42.
11. Wickersham M, Wachtel S, Wong Fok Lung T, et al. Metabolic stress drives keratinocyte defenses against *Staphylococcus aureus* infection. Cell Rep. 2017 Mar 14;18(11):2742-2751.
12. Riquelme SA, Liimatta K, Wong Fok Lung T, et al. *Pseudomonas aeruginosa* utilizes host-derived itaconate to redirect its metabolism to promote biofilm formation. Cell Metabol. 2020 Jun 2;31(6):1091-1106 e6.
13. Tucey TM, Verma J, Harrison PF, et al. Glucose homeostasis is important for immune cell viability during *Candida* challenge and host survival of systemic fungal infection. Cell Metabol. 2018 May 1;27(5):988-1006 e7.
14. Stienstra R, Netea-Maier RT, Riksen NP, et al. Specific and complex reprogramming of cellular metabolism in myeloid cells during innate immune responses. Cell Metabol. 2017 Jul 5;26(1):142-156.
15. Netea MG, Joosten LA, van der Meer JW, et al. Immune defence against *Candida* fungal infections. Nat Rev Immunol. 2015 Oct;15(10):630-42.
16. van de Veerdonk FL, Gresnigt MS, Romani L, et al. *Aspergillus fumigatus* morphology and dynamic host interactions. Nat Rev Microbiol. 2017 Nov;15(11):661-674.
17. Arts RJ, Novakovic B, Ter Horst R, et al. Glutaminolysis and fumarate accumulation integrate immunometabolic and epigenetic programs in trained immunity. Cell Metabol. 2016 Dec 13;24(6):807-819.

18. Bekkering S, Arts RJW, Novakovic B, et al. Metabolic induction of trained immunity through the mevalonate pathway. Cell. 2018 Jan 11;172(1-2):135-146 e9.
19. Dominguez-Andres J, Arts RJW, Ter Horst R, et al. Rewiring monocyte glucose metabolism via C-type lectin signaling protects against disseminated candidiasis. PLoS Pathog. 2017 Sep;13(9):e1006632.
20. Dominguez-Andres J, Novakovic B, Li Y, et al. The itaconate pathway is a central regulatory node linking innate immune tolerance and trained immunity. Cell Metabol. 2018 Oct 1.
21. Millet P, Vachharajani V, McPhail L, et al. GAPDH Binding to TNF-alpha mRNA contributes to posttranscriptional repression in monocytes: a novel mechanism of communication between inflammation and metabolism. J Immunol. 2016 Mar 15;196(6):2541-51.
22. Palsson-McDermott EM, Curtis AM, Goel G, et al. Pyruvate kinase M2 regulates Hif-1alpha activity and IL-1beta induction and is a critical determinant of the warburg effect in LPS-activated macrophages. Cell Metabol. 2015 Jan 6;21(1):65-80.
23. Gustafsson NMS, Farnegardh K, Bonagas N, et al. Targeting PFKFB3 radiosensitizes cancer cells and suppresses homologous recombination. Nat Commun. 2018 Sep 24;9(1):3872.
24. Lu L, Chen Y, Zhu Y. The molecular basis of targeting PFKFB3 as a therapeutic strategy against cancer. Oncotarget. 2017 Sep 22;8(37):62793-62802.
25. Jiang H, Shi H, Sun M, et al. PFKFB3-driven macrophage glycolytic metabolism is a crucial component of innate antiviral defense. J Immunol. 2016 Oct 1;197(7):2880-90.
26. Taniguchi-Ponciano K, Vadillo E, Mayani H, et al. Increased expression of hypoxia-induced factor 1alpha mRNA and its related genes in myeloid blood cells from critically ill COVID-19 patients. Ann Med. 2021 Dec;53(1):197-207.
27. Wang Z, Kong L, Tan S, et al. Zhx2 Accelerates sepsis by promoting macrophage glycolysis via Pfkfb3. J Immunol. 2020 Apr 15;204(8):2232-2241.
28. Campos CF, van de Veerdonk FL, Goncalves SM, et al. Host genetic signatures of susceptibility to fungal disease. Curr Top Microbiol Immunol. 2019;422:237-263.
29. Cunha C, Aversa F, Lacerda JF, et al. Genetic PTX3 deficiency and aspergillosis in stem-cell transplantation. N Engl J Med. 2014 Jan 30;370(5):421-32.
30. Cunha C, Aversa F, Romani L, et al. Human genetic susceptibility to invasive aspergillosis. PLoS Pathog. 2013;9(8):e1003434.
31. Cunha C, Di Ianni M, Bozza S, et al. Dectin-1 Y238X polymorphism associates with susceptibility to invasive aspergillosis in hematopoietic transplantation through impairment of both recipient- and donor-dependent mechanisms of antifungal immunity. Blood. 2010 Dec 9;116(24):5394-402.
32. Fisher CE, Hohl TM, Fan W, et al. Validation of single nucleotide polymorphisms in invasive aspergillosis following hematopoietic cell transplantation. Blood. 2017 May 11;129(19):2693-2701.
33. Gonçalves SM, Lagrou K, Rodrigues CS, et al. Evaluation of bronchoalveolar lavage fluid cytokines as biomarkers for invasive pulmonary aspergillosis in at-risk patients. Front Microbiol. 2017;8:2362.
34. Chai LY, de Boer MG, van der Velden WJ, et al. The Y238X stop codon polymorphism in the human beta-glucan receptor dectin-1 and susceptibility to invasive aspergillosis. J Infect Dis. 2011 Mar 1;203(5):736-43.
35. Yang Z, Fujii H, Mohan SV, et al. Phosphofructokinase deficiency impairs ATP generation, autophagy, and redox balance in rheumatoid arthritis T cells. J Exp Med. 2013 Sep 23;210(10):2119-34.

36. Finucane OM, Sugrue J, Rubio-Araiz A, et al. The NLRP3 inflammasome modulates glycolysis by increasing PFKFB3 in an IL-1beta-dependent manner in macrophages. Sci Rep. 2019 Mar 11;9(1):4034.
37. Zhang R, Li R, Liu Y, et al. The glycolytic enzyme PFKFB3 controls TNF-alpha-induced endothelial proinflammatory responses. Inflammation. 2019 Feb;42(1):146-155.
38. Ando M, Uehara I, Kogure K, et al. Interleukin 6 enhances glycolysis through expression of the glycolytic enzymes hexokinase 2 and 6-phosphofructo-2-kinase/fructose-2,6-bisphosphatase-3. J Nippon Med Sch. 2010 Apr;77(2):97-105.
39. Yi M, Ban Y, Tan Y, et al. 6-Phosphofructo-2-kinase/fructose-2,6-biphosphatase 3 and 4: a pair of valves for fine-tuning of glucose metabolism in human cancer. Mol Metab. 2019 Feb;20:1-13.
40. Mondal S, Roy D, Sarkar Bhattacharya S, et al. Therapeutic targeting of PFKFB3 with a novel glycolytic inhibitor PFK158 promotes lipophagy and chemosensitivity in gynecologic cancers. Int J Cancer. 2019 Jan 1;144(1):178-189.
41. Gong Y, Lan H, Yu Z, et al. Blockage of glycolysis by targeting PFKFB3 alleviates sepsis-related acute lung injury via suppressing inflammation and apoptosis of alveolar epithelial cells. Biochem Biophys Res Commun. 2017 Sep 16;491(2):522-529.
42. De Pauw B, Walsh TJ, Donnelly JP, et al. Revised definitions of invasive fungal disease from the european organization for research and treatment of cancer/invasive fungal infections cooperative group and the national institute of allergy and infectious diseases mycoses study group (EORTC/MSG) consensus group. Clin Infect Dis. 2008 Jun 15;46(12):1813-21.
43. Li Y, Oosting M, Smeekens SP, et al. A Functional genomics approach to understand variation in cytokine production in humans. Cell. 2016 Nov 03;167(4):1099-1110 e14.
44. Gray RJ. A Class of K-sample tests for comparing the cumulative incidence of a competing risk. Ann Stat. 1988;16(3):14.
45. Scrucca L, Santucci A, Aversa F. Competing risk analysis using R: an easy guide for clinicians. Bone Marrow Transplantat. 2007 Aug;40(4):381-7.
46. Scrucca L, Santucci A, Aversa F. Regression modeling of competing risk using R: an in depth guide for clinicians. Bone Marrow Transplant. 2010 Sep;45(9):1388-95.

Chapter IV

Concluding remarks and future perspectives

Concluding remarks and future perspectives

The number of immunocompromised patients with complex immune and metabolic abnormalities is expected to increase in the near future as the result of advances in medical interventions, including broad-spectrum antibiotherapy and immunotherapy, as well as higher rates of inflammatory and metabolic diseases as a consequence of aging and environmental exposures [1]. Therefore, the detrimental impact of infections caused by *Aspergillus* to distinct patient populations across the globe is likely to continue rising. Owing to an increasing incidence, and despite available antifungal therapy, invasive fungal diseases, namely IPA, are a leading cause of mortality primarily among immunocompromised hosts, including hematological patients and stem-cell transplant recipients. Many unanswered and unresolved epidemiological, laboratory, and clinical questions remain to be addressed in order to further foster our knowledge of the host-fungus interaction allowing an improvement in the diagnosis, treatment, and prevention of IPA.

The pathogenesis of IPA is governed by a complex interplay between the pathogen, environmental conditions and host immune responses, the so-called disease triangle, which dictates the occurrence of a disease caused by a particular pathogen in a susceptible host in a given environmental setting [2]. Management of IPA has been focused mainly on targeting the pathogen directly with the use of antifungal drugs. The excessive prescription of these formulations and the emergence of resistant strains, as well as the remarkable burden conveyed by IPA to the healthcare systems, have driven efforts at an improved understanding of the pathogenesis of IPA. Importantly, risk of infection and its clinical outcome vary significantly even among patients with similar predisposing clinical conditions, a finding highlighting patient-intrinsic factors as critical drivers of susceptibility to IPA. In this sense, the development of novel immunomodulatory therapies that boost host specific immune defects or functions may represent a promising strategy to counter IPA. To achieve this purpose, it is essential to improve our understanding of emerging concepts of regulation of host immunity, namely the metabolic regulation of antifungal immunity. In this regard, we demonstrated the critical role of cellular metabolism and its plasticity to the activation of specific programs of antifungal immunity, as highlighted in Chapter 2.

By resorting to different pharmacological and genetic tools manipulating both the host and the fungus, we deciphered the molecular and biochemical mechanisms by which macrophage metabolism is reprogrammed in response to infection with *A. fumigatus* to promote host antifungal defense. Notably, we established fungal melanin as an essential molecule for this process; during infection, removal of fungal melanin within the phagosomal compartment of macrophages activates an immunometabolic

signaling axis leading to the upregulation of glycolysis via the recruitment of mTOR and the downstream activation of HIF-1α. Of note, the AKT–mTOR–HIF-1α pathway represents a major signaling hub that regulates metabolic changes underlying trained immunity in myeloid cells in response to β-1,3-glucan [3]. Induction of a trained immune phenotype in innate immune cells enables them to react more rapidly, stronger, and/or qualitatively different, when challenged with subsequent triggers [4]. The reprogramming of cellular metabolism is therefore a critical mediator of the trained immunity-dependent epigenetic reprogramming of innate immune cells and their progenitors [4]. In this work, we provided evidence that fungal melanin is endowed with the ability to regulate mTOR and HIF-1α signaling resulting in the metabolic reprogramming of macrophages and enhanced antifungal responses. Accordingly, is fungal melanin also able to induce trained immunity similar to β-1,3-glucan? If so, will this melanin-trained immunity be able to boost immune responses in patients at-risk to IPA and improve disease outcome? Although at the moment these questions remain unanswered, we now know that fungal cell wall components play a pivotal role in modulating host immunity and this knowledge opens new opportunities for the development of immunomodulatory strategies to fight deadly fungal infections [5]. Finally, our data (chapter 2) highlight for the first time the interplay between *A. fumigatus* and glucose metabolism in immune cells, revealing a central role for glycolysis in antifungal immunity and representing a promising first step toward the elucidation of the metabolic features that govern antifungal immunity.

Optimal patient management will require not only the development of new host-directed therapies, but also the identification of high–risk groups in which the prevalence of fungal infection is known to be increased. Part of this dissertation (chapter 3) was also developed within this purpose, envisaging that a step forward in this field could be given in risk stratification with the identification of human genetic susceptibility markers allowing identification of patients most at risk. Human genetic association studies have reported an expanding number of SNPs associated with the development of IPA in patients at-risk [6,7]. These SNPs include mainly well-known components of the immune response to *A. fumigatus*, such as dectin-1 [8,9] and PTX3 [10,11]. However, no evidence linking host genetics and immunometabolic responses to *A. fumigatus* has been provided so far. We have now added a further layer of complexity to this scenario, by demonstrating that genetic variation in a major regulator of glycolysis, PFKFB3, contributes to IPA via molecular mechanisms impacting the metabolic homeostasis of immune cells and the signals that orchestrate the antifungal response. Therefore, the identification of these key host determinants of susceptibility may lead to pre-transplant screening algorithms that can identify high-risk patients who would benefit from targeted antifungal prophylaxis or a more intense diagnostic work–up.

Genetic studies are continuously providing irrefutable evidence of the critical impact of host genetic variability in determining the risk and progression of fungal infections. However, efforts in genome-wide analyses of susceptibility to infection have also emphasized the challenges in ascribing a precise role to risk-associated variants: which variant or variants are causal; what are the molecular functions of the causal variants; which genes are affected by the casual variants; and how changes in the function or regulation of the causal genes alter the risk for infection. Also because of this, the clinical implications of this information remain modest, with limited contributions to improved patient outcomes. Although the use of genetic information to predict fungal infection is unlikely to alter clinical practice soon, the predictive performance of genetic profiling may benefit from advanced functional genomics and systems biology approaches. Recent advances in sequencing technologies and computational biology now offer unprecedented opportunities to identify essential genes and pathways involved in the host-fungus interaction at a level of complexity that was previously unattainable. Recently, Matzaraki and collaborators provided evidence that genetic variation influences ROS production of infected PBMCs, by applying a functional genomics approach in a population-based cohort, and more importantly, contribute for IPA in stem-cell transplant recipients [12]. The clinical benefits of identifying the patients that would benefit the most from antifungal prophylaxis, early empiric treatment, or host-directed immunotherapy are multiple, including patient safety and healthcare costs. The clinical applicability of this concept was recently demonstrated by the combined evaluation of relevant genetic and clinical factors in a predictive model that was used to guide preemptive therapy in hematological patients [13].

Although genetic data have historically been investigated in risk stratification strategies, recent studies illustrate the importance of genetic factors in the regulation of antifungal immune responses and in redefining current immunotherapeutic strategies [14]. Most of the clinical trials performed to date did not account for the potential impact that genetic variation may elicit on selected subgroups of individuals, and this may partly explain the disappointing outcomes of several trials involving anti-inflammatory agents. There is therefore an urgent need to portray the genetic profile of patients enrolled in clinical trials of immunomodulatory agents and assess the extent to which it may bias trial results.

Research on the genetics of susceptibility to infection over the next years is expected to transform care in infectious diseases, and fungal infections are not an exception. These efforts will be paralleled by advances in other disciplines, and this will certainly contribute to assessing the relevance of host genetics in the host-fungus interaction with an unprecedented resolution. For example, recently established organ-on-a-chip systems are amenable to the functional testing of genetic variants, and this will provide exciting

possibilities to address their functional consequences in a complex and human disease-relevant model. In conclusion, an improved understanding of how genetic signatures regulate susceptibility to fungal infection will pave the way towards new personalized medical interventions and we will surely witness the results of these advances in the field of medical mycology in the coming years.

The search for novel host-directed therapies has been inspired by the current therapeutic limitations and concerns over the emergence of antifungal resistance. The work presented herein, highlights a possible way toward innovative therapeutic approaches or metabolic adjuncts to reorient host cells towards immune protection against fungal infection. The goal of host-direct approaches targeting immunometabolism is ultimately the exploitation of intrinsic metabolic pathways in the treatment of disease, including fungal infections. The targeting of host metabolism instead of fungal traits would decrease selective pressure and consequently diminish the development of unwanted resistance to antifungals. Selected metabolic pathways may be harnessed to potentiate immune responses or dampen them when they become maladaptive, while considering the pathogen involved, the affected tissue, and the disease state. Importantly, a rational strategy to identify and interpret immunometabolic signatures of susceptibility to fungal infection through the immune profiling by multi-omics approaches, including genomics, metabolomics, and epigenomics, holds the promise to identify patients at high-risk of infection that would benefit the most from targeted preventative measures. To achieve this goal, further studies are needed to better understand the pathogenesis of fungal diseases, their progression profile in time and space, and the host-fungus interplay in the context of effector immune cells. The exploitation of new approaches to study the diverse metabolic programs of specific cells, tissues, and diseased states is ultimately necessary to pave the way toward the effective clinical modulation of immunometabolism in the field of fungal disease.

In summary, the results and considerations presented throughout this dissertation reinforce the requirement for changes in the management of fungal infections, specifically those that involve host-directed medicine. Advances in the understanding of the impact of individual immunometabolic signatures and genetic variation in the outcome of the host–fungus interaction hold promise for an era of new strategies to reduce mortality and improve outcomes in vulnerable populations at risk of fungal disease.

References

1. Latge JP, Chamilos G. *Aspergillus fumigatus* and aspergillosis in 2019. Clin Microbiol Rev. 2019 Dec 18;33(1).
2. Palmieri F, Koutsokera A, Bernasconi E, et al. Recent advances in fungal infections: from lung ecology to therapeutic strategies with a focus on *Aspergillus* spp. Front Med (Lausanne). 2022;9:832510.
3. Cheng SC, Quintin J, Cramer RA, et al. mTOR- and HIF-1alpha-mediated aerobic glycolysis as metabolic basis for trained immunity. Science. 2014 Sep 26;345(6204):1250684.
4. Netea MG, Dominguez-Andres J, Barreiro LB, et al. Defining trained immunity and its role in health and disease. Nat Rev Immunol. 2020 Jun;20(6):375-388.
5. Briard B, Fontaine T, Kanneganti TD, et al. Fungal cell wall components modulate our immune system. Cell Surf. 2021 Dec;7:100067.
6. Campos CF, van de Veerdonk FL, Goncalves SM, et al. Host genetic signatures of susceptibility to fungal disease. Curr Top Microbiol Immunol. 2018 Jul 25.
7. Cunha C, Aversa F, Romani L, et al. Human genetic susceptibility to invasive aspergillosis. PLoS Pathogens. 2013;9(8):e1003434.
8. Cunha C, Di Ianni M, Bozza S, et al. Dectin-1 Y238X polymorphism associates with susceptibility to invasive aspergillosis in hematopoietic transplantation through impairment of both recipient- and donor-dependent mechanisms of antifungal immunity. Blood. 2010 Dec 9;116(24):5394-402.
9. Chai LY, de Boer MG, van der Velden WJ, et al. The Y238X stop codon polymorphism in the human beta-glucan receptor dectin-1 and susceptibility to invasive aspergillosis. J Infect Dis. 2011 Mar 1;203(5):736-43.
10. Cunha C, Aversa F, Lacerda JF, et al. Genetic PTX3 deficiency and aspergillosis in stem-cell transplantation. N Engl J Med. 2014 Jan 30;370(5):421-32.
11. Fisher CE, Hohl TM, Fan W, et al. Validation of single nucleotide polymorphisms in invasive aspergillosis following hematopoietic cell transplantation. Blood. 2017 May 11;129(19):2693-2701.
12. Matzaraki V, Beno A, Jaeger M, et al. Genetic determinants of fungi-induced ROS production are associated with the risk of invasive pulmonary aspergillosis. Redox Biol. 2022 Jul 4;55:102391
13. White PL, Parr C, Barnes RA. Predicting invasive aspergillosis in hematology patients by combining clinical and genetic risk factors with early diagnostic biomarkers. J Clin Microbiol. 2018 Jan;56(1).
14. Williams TJ, Harvey S, Armstrong-James D. Immunotherapeutic approaches for fungal infections. Curr Opin Microbiol. 2020 Dec;58:130-137.